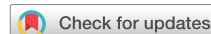


# Guidelines for Performing a Comprehensive Pediatric Transthoracic Echocardiogram: Recommendations From the American Society of Echocardiography



Leo Lopez, MD, FASE (Chair), Daniel L. Saurers, RCS, RDCS, FASE (Co-Chair), Piers C. A. Barker, MD, FASE, Meryl S. Cohen, MD, MEd, FASE, Steven D. Colan, MD, FASE, Jeanine Dwyer, BS, RDCS, FASE, Daniel Forsha, MD, MHS, FASE, Mark K. Friedberg, MD, PhD, FASE, Wyman W. Lai, MD, MPH, MBA, FASE, Beth F. Printz, MD, PhD, FASE, Ritu Sachdeva, MBBS, FASE, Neha R. Soni-Patel, MEd, BSME, RCCS, RDCS, FASE, Dongngan T. Truong, MD, MSCI, FASE, Luciana T. Young, MD, FASE, and Carolyn A. Altman, MD, FASE (Co-Chair), *Palo Alto, Irvine, Orange, and San Diego, California; Nashville, Tennessee; Durham, North Carolina; Philadelphia, Pennsylvania; Boston, Massachusetts; Aurora, Colorado; Kansas City, Missouri; Toronto, Ontario, Canada; Atlanta, Georgia; Cleveland, Ohio; Salt Lake City, Utah; Seattle, Washington; and Houston, Texas*

Echocardiography is a fundamental component of pediatric cardiology, and appropriate indications have been established for its use in the setting of suspected, congenital, or acquired heart disease in children. Since the publication of guidelines for pediatric transthoracic echocardiography in 2006 and 2010, advances in knowledge and technology have expanded the scope of practice beyond the use of traditional modalities such as two-dimensional, M-mode, and Doppler echocardiography to evaluate the cardiac segmental structures and their function. Adjunct modalities such as contrast, three-dimensional, and speckle-tracking echocardiography are now used routinely at many pediatric centers. Guidelines and recommendations for the use of traditional and newer adjunct modalities in children are described in detail in this document. In addition, suggested protocols related to standard operations, infection control, sedation, and quality assurance and improvement are included to provide an organizational structure for centers performing pediatric transthoracic echocardiograms. (*J Am Soc Echocardiogr* 2024;37:119-70.)

**Keywords:** Pediatric transthoracic echocardiography, Congenital echocardiography, Z scores, Echocardiographic protocols, Guidelines

This document is endorsed by the Society of Pediatric Echocardiography (SOPE).

From the Division of Cardiology, Department of Pediatrics, Stanford University School of Medicine and Lucile Packard Children's Hospital Stanford, Palo Alto, California (L.L.); the Department of Pediatrics, Vanderbilt University Medical Center, Nashville, Tennessee (D.L.S.); Duke Children's Hospital & Health Center, Duke University, Durham, North Carolina (P.C.A.B.); the Cardiac Center and Division of Cardiology, Children's Hospital of Philadelphia, Philadelphia, Pennsylvania (M.S.C.); the Department of Cardiology, Boston Children's Hospital, Boston, Massachusetts (S.D.C.); the Pediatric Heart Institute, Children's Hospital Colorado, Aurora, Colorado (J.D.); the Ward Family Heart Center, Children's Mercy Kansas City Hospital, Kansas City, Missouri (D.F.); the Labatt Family Heart Centre, Division of Cardiology, The Hospital for Sick Children and University of Toronto, Toronto, Ontario, Canada (M.K.F.); the Division of Pediatric Cardiology, University of California School of Medicine, Irvine, California (W.W.L.); Department of Pediatrics, Children's Hospital of Orange County, Orange, California (W.W.L.); Rady Children's Hospital San Diego and Heart Institute, University of California, San Diego, San Diego, California (B.F.P.); the Department of Pediatrics, Emory University School of Medicine and Children's Healthcare of Atlanta, Atlanta, Georgia (R.S.); the Pediatric & Adult Congenital Heart Center, Cleveland Clinic Children's Hospital, Cleveland, Ohio (N.R.S.-P.); the University of Utah and Division of Pediatric

Cardiology, Primary Children's Hospital, Salt Lake City, Utah (D.T.T.); Seattle Children's Hospital and Pediatric Cardiology, University of Washington School of Medicine, Seattle, Washington (L.T.Y.); and Baylor College of Medicine and Texas Children's Heart Center, Texas Children's Hospital, Houston, Texas (C.A.A.).

Reprint requests: American Society of Echocardiography, Meridian Corporate Center, 2530 Meridian Parkway, Suite 450, Durham, NC 27713 (E-mail: [ase@asecho.org](mailto:ase@asecho.org)).

#### Attention ASE Members:

Login at [www.ASELearningHub.org](http://www.ASELearningHub.org) to earn continuing medical education credit through an online activity related to this article. Certificates are available for immediate access upon successful completion of the activity and post-work. This activity is free for ASE Members, and \$40 for nonmembers.

0894-7317/\$36.00

Copyright 2023 Published by Elsevier Inc. on behalf of the American Society of Echocardiography.

<https://doi.org/10.1016/j.echo.2023.11.015>

**TABLE OF CONTENTS**

|   |     |
|---|-----|
| Indications                                     | 120 |
| Operations                                      | 121 |
| General Principles                              | 123 |
| Pediatric 2D and Doppler Echocardiography       | 123 |
| Standard Transthoracic Echocardiographic Views  | 124 |
| Echocardiographic Z Scores                      | 127 |
| Agitated Saline and UEAs                        | 128 |
| Three-Dimensional Echocardiography              | 128 |
| Strain Imaging                                  | 136 |
| Segmental Protocols                             | 137 |
| Systemic and Pulmonary Veins                    | 137 |
| Atria and Atrial Septum                         | 139 |
| AV Valves                                       | 143 |
| Right Ventricle                                 | 144 |
| Left Ventricle and Ventricular Septum           | 146 |
| Ventricular Outflow Tracts and Semilunar Valves | 151 |
| Great Arteries and Their Proximal Branches      | 156 |
| Reporting                                       | 163 |
| Quality Assurance                               | 165 |
| Summary   | 166 |
| Notice and Disclaimer                           | 166 |

Echocardiography plays a crucial role in the evaluation of children with acquired and congenital heart disease (CHD). It is the primary noninvasive imaging modality for establishing diagnoses, determining treatment strategies, monitoring disease progression, and assessing the effects of intervention. In 2006, the American Society of Echocardiography (ASE) published guidelines and standards for the performance of pediatric transthoracic echocardiography (TTE),<sup>1</sup> followed in 2010 by recommendations for quantification methods in pediatric TTE.<sup>2</sup> Although the principles highlighted in these documents remain as fundamental tenets in pediatric and congenital echocardiography, evolving knowledge about acquired and CHD, improvements in transducer technology and image processing, and advances in artificial intelligence have expanded the scope and value of echocardiography and transformed the landscape of care for children with heart disease. For example, adjunct advanced imaging modalities involving three-dimensional echocardiography (3DE), contrast or ultrasound enhancing agents (UEAs), and two-dimensional (2D) speckle-tracking echocardiography (STE) have become standard practice rather than research tools at many pediatric centers.

Since 2010, several reference articles with guidelines for echocardiography in the setting of pediatric and CHD have been published, including those related to appropriate use criteria (AUC) for initial outpatient pediatric TTE and for multimodality imaging of patients with known CHD (Table 1).<sup>3-6,8-10,12</sup> The American College of Cardiology Section on Adult Congenital and Pediatric Cardiology (ACPC) has also published quality metrics specific to pediatric TTE as part of its national collaborative Quality Network, including metrics related to elements of a complete pediatric TTE, image quality, and diagnostic accuracy (Table 2).<sup>13</sup> In summarizing the highlights from these and other references while focusing on advances in the field and changes in practice, this reference document will provide a comprehensive set of pediatric TTE guidelines to replace those from the 2006 and 2010 ASE documents. Each section will focus on why pediatric guidelines differ from adult guidelines. Pediatric and congenital echocardiography is unique in its need to address a

wide spectrum of anatomic and physiologic abnormalities in potentially uncooperative patients with smaller hearts and faster heart rates or older children with repaired heart disease and limited imaging windows. The substantial heterogeneity has resulted in clinical practice recommendations that are rarely based on randomized controlled studies with large sample sizes. Unless otherwise stated, all guidelines and recommendations in this document have level of evidence C, which represents the consensus of opinions based on clinical experience, descriptive studies, and reports of expert committees. Lastly, a distinction will be made for elements of the complete pediatric TTE as guidelines that should be done and additional or adjunct recommendations that may be done during the performance of pediatric TTE. It is important to recognize that these guidelines and recommendations do not represent any practice that must be done during a standard examination.

**INDICATIONS**

Typical indications for performing TTE in children are listed in Table 3. The American College of Cardiology has established AUC as a new category of standards promoting the rational use of diagnostic tests and procedures by classifying indications as “appropriate,” “may be appropriate,” or “rarely appropriate.” AUC guidelines do not replace physician judgement or practice experience but rather serve as a framework for improving patient care and outcomes in a cost-effective manner. Seven years after the first AUC document for adult TTE and transesophageal echocardiography was published, AUC guidelines for an initial outpatient pediatric TTE were published in 2014, focusing on a broad spectrum of indications categorized as (1) palpitations and arrhythmias, (2) syncope, (3) chest pain, (4) murmur, (5) other symptoms and signs, (6) prior test results, (7) systemic disorders, (8) positive family history without signs, symptoms, or confirmed cardiac diagnosis, and (9) outpatient indications in the neonatal period without a postnatal cardiac evaluation.<sup>4</sup> Another AUC document published in 2020 focused on multimodality cardiac imaging for children and adults with known CHD.<sup>9</sup> This initiative was particularly challenging as, unlike adult cardiology, evidence-based practice guidelines for individual CHDs are rare. The indications for TTE, transesophageal echocardiography, cardiac magnetic resonance imaging (MRI), computed tomography, stress imaging, and lung scan accounted for age, lesion severity, surveillance before and after intervention, and changes in clinical status. Appropriateness at different time intervals was also evaluated. As with other AUC documents, future revisions will likely need to address gaps and practice changes because of advances in knowledge and technology. Other organizations have also published documents listing indications for pediatric and congenital TTE, although most have focused on specific aspects of TTE such as diastolic function,<sup>14</sup> Kawasaki disease,<sup>7</sup> imaging of young competitive athletes,<sup>11</sup> and newborn screening by adult cardiac sonographers.<sup>12</sup>

**Key Points and Recommendations**

- AUC are available for pediatric TTE.
- TTE should be performed in children with suspected heart disease, established acquired or CHD, systemic or genetic disorders with known cardiac involvement, and significant family history of cardiovascular disease.
- Published AUC guidelines should be considered when ordering TTE.

**Abbreviations**

|   |
|---|
| <b>2D</b> = Two-dimensional   |
| <b>2DE</b> = Two-dimensional echocardiography   |
| <b>3D</b> = Three-dimensional   |
| <b>3DE</b> = Three-dimensional echocardiography   |
| <b>ACPC</b> = American College of Cardiology Section on Adult Congenital and Pediatric Cardiology |
| <b>AoV</b> = Aortic valve   |
| <b>ASE</b> = American Society of Echocardiography   |
| <b>AUC</b> = Appropriate use criteria   |
| <b>AV</b> = Atrioventricular  |
| <b>CA</b> = Coronary artery   |
| <b>CHD</b> = Congenital heart disease   |
| <b>CW</b> = Continuous-wave   |
| <b>EF</b> = Ejection fraction   |
| <b>FAC</b> = Fractional area change   |
| <b>GLS</b> = Global longitudinal strain   |
| <b>IVC</b> = Inferior vena cava   |
| <b>LA</b> = Left atrial   |
| <b>LV</b> = Left ventricular  |
| <b>MPI</b> = Myocardial performance index   |
| <b>MRI</b> = Magnetic resonance imaging   |
| <b>MV</b> = Mitral valve  |
| <b>PA</b> = Pulmonary artery  |
| <b>PHN</b> = Pediatric Heart Network  |
| <b>PV</b> = Pulmonary valve   |
| <b>PW</b> = Pulsed-wave   |
| <b>QA</b> = Quality assurance   |
| <b>QI</b> = Quality improvement   |
| <b>RA</b> = Right atrial  |
| <b>RV</b> = Right ventricular   |
| <b>SF</b> = Shortening fraction   |
| <b>STE</b> = Speckle-tracking echocardiography  |
| <b>SVC</b> = Superior vena cava   |

**OPERATIONS**

Ultrasound systems should have appropriate hardware and software to perform the essential components of standard pediatric TTE (Table 4). Other modalities, such as tissue Doppler imaging (TDI), STE, and 3DE, may provide additional information about cardiac structure and function. Ultrasound machines should achieve sufficiently high frame rates to avoid aliasing errors. Temporal resolution is not usually a problem in adults, but higher heart rates in children require higher frame rates. Reducing the penetration depth and sector width increases frame rate, which can be useful when assessing valve function. Current ultrasound image management systems usually store images at 30 Hz regardless of how they are captured on the machine, such that quantification for younger children may be better at the time of image acquisition rather than after the images have been archived. Multiple transducers used in children should provide an adequate combination of resolution and penetration depth across a wide range of patient sizes, and low-frequency (2-2.5 MHz), high-frequency ( $\geq 7.5$  MHz), and multifrequency transducers should be available in a pediatric laboratory. A non-imaging continuous-wave (CW) Doppler transducer is frequently useful for optimal quantification of peak velocities when evaluating stenotic structures or estimating ventricular systolic pressure from atrioventricular (AV) valve regurgitant velocities. A 3DE matrix transducer may also be useful. The monitor should have an appropriate size and pixel resolution to allow high-quality visualization of small cardiac structures. The display should include depth and focal range markers as well as a real-time electrocardiogram to correlate the images with the timing of cardiac events. Quantification capabilities should include measurements of dis-

|   |
|---|
| <b>TAPSE</b> = Tricuspid annular plane systolic excursion |
| <b>TDI</b> = tissue Doppler imaging                       |
| <b>TTE</b> = Transthoracic echocardiography               |
| <b>TV</b> = Tricuspid valve                               |
| <b>UEA</b> = Ultrasound enhancing agent                   |

tances, areas, blood flow and tissue velocities, and time intervals as well as calculation of volumes, ventricular mass, and peak and mean gradients.

Pediatric TTE must be performed by a competent operator with specialized training in the use of echocardiography to assess a wide range of clinical scenarios and cardiovascular abnormalities. The required knowledge base and skills for a physician or sonographer per-

forming TTE have been described previously as part of the 2006 pediatric TTE guidelines (Table 5).<sup>1</sup> The cognitive and technical elements listed in Table 5 are divided into those needed to achieve a core vs those needed to achieve an advanced level of expertise. Core expertise is usually gained during a pediatric cardiology fellowship training program or after graduating from a cardiac sonography school with exposure to pediatric and CHD. Advanced expertise usually requires additional training for physicians and higher levels of certification for sonographers. Physicians and sonographers with a core level of expertise should be able to perform TTE in normal infants, children, and adolescents as well as those with heart disease under direct supervision by individuals with an advanced level of expertise. Advanced operators must have a sufficient level of knowledge about pediatric and CHD as well as enough technical expertise to perform a complex pediatric TTE independently and to train and supervise learners and individuals with a core level of expertise.

Performance of a complete uncomplicated outpatient pediatric TTE generally requires 30 to 60 min. Inpatient studies may require more time to prepare the equipment, allow other activities at the bedside, target the initial part of the study to answer a critical question, and receive feedback from the interpreting physician regarding additional information that may be needed before leaving the bedside. Good communication with the nursing team is essential before and during the study to ensure appropriate monitoring of vital signs and clinical status. A respiratory therapist or nurse should assist in positioning patients receiving mechanical respiratory or cardiovascular support. Infection protocols should be implemented. The procedure should be explained to the patient and/or family before starting. Ambient light at the bedside should be minimized if possible. Appropriate patient positioning is crucial, using a supine position, often with knees flexed to relax the abdominal muscles, for subcostal (subxiphoid) imaging, a left lateral decubitus position for apical and left parasternal imaging, a right lateral decubitus position for right parasternal imaging, and a supine position with neck extension using a pillow or rolled towel under the shoulders for suprasternal imaging. Infants may need to be swaddled, and calming maneuvers such as feeding, a pacifier, and/or warm gel can aid with image acquisition. Distractions such as toys, music, or a television should be available for young children, and a parent or guardian should accompany all children when possible. Procedural sedation is often needed for children  $< 3$  years of age or those with developmental challenges, and a policy should be in place delineating (1) necessary personnel; (2) criteria for patient selection; (3) contraindications; (4) dosing, method, and timing of specific medications; (5) appropriate monitoring during and after the procedure; and (6) documentation of sedation successes, failures, and adverse events (Table 6). If saline contrast

**Table 1** Recent published guidelines and reference documents related to pediatric and congenital echocardiography

| Document  | Authors                               | Year | Comments and highlights   |
|---|---------------------------------------|------|---|
| Multimodality imaging guidelines for patients with repaired tetralogy of Fallot   | Valente <i>et al.</i> <sup>3</sup>    | 2013 | Approach to multimodality imaging of patients after tetralogy of Fallot repair, including patient-specific considerations, strengths and weaknesses of each modality, and institutional resources and expertise   |
| AUC for initial TTE in outpatient pediatric cardiology  | Campbell <i>et al.</i> <sup>4</sup>   | 2014 | List of 113 indications for initial outpatient TTE in children, using evidence-based data and expert consensus to rate them as “appropriate,” “may be appropriate,” or “rarely appropriate”   |
| Multimodality imaging guidelines of patients with transposition of the great arteries                                       | Cohen <i>et al.</i> <sup>5</sup>      | 2016 | Approach to multimodality imaging of patients with transposition of the great arteries before and after surgical intervention, focusing on the benefits and limitations of each modality for this patient population  |
| 3DE in CHD  | Simpson <i>et al.</i> <sup>6</sup>    | 2017 | Optimal application of 3DE in CHD, including technical considerations, image orientation, application to different lesions, procedural guidance, and functional assessment  |
| Diagnosis, treatment, and long-term management of Kawasaki disease  | McCrinkle <i>et al.</i> <sup>7</sup>  | 2017 | Updated and evidence-based recommendations for the diagnosis and management of patients with Kawasaki disease, including guidelines related to the use of echocardiography and Z scores for determining CA involvement  |
| Guidelines for performing comprehensive transesophageal echocardiographic examination in children and all patients with CHD | Puchalski <i>et al.</i> <sup>8</sup>  | 2019 | Updated guidelines on the use of transesophageal echocardiography in pediatric and congenital cardiology focusing on indications, protocols, components of each view, and anatomic and disease-specific considerations  |
| AUC for multimodality imaging during the follow-up care of patients with CHD  | Sachdeva <i>et al.</i> <sup>9</sup>   | 2020 | List of 324 indications for multimodality imaging of patients with established CHD, considering patient age, lesion severity, surveillance before and after intervention, and changes in clinical status, and using evidence-based data and expert consensus to rate them as “appropriate,” “may be appropriate,” or “rarely appropriate” at different time intervals |
| Recommendations for multimodality assessment of congenital coronary anomalies   | Frommelt <i>et al.</i> <sup>10</sup>  | 2020 | Approach to multimodality imaging of patients with congenital coronary anomalies, highlighting the benefits and limitations of each modality, and establishing coronary imaging strategies for anomalies in isolation and those associated with other CHD   |
| Recommendations on the use of multimodality cardiovascular imaging in young adult competitive athletes                      | Baggish <i>et al.</i> <sup>11</sup>   | 2020 | Guidelines focusing on the assessment of young competitive athletes, including key issues related to imaging in the setting of CHD  |
| Recommendations for the adult cardiac sonographer performing echocardiography to screen for critical CHD in the newborn     | Wasserman <i>et al.</i> <sup>12</sup> | 2021 | Echocardiographic approach for the adult sonographer who does not typically screen for CHD, providing essential information and tools needed to detect critical heart disease in newborns   |

or an UEA is needed, a protocol should be established for intravenous line insertion and administration. In laboratories associated with an inpatient facility, a fully equipped and regularly inspected resuscitation cart and masks for supplemental oxygen delivery to accommodate pediatric patients of all sizes should be readily accessible.<sup>15</sup>

Echocardiograms should be stored digitally in a system that allows (1) smooth playback of recorded moving images; (2) offline quantification, as performing measurements during a study is frequently difficult in children with limited cooperation; (3) encryption and data security against unauthorized access; and

(4) backup redundancy. Archived images and associated data should be accessible for comparison against prior studies. Using the Digital Imaging and Communications in Medicine (DICOM) standard, all images should have an associated DICOM header that can be displayed on the monitor and includes patient information as well as date, time, and location of the study. Password access should be used to ensure confidentiality of all data. Digital output from multiple systems should be accessible for interpretation, and final reports should become part of the hospital electronic medical records.

**Table 2** ACPC quality metrics related to pediatric and congenital echocardiography<sup>13</sup>

| Quality metric   | Highlights   | Link  |
|--|--|---|
| Comprehensive echocardiographic examination  | Comprehensiveness examination assessment tool to determine whether all necessary structures were appropriately assessed by 2D imaging, color mapping, and spectral Doppler interrogation               | <a href="https://cvquality.acc.org/docs/default-source/acpc/quality-metrics/study-comprehensiveness-metric-specifications.pdf?sfvrsn=787180bf_4">https://cvquality.acc.org/docs/default-source/acpc/quality-metrics/study-comprehensiveness-metric-specifications.pdf?sfvrsn=787180bf_4</a>                                     |
| Initial transthoracic echocardiographic image quality  | Image quality assessment tool to evaluate specific elements related to image orientation, 2D image appearance, and presentation of color and spectral Doppler analysis                                 | <a href="https://cvquality.acc.org/docs/default-source/acpc/quality-metrics/acpc-qnet-metric-026-initial-echo-image-quality-as-of-4-18-2018.pdf?sfvrsn=ed5480bf_4">https://cvquality.acc.org/docs/default-source/acpc/quality-metrics/acpc-qnet-metric-026-initial-echo-image-quality-as-of-4-18-2018.pdf?sfvrsn=ed5480bf_4</a> |
| Echocardiographic diagnostic accuracy  | Diagnostic accuracy tool to track errors in preoperative TTE, categorizing levels of clinical impact and error preventability  | <a href="https://cvquality.acc.org/docs/default-source/acpc/quality-metrics/diagnostic-accuracy-metric-specification.pdf?sfvrsn=7e7180bf_4">https://cvquality.acc.org/docs/default-source/acpc/quality-metrics/diagnostic-accuracy-metric-specification.pdf?sfvrsn=7e7180bf_4</a>   |
| Critical results reporting in pediatric echocardiography   | Tracking tool to identify specific critical results, components that should be documented in the report, and the time for critical result reporting  | <a href="https://cvquality.acc.org/docs/default-source/ACPC/Quality-Metrics/004critical-reporting-echo1816.pdf?sfvrsn=39528cbf_0">https://cvquality.acc.org/docs/default-source/ACPC/Quality-Metrics/004critical-reporting-echo1816.pdf?sfvrsn=39528cbf_0</a>   |
| Adverse events with sedated pediatric echocardiography   | Tracking tool to identify adverse events associated with sedation during the performance of an echocardiogram, categorizing them as minor, moderate, or severe events                                  | <a href="https://cvquality.acc.org/docs/default-source/ACPC/Quality-Metrics/005aes-w-echo1092015.pdf?sfvrsn=4f528cbf_0">https://cvquality.acc.org/docs/default-source/ACPC/Quality-Metrics/005aes-w-echo1092015.pdf?sfvrsn=4f528cbf_0</a>   |
| Application of the pediatric AUC to initial outpatient echocardiographic orders                                | Metric to determine the proportion of initial outpatient TTE performed for indications rated “rarely appropriate”  | <a href="https://cvquality.acc.org/initiatives/acpc-quality-network/quality-metrics">https://cvquality.acc.org/initiatives/acpc-quality-network/quality-metrics</a>   |
| Echocardiogram performed as an outpatient during the first year of life for arterial switch operation patients | Tracking tool to identify an echocardiogram performed in infants after the arterial switch operation for transposition of the great arteries, highlighting the necessary components of the examination | <a href="https://cvquality.acc.org/docs/default-source/default-document-library/021tga-asoecho06012016.pdf?sfvrsn=3f538cbf_0">https://cvquality.acc.org/docs/default-source/default-document-library/021tga-asoecho06012016.pdf?sfvrsn=3f538cbf_0</a>   |

## Key Points and Recommendations

- Several different transducers should be available with the full array of functionalities needed to perform pediatric TTE.
- A protocol should be in place outlining all the necessary components of patient preparation, image acquisition, and image storage in a system that allows easy review and comparison with prior studies, offline quantification, encryption and data security, and backup redundancy.

## GENERAL PRINCIPLES

Standard pediatric TTE should provide comprehensive anatomic data and quantitative evaluation of ventricular function and cardiovascular physiology. It is composed of 2D echocardiographic (2DE) images with spectral and color Doppler information in multiple imaging planes, and it may include M-mode, TDI, 3DE, and strain evaluation. During an examination, the person performing the study should un-

derstand the study indication, address issues that may affect management, and consider patient position, comfort, anxiety, and clinical stability. Standard pediatric TTE should evaluate all abnormal structures or flow jets and assess for pulmonary hypertension. Exclusion of pericardial effusion from multiple views should be part of the standard protocol, especially after cardiac surgery. The protocol may also include evaluation for pleural effusion and abnormal diaphragmatic motion in the subcostal coronal view. Extracardiac structures, such as the thymus, may be evaluated, recognizing that its absence may be important in some scenarios. Mediastinal abnormalities such as solid or cystic masses may be present and should be reported.

## Pediatric 2D and Doppler Echocardiography

Image quality optimization is crucial for diagnostic accuracy, requiring appropriate selection of probe and frequency range as well as constant technical adjustments during the examination to improve signal-to-noise ratio and image resolution. The ACPC Quality Network has published a quality metric to quantify the frequently

**Table 3** Indications for initial and follow-up TTE in children

|                    |  |
|--------------------|--|
| Initial evaluation | <ul style="list-style-type: none"> <li>• Abnormal fetal echocardiogram</li> <li>• Concerning maternal history during pregnancy</li> <li>• Signs, symptoms, or physical findings suggestive of heart disease</li> <li>• Abnormal test results suggestive of heart disease</li> <li>• Systemic or genetic disorders associated with heart disease</li> <li>• Family history of inheritable heart disease</li> <li>• Baseline before receiving a therapy that affects cardiac function</li> </ul> |
| Follow-up study    | <ul style="list-style-type: none"> <li>• Established CHD before and after therapeutic intervention</li> <li>• Established CHD with potential for change in chamber size, hemodynamics, ventricular function, or valvar function</li> <li>• Established acquired heart disease</li> <li>• Systemic or genetic disorders with associated heart disease</li> <li>• Familial cardiomyopathy</li> <li>• Pulmonary hypertension</li> <li>• Therapy that affects cardiac function</li> </ul>          |

subjective elements of image quality in pediatric TTE, namely image orientation, 2D image appearance, and presentation of color and spectral Doppler analysis (Table 7).<sup>13</sup> Structures of interest should be displayed in the center of the image with appropriate image sector depth, acoustic focus depth and length, and magnification when necessary, choosing a window where the structure is perpendicular to the ultrasound beam for optimal 2DE characterization. When possible, linear measurements should be performed along the direction of the ultrasound beam, as spatial resolution is better along this axial plane than along the perpendicular lateral plane. Lateral resolution decreases with increasing depth because of beam spread, so image views for measurements should be chosen to minimize the distance between the transducer and the structure of interest. Complete sweeps should be performed from base to apex and from right to left, keeping the transducer indicator in a fixed position while angling (or tilting) the transducer to obtain a series of 2D planar images along the three-dimensional (3D) space of the entire heart.<sup>12</sup> The images should be recorded as a combination of complete sweeps and single-plane clips, and the protocol should provide the framework for the number and order of these sweeps and clips in a standard TTE study (Table 8).

Unlike 2DE, the ultrasound beam should be parallel to the direction of flow for color mapping and pulsed-wave (PW) and CW Doppler interrogation. Color mapping should precede spectral Doppler interrogation to ensure proper sample volume placement and optimize the angle of interrogation. The color box size and the color velocity range should be adjusted to maintain a frame rate of  $\geq 20$  Hz. A narrower color box with decreased penetration depth over the area of interest results in a higher frame rate. Color-compare mode with simultaneous display of the 2DE image alone and with color mapping should be used sparingly, as the image frame rate and therefore temporal resolution are decreased in this mode compared with a 2DE image alone. This modality may be helpful when evaluating small structures with low-velocity flow, such as pul-

monary veins and coronary arteries (CAs). When TDI is used to quantify the higher amplitude and lower velocity signals of myocardial tissue motion, the ultrasound beam should be as parallel to the direction of motion as possible. Longitudinal myocardial velocities should be measured in apical views with placement of the sample volume at the ventricular myocardium immediately adjacent to the valve annulus.

## Key Points and Recommendations

- Pediatric TTE laboratories should follow standard practices for image quality optimization.

### Standard Transthoracic Echocardiographic Views

The standard pediatric TTE views are described in the 2006 ASE guidelines<sup>1</sup> and summarized in Table 9. They provide multiple opportunities to evaluate anatomic and physiologic details that may be difficult to characterize in a single plane. They also mitigate the challenges with artifacts caused by false dropout of structures parallel to the ultrasound beam or shadowing from reflective structures proximal to the structure of interest. Images are usually displayed with anatomically correct spatial orientation on the monitor, so that anterior or superior structures are at the top and rightward structures on the left side of the monitor. Consequently, display of subcostal and apical views requires the near field (or vertex) of the imaging sector to be at the bottom of the monitor, a practice in pediatric laboratories that is different from most adult laboratories. A standard pediatric protocol should outline the order of standard views, appropriate modalities for each view, and preferred methods for display and recording (Table 8). In addition, it should include a list of structures to be evaluated in each view as well as required vs optional measurements. Each view should be associated with an initial reference image that identifies the view and serves as an anchoring plane for sweeps. The segmental approach should be used to characterize the major cardiovascular segments in sequence.<sup>16,17</sup> Using this approach, the ACPC Quality Network has published a quality metric evaluating the completeness of pediatric TTE by listing the necessary components of an initial study, potentially serving as a reference when developing the protocols (Table 10).<sup>13</sup>

Pediatric echocardiography laboratories may begin TTE with either the subcostal or left parasternal view, and the order of views varies among centers. Although a specific order is presented in the 2006 guidelines and in Table 8, this document does not endorse one order over another, recognizing that each center will choose its own approach and specify the order in its TTE protocol. Views that are used more routinely in pediatric TTE than in adult TTE include subcostal coronal (long-axis), subcostal sagittal (short-axis), right parasternal, and suprasternal short-axis views. Because of the complex anatomy and/or abnormal cardiac position frequently encountered in CHD, pediatric TTE often requires modified or “in between” views for better characterization of individual structures, with subcostal left and right anterior oblique views representing the most common modified views. Sweeps can provide valuable information about the complex 3D spatial relationships among the cardiovascular structures in the setting of CHD.

The subcostal coronal (long-axis) view provides information on visceral situs and cardiac position, and the reference image shows the relative locations of the spine, inferior vena cava (IVC), and descending aorta at the level of the diaphragm (Figure 1, Videos 1 and 2). The subcostal sagittal (short-axis) view shows the proximal

**Table 4** Recommended hardware and software for standard pediatric and congenital TTE

|   |   |
|---|---|
| <p>Standard modalities</p> <ul style="list-style-type: none"> <li>• 2D imaging</li> <li>• M-mode</li> <li>• Color mapping</li> <li>• PW Doppler interrogation</li> <li>• CW Doppler interrogation</li> </ul>  | <p>Additional modalities</p> <ul style="list-style-type: none"> <li>• TDI</li> <li>• 2D strain echocardiography</li> <li>• 3DE</li> </ul>   |
| <p>Video monitor</p> <ul style="list-style-type: none"> <li>• High resolution</li> <li>• Depth markers</li> <li>• Focal range markers</li> <li>• Real-time electrocardiogram</li> </ul>   | <p>Digital storage</p> <ul style="list-style-type: none"> <li>• Password protection</li> <li>• Viewable DICOM header associated with each study consisting of patient identifiers as well as study time, date, and location</li> <li>• Easy access to stored images from all ultrasound platforms for review and comparison with prior studies</li> <li>• Associated structured reporting system</li> </ul> |
| <p>Standard transducers</p> <ul style="list-style-type: none"> <li>• Low frequency (2-2.5 MHz)</li> <li>• High frequency (&gt;7.5 MHz)</li> <li>• Multifrequency</li> <li>• Nonimaging CW Doppler</li> </ul>  | <p>Optional transducers</p> <ul style="list-style-type: none"> <li>• 3D echocardiographic matrix</li> </ul>   |
| <p>Standard quantification tools</p> <ul style="list-style-type: none"> <li>• Distances</li> <li>• Areas</li> <li>• Calculated chamber volumes</li> <li>• Calculated LV mass</li> <li>• Calculated SF and EF</li> <li>• Blood flow velocities</li> <li>• Tissue velocities</li> <li>• Time intervals</li> <li>• Peak gradients</li> <li>• Mean gradients</li> </ul> | <p>Optional quantification tools</p> <ul style="list-style-type: none"> <li>• 3D volumes</li> <li>• Calculated EF from 3D volumes</li> <li>• Global strain values</li> </ul>  |
| <p>Standard patient safety equipment</p> <ul style="list-style-type: none"> <li>• Regularly inspected and readily available resuscitation equipment appropriate to the practice setting</li> <li>• Supplemental oxygen</li> <li>• Respiratory masks of various sizes</li> </ul>   |   |

DICOM, Digital Imaging and Communications in Medicine.

superior vena cava (SVC), intrahepatic IVC, and hepatic veins, with the bicaval view serving as the reference image (Figure 2, Videos 3 and 4). This view allows optimal Doppler interrogation of abdominal aortic flow to assess for blunting or delay in return to baseline (seen with obstruction along the aortic arch or descending thoracic aorta) or diastolic flow reversal (seen with aortic regurgitation, a significant patent ductus arteriosus, aortopulmonary collateral, or arteriovenous malformation, or in the setting of general anesthesia or moderate sedation (Figure 3). The atrial septum is easily evaluated in subcostal views because it is perpendicular or nearly perpendicular to the ultrasound beam (Figures 2 and 4). In contrast, the atrial septum is usually parallel to the ultrasound beam in apical and left parasternal views, frequently resulting in dropout that can be mistaken for a septal defect. The right upper pulmonary vein is seen well in the subcostal sagittal view, entering the left atrium inferior to the right pulmonary artery (PA) and posterior to the SVC (Figure 5). Lastly, right ventricular (RV) outflow tract obstruction, secondary to infundibular hypertrophy, a deviated conal septum, or prominent muscle bundles in the setting of a double-chambered right ventricle, is well visualized in subcostal views. Counterclockwise rotation of the transducer from the subcostal coronal view (right anterior oblique view; Video 5) shows the RV inflow and outflow tracts in the same plane and can display anterior deviation of the conal septum into the RV outflow tract in the setting of tetralogy of Fallot (Figure 6). Clockwise rotation

of the transducer from the subcostal coronal view so that it is positioned between the coronal and sagittal views (left anterior oblique view) can provide excellent en face characterization of the AV valves, particularly when there is a common AV valve in the setting of an AV septal defect, as well as evaluation of the left ventricular (LV) outflow tract (Figure 7).

Methodologies for standard apical four-chamber, three-chamber, and two-chamber views have been described previously (Figure 8, Videos 6 and 7).<sup>1</sup> Moving the transducer medially on the chest allows modified apical views that are focused on the right ventricle (Figure 8). Posterior angulation from the standard apical four-chamber view is another opportunity to evaluate the IVC and hepatic venous connection to the right atrium as well as the IVC pathway in patients who have undergone the atrial switch procedure. It is also helpful in identifying a dilated coronary sinus before it enters the right atrium. Anterior angulation provides information about the LV and RV outflow tracts and semilunar valve function. Color mapping of the ventricular septum with a low Nyquist limit during an apical sweep from its posteroinferior to anterosuperior aspect may reveal small muscular ventricular septal defects or coronary blood flow in the setting of CHD with associated coronary collateral vessels. Apical views can also be useful when there are dilated CAs that can be seen traversing the AV groove or the anterior interventricular groove.

**Table 5** Required knowledge elements and skills for core and advanced level of expertise<sup>1</sup>

| Level of expertise | Required knowledge elements  |
|--------------------|--|
| Core               | <ul style="list-style-type: none"> <li>• Understanding of the basic principles of ultrasound physics</li> <li>• Knowledge of the indications for TTE in pediatric patients</li> <li>• Knowledge of common CHDs and surgical interventions</li> <li>• Knowledge of Doppler methods and their application for assessment of blood flow and prediction of intracardiac pressures</li> <li>• Knowledge of the limitations of echocardiography and Doppler techniques</li> <li>• Knowledge of alternative diagnostic imaging techniques</li> <li>• Knowledge of standard acoustic windows and transducer positions</li> <li>• Knowledge of image display and orientation used in pediatric echocardiography</li> <li>• Ability to recognize normal and abnormal cardiovascular structures by 2D imaging and to correlate the cross-sectional images with anatomic structures</li> <li>• Familiarity with standard echocardiographic methods of ventricular function assessment</li> <li>• Familiarity with major developments in the field of noninvasive diagnostic imaging</li> </ul> |
| Advanced           | <ul style="list-style-type: none"> <li>• All required core level knowledge elements</li> <li>• In-depth knowledge of ultrasound physics</li> <li>• Ability to recognize and characterize rare and complex acquired and CHDs in a variety of clinical settings</li> <li>• In-depth understanding of Doppler methods and their application to the assessment of cardiovascular physiology</li> <li>• Familiarity with all echocardiographic methods available for assessment of global and regional ventricular function and knowledge of the strengths and weaknesses of these techniques</li> <li>• Up-to-date knowledge of recent advances in the field of noninvasive cardiac imaging, including ability to review critically published research that pertains to the field</li> <li>• Knowledge of current training guidelines and regulations relevant to pediatric echocardiography</li> </ul>  |

| Level of expertise | Required skills  |
|--------------------|--|
| Core               | <ul style="list-style-type: none"> <li>• Ability to safely, properly, and efficiently use cardiac ultrasound equipment</li> <li>• Ability to perform a complete TTE examination with proper use of M-mode, 2D, and Doppler techniques in normal pediatric patients and in those with heart disease, with consultation as needed</li> </ul> |
| Advanced           | <ul style="list-style-type: none"> <li>• All required core level skills</li> <li>• Ability to independently perform a complete TTE examination with proper use of all</li> </ul>   |

(Continued)

**Table 5** (Continued)

| Level of expertise | Required skills   |
|--------------------|---|
|                    | <ul style="list-style-type: none"> <li>• available ultrasound techniques in patients with all types of CHD</li> <li>• Ability to assess cardiovascular physiology and global and regional ventricular function using a variety of ultrasound techniques</li> <li>• Ability to supervise and teach pediatric echocardiography to sonographers, pediatric cardiography fellows, and other physicians</li> </ul> |

Left parasternal views are standard for all TTE. The long-axis view with the cardiac apex displayed on the left side is one exception to the rule that rightward structures are displayed on the left (Figure 9, Videos 8 and 9). Besides information about the ventricular septum, parasternal long- and short-axis views (Videos 10 and 11) are particularly useful in evaluating mitral valve (MV) and aortic valve (AoV) morphology, presence or absence of fibrous continuity between the MV and AoV when there is a conotruncal abnormality, and mechanism for subvalvar aortic or pulmonary stenosis when present. These views can provide information about the origin, course, and relative sizes of the CAs, which is not standard in adult TTE protocols (Figure 10).<sup>1</sup> In the setting of dextrocardia, right parasternal views provide similar images as left parasternal views with levocardia, except that the transducer is rotated by 90° in a clockwise direction so that the transducer indicator is directed toward the left shoulder for the long-axis view and toward the left hip for the short-axis view (Table 11). This modification maintains the rule in the short-axis view that right-sided structures are displayed on the left side of the screen. In the setting of levocardia, the right parasternal sagittal view can provide good visualization of the atrial septum in the reference bicaval image and can be useful when evaluating superior sinus venosus defects (Figure 11, Video 12). Doppler interrogation of subvalvar, valvar, or supravulvar aortic stenosis can also be done effectively in the right parasternal sagittal view. The right parasternal transverse view can provide another opportunity to evaluate the right upper pulmonary vein coursing inferior to the right PA before draining into the left atrium.

The high left parasternal sagittal view, known as the ductal view, allows long-axis evaluation of a patent ductus arteriosus if present (Figure 12, Video 13) as well as the aortic isthmus and proximal descending aorta. It provides excellent evaluation of aortic coarctation, especially if suprasternal windows are unavailable. During a ductal sweep from right to left, one begins with the reference image of the long axis of the ascending aorta, followed in order by the main PA, the proximal left PA, and finally the descending aorta. The transition from the proximal left PA to the descending aorta is generally where a patent ductus arteriosus is located, usually with a good angle of insonation for Doppler interrogation. The high left parasternal transverse view is also excellent for evaluating the proximal branch PAs (Figure 13).

The reference image for the suprasternal long-axis view provides excellent characterization of the entire aortic arch (Videos 14 and 15).<sup>1</sup> The short-axis reference image shows the ascending aorta in cross-section with the SVC to the right and the left innominate vein coursing anterior to the aorta as it drains into the SVC (Figure 14, Video 16). Color mapping along the leftward aspect of the left innominate vein can reveal a left SVC, left azygos vein, supreme left

**Table 6** Suggested components of a conscious sedation policy and protocol

|  |
|--|
| <p><b>Personnel</b></p> <ul style="list-style-type: none"> <li>• Credentialed provider to administer sedation</li> <li>• Provider to monitor clinical status during and after sedation</li> <li>• Trained sonographer</li> </ul>   |
| <p><b>Medications</b></p> <ul style="list-style-type: none"> <li>• List of medications used for sedated echocardiographic studies</li> <li>• Appropriate dosing and routes of administration for each medication</li> <li>• Timing and indications for repeat dosing</li> </ul>  |
| <p><b>Patient care</b></p> <ul style="list-style-type: none"> <li>• Assessment of candidacy</li> <li>• Documentation of history and physical</li> <li>• Explanation of procedure to patient and/or family members</li> <li>• Consent</li> <li>• Guidelines for cessation of oral intake of solids and liquids before procedure</li> </ul>  |
| <p><b>Patient monitoring</b></p> <ul style="list-style-type: none"> <li>• Vital signs before, during, and after sedation</li> <li>• Criteria for escalation of care</li> <li>• Criteria for discharge after sedation</li> </ul>  |
| <p><b>Sonographer preparation</b></p> <ul style="list-style-type: none"> <li>• Review of study indication</li> <li>• Review of patient history, including prior echocardiograms</li> <li>• Review of necessary information to obtain from sedated study</li> <li>• Consideration of 3DE and other adjunct modalities if appropriate</li> <li>• Review for completeness with interpreting physician before emergence from sedation</li> </ul> |
| <p><b>QA documentation</b></p> <ul style="list-style-type: none"> <li>• All successful cases</li> <li>• All failed sedation cases</li> <li>• Adverse events</li> </ul>   |

intercostal vein, or anomalous pulmonary venous drainage via a vertical vein. Sweeping superiorly with 2D imaging and color mapping can determine arch sidedness by characterizing the arch branches (the first branch in a normal left aortic arch should be the innominate artery coursing to the right and bifurcating into the right common carotid and right subclavian arteries). Inferior tilting from the reference view with color mapping should reveal normal drainage of all four pulmonary veins into the left atrium (“crab view”). In this view, one must not mistake the right middle pulmonary vein for the right upper pulmonary vein or the left atrial (LA) appendage for the left upper pulmonary vein (Figure 15, Video 17).

### Key Points and Recommendations

- Every standard view in pediatric TTE involves focused and optimized evaluation of specific cardiovascular segments and connections, particularly in the setting of CHD.
- A protocol should be established outlining the required elements and preferred order for all the standard views of a comprehensive pediatric TTE, understanding that modified views are often needed to evaluate abnormal findings.

### Echocardiographic Z Scores

Most parameters of cardiovascular size, function, and blood flow patterns change with total body growth and maturation in children. Because these are also frequently affected by the abnormal hemodynamics of a disease state, it is important to distinguish between the expected physiologic changes associated with increasing body size or age and the pathologic changes in the setting of acquired or CHD. Normal pediatric reference values that account for growth and maturation should be readily available so that clinicians and researchers can distinguish a normal finding from an abnormal one, particularly as many of these parameters help predict outcome in the setting of heart disease, determine the type and timing of intervention, and quantify the response to therapy. The most widely accepted and predictive determinant of the growth of cardiovascular structures in children is total body size, usually expressed as body surface area or height, because of the known relationship between cardiovascular growth and cardiac output and between cardiac output and total body size.<sup>18</sup> Age is usually the best determinant of most functional indices. Once the relationship between a measurement and body size and/or age is characterized in a mathematical model, describing the mean behavior of the measurement in a normal pediatric population becomes the first step in establishing a normal reference range for the measurement. Ideally, the mathematical model should be simple, based on physiologic principles rather than purely statistical rules, and be applicable across the full range of body sizes encountered in pediatrics.

The next step involves characterizing the distribution of measurement values around the mean. When there is a normal distribution of the adjusted measurement values around the mean, the SD can be calculated as Z scores. A Z score of +2 or -2 represents a measurement value that is two SDs above or below the mean value, usually recognized as the thresholds for normal in a pediatric population. Multiple Z score models have been published over the past several decades to determine how abnormal a measurement is in growing children (Table 12). Because they use variable measurement performance and statistical methodologies, there may be a wide range of Z scores for a particular measurement in the same patient depending on which model was used.<sup>24</sup> The most commonly used models are each derived from single-center data.<sup>21-23</sup> More recently, the Pediatric Heart Network (PHN) used the 2010 ASE pediatric quantification guidelines<sup>2</sup> to establish a normative echocardiographic database from 3,215 North American children enrolled at 19 different centers and divided equally by sex and race.<sup>20</sup> The PHN model calculated Z scores that correlated well with the most commonly used models.<sup>19</sup> However, there were some significant differences, particularly for the smallest structures such as the left anterior descending CA diameter. This finding highlights the importance of using the same Z score model when determining growth trends over time in an individual patient and when assessing clinical outcomes and risk in a particular patient population. In the current era, online Z score calculators have provided easy access to normal reference ranges for clinical use and for research.<sup>21,25,26</sup> It is important to recognize the limitations with extrapolating “normal” reference values to abnormal populations, such as premature babies, obese children, and children with CHD, highlighting the value of Z score models based on physiologic principles.<sup>18</sup> This is especially true in the obese population, since excess adiposity disrupts the usual relationships between body surface area and the sizes of cardiovascular structures, precluding the reliance on normal Z scores in the setting of obesity.<sup>27</sup>

## Key Points and Recommendations

- Z scores for echocardiographic measurements are available for growing children.
- Different published Z score models can provide variable Z scores for the same measurement in the same patient.
- Echocardiographic Z scores should be used in children, recognizing the need to use the same Z score model when trending measurements over time in the same patient and when assessing risk in a particular patient population.

### Agitated Saline and UEAs

During a “bubble study,” an agitated mixture of sterile saline, a small volume of air or carbon dioxide, and a small volume of blood is injected into a vein, resulting in echogenic microbubbles that are too large to cross the pulmonary capillary circuit.<sup>28</sup> Agitated saline contrast is used to detect intracardiac and intrapulmonary right-to-left shunting in a wide range of patient ages and diagnoses. A protocol should be established to ensure proper use and maximize the benefits of this adjunct modality in children (Table 13).<sup>28,29</sup> The intravenous line for injection is usually placed in the upper extremity on the same side as the SVC unless a systemic venous anomaly is suspected and requires confirmation. In some patients, bilateral upper extremity venous injections may help define abnormal venous drainage patterns. Various methods for optimizing agitated saline contrast injection have been published for adult patients,<sup>28-30</sup> including (1) filling a 10-mL syringe with saline plus approximately 1 mL blood if available and 0.5 to 1 mL air, (2) connecting that syringe via a three-way stopcock to a second 10-mL syringe, and (3) agitating the mixture by passing it back and forth from one syringe to the other before injection. Apical four-chamber or subcostal coronal views are typically used, and harmonic imaging should be considered to improve contrast visualization. Appearance of contrast in the left atrium and left ventricle within three to six cardiac cycles after RA opacification with or without a Valsalva maneuver suggests interatrial shunting. Intrapulmonary shunting is highly suspected if contrast is seen in the left atrium later than six car-

diac cycles after RA opacification. A false-positive result may be seen with release of pooled blood in the pulmonary veins after a prolonged Valsalva maneuver, and a false negative result may occur with (1) elevated LA pressures precluding interatrial right-to-left shunting or (2) a prominent Eustachian valve that causes preferential interatrial right-to-left streaming from the IVC rather than the SVC.<sup>28</sup>

UEAs are manufactured microbubbles composed of a phospholipid or human albumin membrane around a high molecular weight gaseous core that (1) are small enough to pass from the systemic veins through the pulmonary capillary circuit into the left atrium and left ventricle and (2) can generate increased acoustic signals compared with the myocardium and surrounding structures, enhancing LV cavity visualization.<sup>30</sup> UEAs are used routinely in adult TTE. Initial safety concerns in patients with pulmonary hypertension, intracardiac shunts, and unstable cardiopulmonary disease have abated with cumulative research,<sup>31</sup> so that the US Food and Drug Administration removed the black box warning for the use of UEAs in these patients in 2017. LV opacification is the only approved indication for UEAs, and off-label uses have included detection and characterization of intracardiac masses, apical hypertrophic cardiomyopathy, LV noncompaction, as well as differences in regional myocardial perfusion at rest and with stress.<sup>30</sup> Lumason (sulfur hexafluoride lipid-type A microspheres) has been approved for pediatric use, particularly in the setting of obesity, prior cardiac surgery, and perfusion imaging for repaired CHD and acquired problems such as Kawasaki disease and the multi-system inflammatory syndrome in children with COVID-19 infection.

## Key Points and Recommendations

- Agitated saline contrast injection should be considered when evaluating intracardiac and intrapulmonary shunting.
- UEA use has been approved for children.
- A UEA may be considered when delineation of the LV endocardium to evaluate function by 2DE alone is challenging.

**Table 7** Elements of image quality optimization<sup>13</sup>

|                          |  |
|--------------------------|--|
| Image orientation        | <ul style="list-style-type: none"> <li>• Adherence to standards for each view</li> </ul>   |
| 2D imaging               | <ul style="list-style-type: none"> <li>• Transducer choice</li> <li>• Presentation of region of interest (focus depth and length, and magnification when necessary)</li> <li>• Balance between resolution and penetration</li> <li>• Appropriate brightness level</li> </ul> |
| Color mapping            | <ul style="list-style-type: none"> <li>• Frame rate <math>\geq</math> 20 Hz</li> <li>• Appropriate color gain</li> <li>• Appropriate Nyquist limit</li> <li>• Deliberate and limited use of color-compare mode</li> </ul>  |
| Spectral Doppler display | <ul style="list-style-type: none"> <li>• Appropriate placement of Doppler sample volume</li> <li>• PW vs CW Doppler interrogation</li> <li>• Appropriate spectral Doppler gain</li> <li>• Scale adjusted to maximize Doppler signal</li> </ul>                               |

### Three-Dimensional Echocardiography

Guidelines have been published highlighting the value of 3DE in the quantification of ventricular volumes and function, characterization of valvar morphology, and evaluation of the atrial septum, ventricular septum, and outflow tracts.<sup>6,32</sup> Three-dimensional echocardiography is especially useful when planning surgical interventions that involve complex intracardiac baffles or complex AV valve repair. Effective 3DE requires optimization of 2DE images, aligning the region of interest in the axial plane and choosing whether to prioritize temporal resolution (volume sampling rate) or spatial resolution. Ventricular volumes are best assessed with high temporal resolution, septal defects and the outflow tracts with high spatial resolution, and valvar morphology and function with a balance of good temporal and spatial resolution. Prioritizing temporal or spatial resolution drives the selection of the data acquisition mode, whether it is acquisition of electrocardiographically gated multibeat volumes, real-time 3DE volumes, or focused wide-sector volumes (3D zoom). Gated volumes provide the best combination of temporal and spatial resolution, but the patient must remain still and suspend respiration during acquisition, which is problematic for most young children. In addition, gated volumes are difficult to obtain in patients with ectopy or other arrhythmias. Three-dimensional echocardiography with color mapping usually results in lower temporal resolution, limiting its use in children.

**Table 8** Suggested components of a standard comprehensive transthoracic echocardiographic protocol

Subcostal coronal situs view (vertex up or down)

- 2D + color clip: cross-section of IVC, DAo, spine, liver, stomach
- 2D + color sweep: hepatic veins to IVC to RA

Subcostal sagittal IVC and DAo view (vertex up or down)

- 2D + color clip: IVC
- 2D + color clip: abdominal DAo
- PW: abdominal DAo below diaphragm

Subcostal coronal (long-axis) view (vertex down)

- 2D + color sweep: IVC to RV outflow tract
- Focused 2D + color sweep at low Nyquist limit: atrial septum

Subcostal sagittal (short-axis) view (vertex down)

- 2D + color sweep: bicaval view to LV apex
- Focused 2D + color sweep at low Nyquist limit: atrial septum
- 2D + color clip: right upper pulmonary vein
- 2D + color clip  $\pm$  PW  $\pm$  CW: RV outflow tract

Subcostal right anterior oblique view (vertex down)

- 2D + color clip: RV inflow and outflow

Subcostal left anterior oblique view (vertex down)

- 2D + color sweep: atrial septum
- 2D + color clip: TV and MV en face

Apical four-chamber view (vertex down)

- 2D + color clip: TV
- PW + CW  $\pm$  tissue Doppler: TV
- CW: tricuspid regurgitation jet if present
- 2D + color clip: MV
- PW + CW + tissue Doppler: MV
- 2D + color sweep: coronary sinus to RV outflow tract
- 2D + color sweep at low Nyquist limit: ventricular septum
- Focused 2D clip: LA and LV
- Color + PW: one right pulmonary vein
- Focused 2D clip: RA and RV (RV-centered view)
- TAPSE
- 2D + color clip  $\pm$  PW  $\pm$  CW: RV outflow tract
- Measurements: TV and MV annular diameters; LA end-systolic area; LV end-diastolic and end-systolic area and length, LV end-diastolic epicardial length; RV end-diastolic and end-systolic area

Apical two-chamber view (vertex down)

- 2D clip: LA and LV
- 2D + color clip: MV
- Measurements: LA end-systolic area; LV end-diastolic and end-systolic area and length

Apical three-chamber (long-axis) view (vertex down)

- 2D + color clip: LV outflow tract, AoV, and proximal aorta
- PW + CW: LV outflow tract, AoV, and proximal aorta

Parasternal long-axis view (vertex up)

- 2D + color sweep: reference to TV back to reference to PV
- Focused color sweep: ventricular septum
- 2D + color clip: MV
- 2D + color clip: AoV
- 2D + color clip: TV
- CW: tricuspid regurgitation jet if present
- 2D + color clip: PV
- PW + CW: PV
- Measurements: AoV annular, aortic root, sinotubular junction, and AAO diameters; MV and TV annular diameters; PV annular and main PA diameters

Parasternal short-axis view (vertex up)

- 2D + color sweep: AoV to apex then back to AoV to main and branch PAs
- Focused color sweep: ventricular septum
- 2D + color clip: AoV
- Focused simultaneous 2D + color clip (color-compare): left main, left anterior descending, and circumflex CAs
- Focused simultaneous 2D + color clip (color-compare): right CA
- 2D + color clip: MV
- 2D + color clip: TV
- CW: tricuspid regurgitation if present
- 2D + color clip: PV
- PW + CW: PV, main PA, proximal branch PAs
- 2D clip and M-mode: LV cross-section at level of papillary muscles
- Measurements: LV end-diastolic and end-systolic areas, LV end-diastolic epicardial area; LV M-mode end-diastolic and end-systolic internal diameters, LV M-mode end-diastolic septal and posterior wall thickness; PV annular, main PA, and proximal branch PA diameters; left main, proximal left anterior descending, and proximal right CA diameters

High left parasternal sagittal (ductal) view (vertex up)

- 2D + color sweep: AAO to main PA to left PA and aortic arch to patent ductus arteriosus (if present) to DAo
- PW + CW: patent ductus arteriosus if present

Suprasternal long-axis view (vertex up)

- 2D + color clip: aortic arch and its branches
- PW + CW: distal transverse aortic arch, aortic isthmus, and proximal DAo
- Measurements: proximal and distal transverse aortic arch and aortic isthmus diameters

Suprasternal short-axis view (vertex up)

- 2D + color sweep: AAO superiorly to first branch bifurcation, showing arch descending to the right or left during sweep with color mapping
- 2D + color sweep: leftward aspect of left innominate vein (exclude left SVC or partial anomalous pulmonary venous return to left innominate vein)
- Focused 2D + color clip  $\pm$  PW: two right and two left pulmonary veins draining into the left atrium (crab view; caution: right middle pulmonary vein may be confused with right upper pulmonary vein)

Right parasternal sagittal view (vertex up)

- 2D + color clip: SVC, IVC, atrial septum (exclude sinus venosus defect)

Right parasternal transverse view (vertex up)

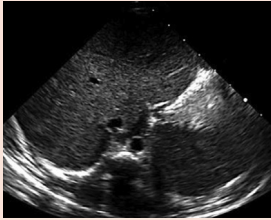
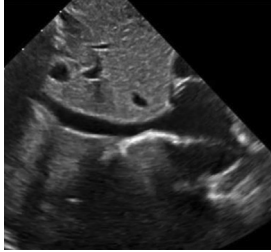
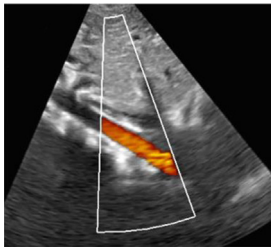
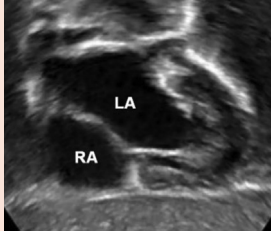
- 2D + color clip: right upper pulmonary vein draining into LA below level of right PA

Calculations

- LV end-diastolic and end-systolic endocardial volumes
- LV end-diastolic epicardial volume
- LV mass
- LV mass-to-volume ratio
- LVEF (5/6 area-length method or method of disks)
- LV M-mode SF
- LA volume
- RV systolic pressure from tricuspid regurgitation gradient or from ventricular septal defect gradient
- PA systolic pressure from PDA gradient

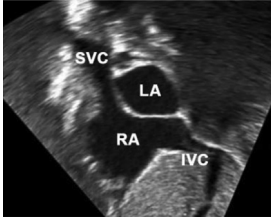
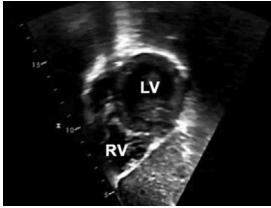
AAo, Ascending aorta; DAo, descending aorta; PDA, patent ductus arteriosus.

**Table 9** Standard transthoracic echocardiographic views

| View                                | Patient/probe position*  | Reference/sample images   | Utility   |
|-------------------------------------|--|---|---|
| Subcostal coronal situs view        | <ul style="list-style-type: none"> <li>• Patient position: supine with flexed knees for older patients</li> <li>• Probe indicator direction: 3 o'clock</li> <li>• Probe position: between xiphoid process and navel on abdomen</li> </ul>  |   | <ul style="list-style-type: none"> <li>• Determine abdominal visceral situs</li> <li>• Evaluate relative locations of IVC, DAo, spine, liver, and stomach</li> </ul>  |
| Subcostal sagittal IVC and DAo view | <ul style="list-style-type: none"> <li>• Patient position: supine with flexed knees for older patients</li> <li>• Probe indicator direction: 12 o'clock</li> <li>• Probe position: between xiphoid process and navel on abdomen</li> </ul> | <br><br>   | <ul style="list-style-type: none"> <li>• Display connection between hepatic segment of IVC and RA</li> <li>• If prominent azygos or hemiazygos vein is present, consider interrupted IVC</li> <li>• Evaluate pulsatility and flow in abdominal aorta by color mapping and PW Doppler</li> </ul> |
| Subcostal coronal (long-axis) view  | <ul style="list-style-type: none"> <li>• Patient position: supine with flexed knees for older patients</li> <li>• Probe indicator direction: 3 o'clock</li> <li>• Probe position: below xiphoid process</li> </ul>                         | <br><br><p>Reference image: cross-section of IVC, DAo, spine, liver, and stomach</p>  | <ul style="list-style-type: none"> <li>• Evaluate coronary sinus, atrial septum, AV connections, LV outflow tract, RV outflow tract, anterior muscular ventricular septum, and ventriculoarterial connections</li> </ul>  |

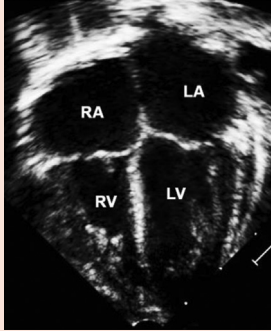
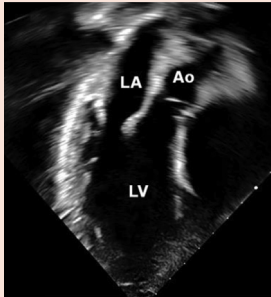
(Continued)

**Table 9** (Continued)

| View                                  | Patient/probe position*  | Reference/sample images  | Utility  |
|---------------------------------------|--|--|--|
| Subcostal sagittal (short-axis) view  | <ul style="list-style-type: none"> <li>• Patient position: supine with flexed knees for older patients</li> <li>• Probe indicator direction: 6 o'clock</li> <li>• Probe position: below xiphoid process</li> </ul> |  <p>Reference image: bicaval view with SVC and IVC draining into RA</p>  | <ul style="list-style-type: none"> <li>• Evaluate SVC, IVC, right upper pulmonary vein, atrial septum, LV outflow tract, RV outflow tract, ventricular septum, and LV cross-section</li> </ul>   |
| Subcostal right anterior oblique view | <ul style="list-style-type: none"> <li>• Patient position: supine with flexed knees for older patients</li> <li>• Probe indicator direction: 2 o'clock</li> <li>• Probe position: below xiphoid process</li> </ul> |   | <ul style="list-style-type: none"> <li>• Display RV inflow and outflow simultaneously along with en face AoV view</li> <li>• For tetralogy of Fallot, evaluate degree of anterosuperior malalignment of conal septum</li> <li>• For perimembranous ventricular septal defect, display area of fibrous continuity between TV and AoV</li> </ul> |
| Subcostal left anterior oblique view  | <ul style="list-style-type: none"> <li>• Patient position: supine with flexed knees for older patients</li> <li>• Probe indicator direction: 5 o'clock</li> <li>• Probe position: below xiphoid process</li> </ul> |    | <ul style="list-style-type: none"> <li>• Evaluate atrial septum</li> <li>• Display both AV valves en face</li> <li>• For AV septal defect, display common AV valve en face</li> </ul>  |

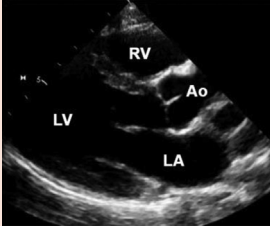
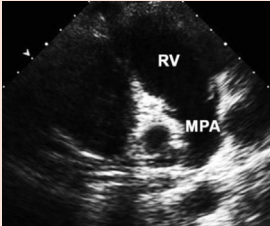
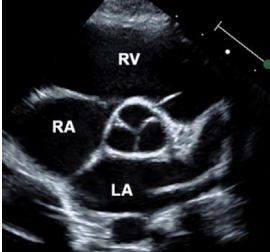
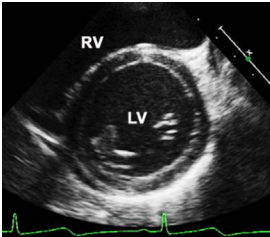
(Continued)

Table 9 (Continued)

| View                      | Patient/probe position*  | Reference/sample images  | Utility  |
|---------------------------|--|--|--|
| Apical four-chamber view  | <ul style="list-style-type: none"> <li>• Patient position: left lateral decubitus (on left side) with left arm up</li> <li>• Probe indicator direction: 3 o'clock</li> <li>• Probe position: laterally at apex of heart</li> </ul>                                   |  <p>Reference image: simultaneous display of four chambers with TV and MV at crux of heart</p> | <ul style="list-style-type: none"> <li>• Evaluate TV morphology, function, and flow</li> <li>• Estimate RV systolic pressure from the tricuspid regurgitation gradient</li> <li>• Evaluate MV morphology, function, and flow</li> <li>• Evaluate ventricular septum</li> <li>• Measure LV size</li> <li>• Evaluate LV systolic and diastolic function</li> <li>• Measure LA size</li> <li>• Evaluate at least one right and/or one left pulmonary vein entering the left atrium</li> </ul> |
| Apical two-chamber view   | <ul style="list-style-type: none"> <li>• Patient position: left lateral decubitus (on left side) with left arm up</li> <li>• Probe indicator direction: 2 o'clock</li> <li>• Probe position: laterally at apex of heart</li> </ul>                                   |   | <ul style="list-style-type: none"> <li>• Evaluate LV systolic function</li> </ul>  |
| Apical three-chamber view | <ul style="list-style-type: none"> <li>• Patient position: left lateral decubitus (on left side) with left arm up</li> <li>• Probe indicator direction: 11 o'clock</li> <li>• Probe position: laterally at apex of heart</li> </ul>                                  |    | <ul style="list-style-type: none"> <li>• Evaluate mitral-to-AoV fibrous continuity</li> <li>• Evaluate LV outflow tract and proximal aorta</li> <li>• Evaluate AoV morphology, function, and flow</li> <li>• Measure LV outflow tract and AoV gradient if elevated</li> </ul>  |
| Apical RV-centered view   | <ul style="list-style-type: none"> <li>• Patient position: left lateral decubitus (on left side) with left arm up</li> <li>• Probe indicator direction: 3 o'clock</li> <li>• Probe position: medial repositioning at apex of heart to bring RV into focus</li> </ul> |    | <ul style="list-style-type: none"> <li>• Evaluate RV size and systolic function</li> </ul>   |

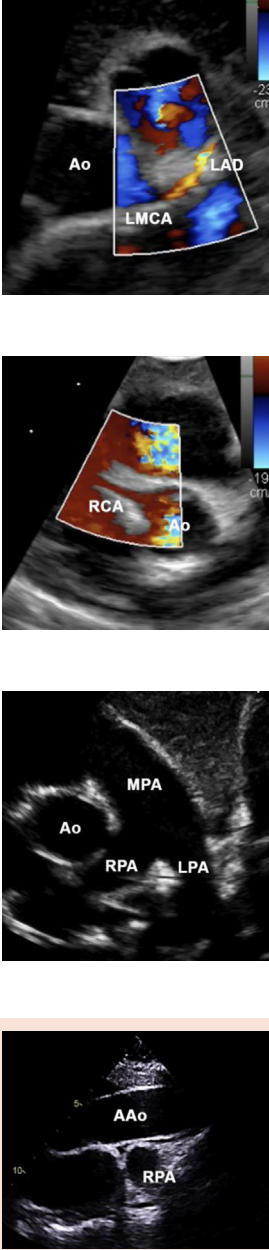
(Continued)

**Table 9** (Continued)

| View                        | Patient/probe position*   | Reference/sample images  | Utility   |
|-----------------------------|---|--|---|
| Parasternal long-axis view  | <ul style="list-style-type: none"> <li>• Patient position: left lateral decubitus (on left side) with left arm up</li> <li>• Probe indicator direction: 10 o'clock</li> <li>• Probe position: midway along left side of sternum</li> </ul>  |  <p>Reference image: LV long axis with apex to left of screen, proximal aorta long axis</p>   | <ul style="list-style-type: none"> <li>• Evaluate mitral-to-AoV fibrous continuity</li> <li>• Evaluate MV morphology and function</li> <li>• Evaluate AoV morphology and function</li> <li>• Measure diameters of AoV annulus, aortic root, sinotubular junction, and AAO</li> <li>• Display origin of RCA from aortic root by 2D and color mapping</li> <li>• Evaluate TV morphology, function, and flow</li> <li>• Estimate RV systolic pressure from the tricuspid regurgitation gradient</li> <li>• Evaluate PV morphology, function, and flow</li> <li>• Measure diameters of PV annulus and MPA</li> <li>• Measure PV and MPA gradient if elevated</li> </ul>   |
| Parasternal short-axis view | <ul style="list-style-type: none"> <li>• Patient position: left lateral decubitus (on left side) with left arm up</li> <li>• Probe indicator direction: 2 o'clock</li> <li>• Probe position: midway along left side of sternum (evaluation of pulmonary veins may be better higher along the left side of the sternum)</li> </ul> |  <p>Reference image: AoV cross-section with RA to the right, RV anteriorly, main PA to the left, and LA posteriorly</p>    | <ul style="list-style-type: none"> <li>• Evaluate AoV morphology</li> <li>• Evaluate MV morphology</li> <li>• Evaluate ventricular septum</li> <li>• Measure LV size</li> <li>• Evaluate LV systolic function</li> <li>• Display origin of LMCA from aortic root as well as its bifurcation into the left circumflex and LAD branches by 2D and color mapping</li> <li>• Measure LMCA, left circumflex, and LAD diameters by 2D</li> <li>• Display origin of RCA from aortic root by 2D and color mapping</li> <li>• Measure RCA diameter by 2D</li> <li>• Evaluate TV morphology, function, and flow</li> <li>• Estimate RV systolic pressure from the tricuspid regurgitation gradient</li> <li>• Evaluate PV morphology, function, and flow</li> <li>• Measure diameters of PV annulus, MPA, and proximal branch PAs</li> <li>• Measure PV and MPA gradient if elevated</li> </ul> |

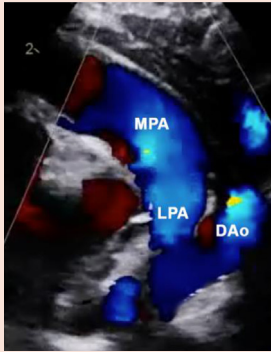
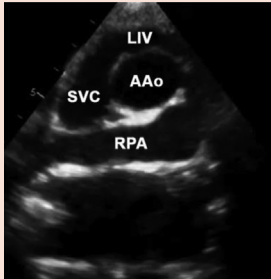
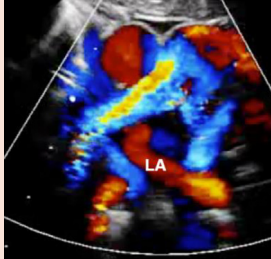
(Continued)

**Table 9** (Continued)

| View   | Patient/probe position*   | Reference/sample images   | Utility  |
|--|---|---|--|
| High left parasternal sagittal (ductal) view | <ul style="list-style-type: none"> <li>• Patient position: left lateral decubitus (on left side) with left arm up</li> <li>• Probe indicator direction: 12 o'clock</li> <li>• Probe position: left side of sternum high on chest</li> </ul> |  | <ul style="list-style-type: none"> <li>• Evaluate AAO</li> <li>• Exclude a patent ductus arteriosus</li> <li>• Evaluate morphology and flow in patent ductus arteriosus if present</li> <li>• Evaluate flow in proximal DAo</li> </ul> |

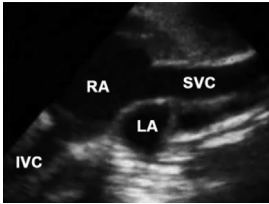
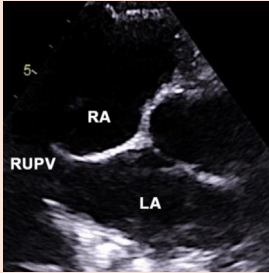
(Continued)

**Table 9** (Continued)

| View                         | Patient/probe position*  | Reference/sample images   | Utility  |
|------------------------------|--|---|--|
| Suprasternal long-axis view  | <ul style="list-style-type: none"> <li>• Patient position: supine</li> <li>• Probe indicator direction: around 12 o'clock</li> <li>• Probe position: suprasternal notch</li> </ul> |   | <ul style="list-style-type: none"> <li>• Evaluate aortic arch and origin of right innominate, left common carotid, and left subclavian arteries</li> <li>• Measure diameters of proximal and distal transverse aortic arch and aortic isthmus</li> <li>• Evaluate flow along aortic arch and proximal DAo</li> </ul>   |
| Suprasternal short-axis view | <ul style="list-style-type: none"> <li>• Patient position: supine</li> <li>• Probe indicator direction: 3 o'clock</li> <li>• Probe position: suprasternal notch</li> </ul>         |  <p data-bbox="696 1010 1044 1062">Reference image: aortic arch and its branches</p>   | <ul style="list-style-type: none"> <li>• Display right innominate artery as first aortic arch branch and its bifurcation into the right subclavian and right common carotid arteries</li> <li>• Display left common carotid artery as the second aortic arch branch and the left subclavian artery as the third aortic arch branch</li> <li>• Evaluate drainage of two right and two left pulmonary veins into LA by 2D, color mapping, and PW (crab view; caution: right middle pulmonary vein may be confused with RUPV, and LA appendage may be confused with the left upper pulmonary vein)</li> </ul> |
|                              |  |  <p data-bbox="696 1381 1044 1461">Reference image: AAO cross-section with SVC to the right, left innominate vein anteriorly, and RPA posteriorly</p> |  |
|                              |  |   |  |

(Continued)

**Table 9** (Continued)

| View                              | Patient/probe position*  | Reference/sample images   | Utility   |
|-----------------------------------|--|---|---|
| Right parasternal sagittal view   | <ul style="list-style-type: none"> <li>• Patient position: right lateral decubitus (on right side) with right arm up</li> <li>• Probe indicator direction: 12 o'clock</li> <li>• Probe position: right side of sternum</li> </ul>              |  <p>Reference image: bicaval view with SVC and IVC draining into RA</p> | <ul style="list-style-type: none"> <li>• Evaluate SVC and IVC flow into RA by color mapping</li> <li>• Evaluate atrial septum</li> <li>• Exclude superior sinus venosus defect</li> <li>• Evaluate right pulmonary veins entering the left atrium</li> <li>• Evaluate AoV flow if subvalvar, valvar, or supra-valvar aortic stenosis present</li> </ul> |
| Right parasternal transverse view | <ul style="list-style-type: none"> <li>• Patient position: right lateral decubitus (on right side) with right arm up</li> <li>• Probe indicator direction: 3 o'clock</li> <li>• Probe position: right side of sternum high on chest</li> </ul> |   | <ul style="list-style-type: none"> <li>• Evaluate RUPV flow into LA by imaging and color mapping</li> </ul>   |

AAo, Ascending aorta; DAo, descending aorta; LAD, left anterior descending CA; LIV, left innominate vein; LMCA, left main CA; LPA, left PA; MPA, main PA; RCA, right CA; RPA, right PA; RUPV, right upper pulmonary vein.

\*Probe indicator direction oriented with the clock face on patient chest so that 12 o'clock points to patient head, 3 o'clock to patient left, 6 o'clock to patient feet, and 9 o'clock to patient right.

Once the 3DE data set is acquired, it can be reconstructed as a volume, surface, or series of tomographic slices (multiplane 2DE image display; Figure 16). Quantification of ventricular volumes and function, valvar shape and function,<sup>33</sup> and short-axis aortic root dimensions can then be performed on the 3DE data set. Three-dimensional echocardiography is now available on most ultrasound platforms, with smaller high-frequency pediatric 3DE probes and more automated display options, allowing increased and more routine use in children. Protocols should be established, including sufficient training of staff in image acquisition and postprocessing, identification of clinical scenarios when 3DE should be used, and establishing a robust quality assurance (QA) process. Designating specific members of an echocardiography laboratory to be the 3DE experts or champions can help maximize its acceptance and use, especially in the setting of complex CHD. Future directions in 3DE involve advances in sampling speed, image gating, frame reordering,<sup>34</sup> strain evaluation, and segmentation algorithms for fully or semiautomated assessment of ventricular function.

### Key Points and Recommendations.

- Three-dimensional echocardiography is useful in the evaluation of the atrial and ventricular septum, ventricular outflow tracts, AV and semilunar valves, and ventricles.
- Three-dimensional echocardiography should be considered when evaluating septal defects, outflow tract abnormalities, valvar morphology and function, and ventricular volumes.

### Strain Imaging

Strain, also known as deformation, is defined for the myocardium as the percentage change in muscle length relative to its baseline length

in one direction. It can be measured by tracking speckles (natural acoustic markers) on a 2DE image using STE. In patients with CHD and abnormal ventricular geometry, STE provides reliable quantification of myocardial function as a complement to traditional geometric parameters such as LV shortening fraction (SF) or ejection fraction (EF). While peak global longitudinal strain (GLS) is now part of the routine clinical work flow for adult patients,<sup>35</sup> the use of STE in pediatrics has been variable, even with growing evidence for its value and reliability. For example, in children who have received chemotherapy, LV GLS has identified subtle LV dysfunction earlier than traditional measures.<sup>36</sup> In patients with repaired tetralogy of Fallot, RV GLS can identify clinically significant dyssynchrony<sup>37</sup> and appropriate timing for pulmonary valve (PV) replacement.<sup>38</sup> In patients with a single ventricle, STE can evaluate function across variable morphologies by tracking myocardial motion without geometric assumptions, identify electromechanical dyssynchrony, allow serial monitoring of progressive dysfunction, and predict outcomes.<sup>39,40</sup>

STE is most reliable when the 2DE image is optimized in terms of frame rate and tissue characterization.<sup>35</sup> Because of faster heart rates in children, strain analysis requires higher frame rates for adequate sampling.<sup>41</sup> Strain can be measured as shortening (negative values) in the longitudinal and circumferential direction and as thickening (positive values) in the radial direction (Figure 17), and GLS appears to have the most clinical value.<sup>35</sup> Reproducibility of strain values is acceptable when measured on the same ultrasound platform but is poor when measured on different platforms, even with joint standardization efforts by the ASE, European Association of Cardiovascular Imaging, and industry representatives.<sup>42,43</sup> Reproducibility for LV global circumferential strain is not as good as LV GLS but remains adequate for clinical use.<sup>43</sup> Radial strain is not routinely used because of poor reproducibility. Strain rate peaks in early systole, and compared with strain, it provides a

**Table 10** Elements of an initial comprehensive transthoracic echocardiogram (adapted from ACPC Quality Network echology metrics)<sup>13</sup>

| Segment             | TTE elements  |
|---------------------|---|
| Situs, veins, atria | <ul style="list-style-type: none"> <li>• Liver and stomach (2D)</li> <li>• Cardiac position (2D)</li> <li>• IVC, DAo, spine (2D)</li> <li>• IVC to RA (2D + color)</li> <li>• SVC to RA (2D + color)</li> <li>• Two right and two left pulmonary veins to LA (2D + color)</li> <li>• Coronary sinus (2D + color)</li> <li>• RA size (qualitative)</li> <li>• LA size (qualitative)</li> <li>• Atrial septum (2D + color)</li> </ul> |
| AV valves           | <ul style="list-style-type: none"> <li>• TV (2D + color + PW + CW)</li> <li>• Tricuspid regurgitation (CW)</li> <li>• MV (2D + color + PW + CW)</li> <li>• MV short-axis (2D + color)</li> </ul>  |
| Ventricles          | <ul style="list-style-type: none"> <li>• Ventricular septum (2D + color)</li> <li>• RV size and function (qualitative)</li> <li>• LV size and function (qualitative + quantitative)</li> <li>• LV mass or LV end-diastolic septal and posterior wall thickness</li> <li>• RV outflow tract (2D + color + PW + CW)</li> <li>• LV outflow tract (2D + color + PW + CW)</li> </ul>   |
| Semilunar valves    | <ul style="list-style-type: none"> <li>• PV (2D + color + PW + CW)</li> <li>• AoV (2D + color + PW + CW)</li> </ul>   |
| Vessels             | <ul style="list-style-type: none"> <li>• Branch PAs (2D + color + PW + CW)</li> <li>• Patent ductus arteriosus if present (2D + color + PW + CW)</li> <li>• CAs (2D + color)</li> <li>• AAo (2D + color + PW + CW)</li> <li>• Aortic arch sidedness and branching pattern (2D + color)</li> <li>• Aortic arch (2D + color + PW + CW)</li> <li>• Abdominal aorta (color + PW)</li> </ul>   |
| Pericardium         | <ul style="list-style-type: none"> <li>• Pericardial effusion if present (2D)</li> </ul>  |

AAo, Ascending aorta.

less load-dependent parameter that correlates better with contractility. However, it requires high frame rates, and its inherent noise and poor reproducibility limit routine clinical use in children. STE can evaluate regional mechanics through quantitative and qualitative assessment of regional strain curves, but reproducibility of this approach is poor.<sup>44</sup> Pattern analysis of segmental strain curves can distinguish electromechanical dyssynchrony from nonspecific discoordination (or mechanical dispersion), helping identify potential candidates for cardiac resynchronization therapy (Figure 18).<sup>45,46</sup>

The determination of normal STE reference values for children has been limited by variable techniques and segmentation methodologies from multiple ultrasound platforms.<sup>47,48</sup> In general, the lower limit of normal for LV endocardial GLS ranges from  $-17\%$  to  $-18\%$ .<sup>47,49</sup> Beyond the newborn period, pediatric strain values decrease mildly with age, although the variability in normal values tends to be more pronounced than age-related changes, presumably because of differences in measurement techniques, vendor-specific ultrasound systems, and software versions.<sup>49,50</sup> For example, various ultrasound

platforms evaluate strain at different layers of the myocardium, often yielding different strain values for the same ventricular segment. In addition, including the pericardium in the region of interest can spuriously reduce myocardial strain values.

Other STE parameters have been used in children, although their clinical value is still limited at this time. LA strain and other measures of LA function may help assess pediatric LV diastolic function and risk for various acquired and CHD.<sup>51,52</sup> Myocardial work, defined as the product of arterial pressure and myocardial strain, may provide a novel and more sensitive index of myocardial function independent of loading conditions in specific situations.<sup>53,54</sup> Three-dimensional strain analysis to measure longitudinal, circumferential, and area strain as well as measures of rotational mechanics may provide valuable information about ventricular mechanics in some pediatric populations.<sup>55,56</sup> Finally, artificial intelligence algorithms to automatically identify standard apical views, segment cardiac chambers, and perform strain analysis have been studied in adults and may facilitate increased use of STE because it is faster and less operator dependent.<sup>57</sup> However, this has not yet been adequately evaluated in children.

## Key Points and Recommendations

- STE has become standard practice in many pediatric TTE laboratories.
- Measurement of LV GLS may be incorporated into LV functional protocols.
- RV and single ventricular GLS, LV circumferential strain, and regional strain pattern analysis may be useful in targeted populations.
- Optimal STE requires high frame rates, and serial evaluations should use a single ultrasound platform.

## SEGMENTAL PROTOCOLS

### Systemic and Pulmonary Veins

Anomalies of the systemic and pulmonary veins usually involve abnormal drainage or obstruction and can present as an isolated finding or in combination with other CHD. TTE is the primary imaging modality to evaluate venous connections and size and possible obstruction. Obstruction should be suspected when turbulence is seen with color mapping, and spectral Doppler interrogation will reveal loss of the usual phasic variation with higher velocity flow (Figure 19). Doppler interrogation of systemic and pulmonary veins can also aid in evaluation of ventricular systolic and diastolic function as discussed below. Occasionally, transesophageal echocardiography, cardiac computed tomography, cardiac MRI, and/or angiography is needed for diagnostic confirmation of abnormal anatomy.

SVC, IVC, hepatic venous, and coronary sinus connections to the right atrium should be evaluated with sweeps in subcostal coronal and sagittal views as well as parasternal and modified apical views with posterior tilting.<sup>1</sup> These views can often identify a persistent left SVC connected to a dilated coronary sinus or LA (Figure 20). Interruption of the intrahepatic IVC should be suspected if (1) the IVC is not seen within the liver in the subcostal coronal view and (2) subcostal sagittal sweeps with color mapping reveal the azygos vein as a prominent vertical venous structure behind the descending aorta with flow directed superiorly. A prominent hepatic vein should not be confused with the IVC in this setting. A suprasternal short-axis view should show normal drainage of the left innominate vein into the right SVC (Figure 14A) and identify a retroaortic left innominate

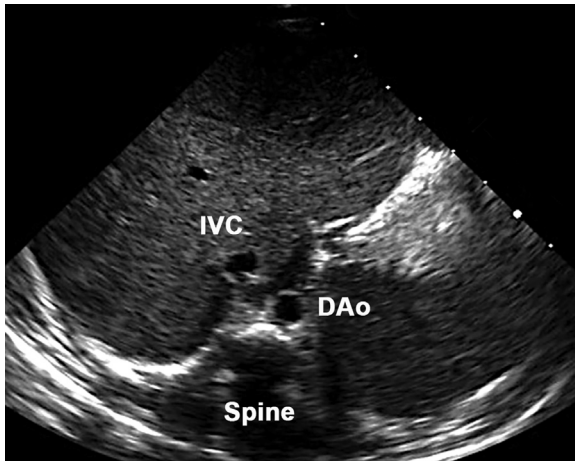


**Figure 1** Subcostal coronal situs view: reference image showing the relative locations of the spine, inferior vena cava (IVC), and descending aorta (DAo) at the level of the diaphragm.

vein, left SVC, or a connecting vein between bilateral SVCs. Right parasternal sagittal views also provide information about the SVC and IVC, especially in older children and adults (Figure 11A), and particularly if there is an overriding SVC in the setting of a sinus venosus defect (Figure 11B). Although adult TTE protocols usually include IVC diameter measurements during the respiratory cycle,<sup>29</sup> systemic venous sizes are not routinely measured in pediatrics, because there are no studies showing good correlation between IVC size and RA pressure in children. Like color mapping and Doppler interrogation, agitated saline contrast can provide information about anomalous systemic venous connections or obstruction.

Pulmonary venous return should be evaluated in high left parasternal or suprasternal short-axis “crab” views (Figure 15).<sup>1</sup> These views may reveal the right lower and right middle pulmonary veins connected to the left atrium, but they may not exclude anomalous drainage of the right upper pulmonary vein into the SVC. Subcostal sagittal and right parasternal views are best at showing the right upper pulmonary vein coursing inferior to the right PA and posterior to the right SVC before draining into the LA (Figure 5). Apical views have also been used to evaluate pulmonary venous return to the left atrium, although this view may not be able to distinguish the upper

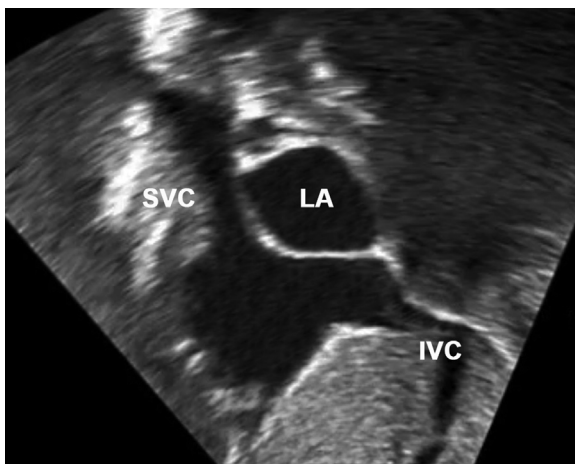


**Figure 2** Subcostal sagittal (short-axis) bicaval view: reference image showing the superior vena cava (SVC) and intrahepatic inferior vena cava (IVC) connecting to the right atrium as well as the atrial septum between the right atrium and left atrium (LA).

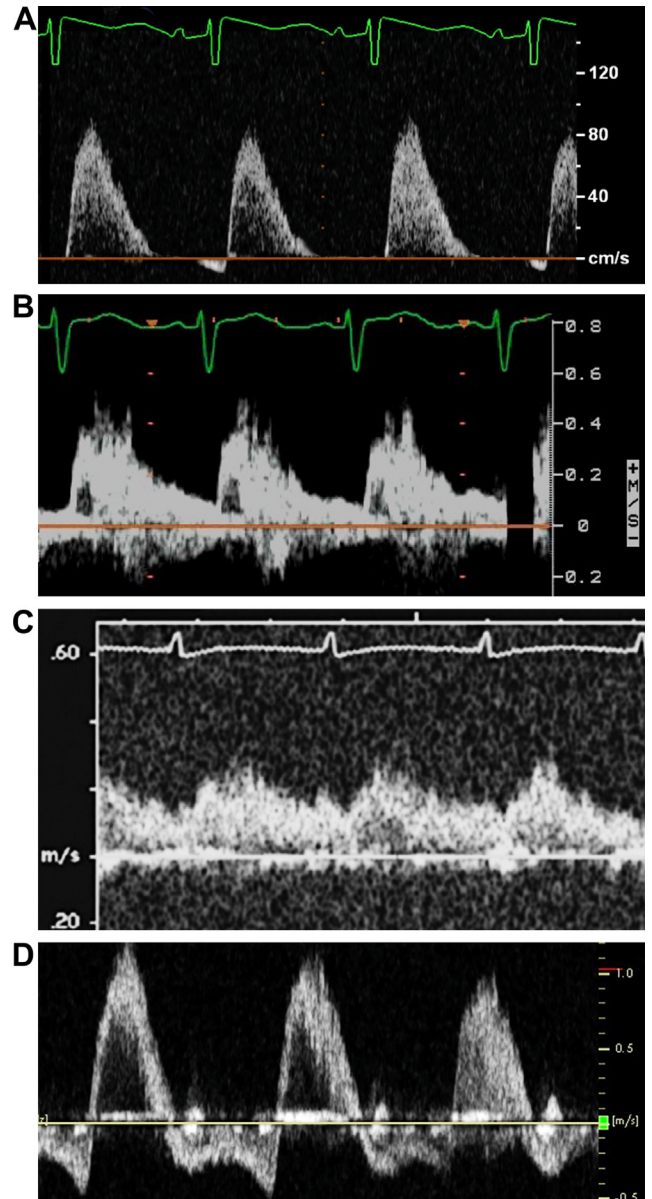


**Figure 3** Abdominal aortic Doppler flow patterns from the subcostal sagittal view: (A) normal pulsatile flow pattern with brisk upstroke and return to baseline; (B) diastolic delay in return to baseline suggestive of aortic arch obstruction; (C) blunted flow pattern and no return to baseline consistent with significant aortic arch obstruction; and (D) holodiastolic flow reversal as seen with at least moderate aortic regurgitation, a significant patent ductus arteriosus, aortopulmonary collateral artery, arteriovenous malformation, shock, or moderate sedation.

from the lower pulmonary vein on both sides. Careful sweeps with color mapping in subcostal, parasternal, and suprasternal views are needed to exclude anomalous pulmonary venous connections. Total anomalous pulmonary venous return should be suspected in newborns with cyanosis when subcostal imaging reveals right-to-left shunting across a patent foramen ovale throughout the cardiac cycle in association with a small LA. Partial anomalous pulmonary venous return may or may not be associated with RV dilation; typical locations for anomalous connections include the right SVC for the right upper pulmonary vein, the IVC for the right lower pulmonary vein

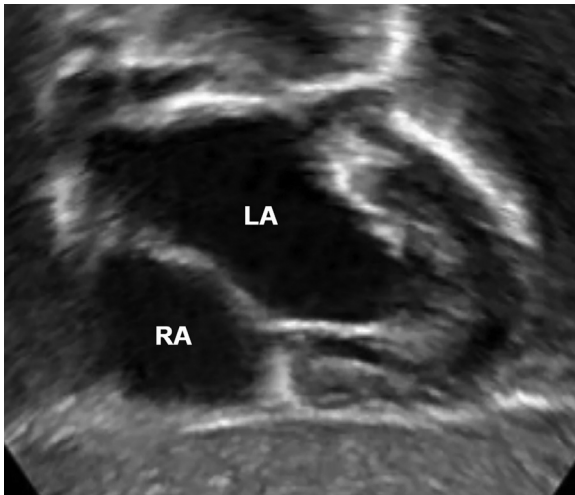


**Figure 4** Subcostal coronal (long-axis) view: optimal visualization of the atrial septum because it is perpendicular to the direction of the ultrasound beam in this view. *LA*, Left atrium; *RA*, right atrium.

(as seen with scimitar syndrome), the left innominate vein for the left upper pulmonary vein, and the coronary sinus for the left lower pulmonary vein.

### Key Points and Recommendations

- Evaluation of the systemic and pulmonary veins by 2DE, color mapping, and spectral Doppler interrogation should be performed for all initial pediatric TTE.

### Atria and Atrial Septum

Standard protocols should include evaluation of atrial size and morphology as well as atrial connections to the systemic and pulmonary veins and to the AV valves. The appearance and location of the atrial appendages should be evaluated when possible, making sure to distinguish the LA appendage with its to-and-fro flow from the left upper pulmonary vein with antegrade flow into the left atrium. Atrial size is best assessed in apical four-chamber or subcostal coronal views, although subcostal sagittal and parasternal views can also be helpful. Atrial dilation usually results from associated AV valve stenosis or regurgitation, ventricular volume overload or hypertrophy, or

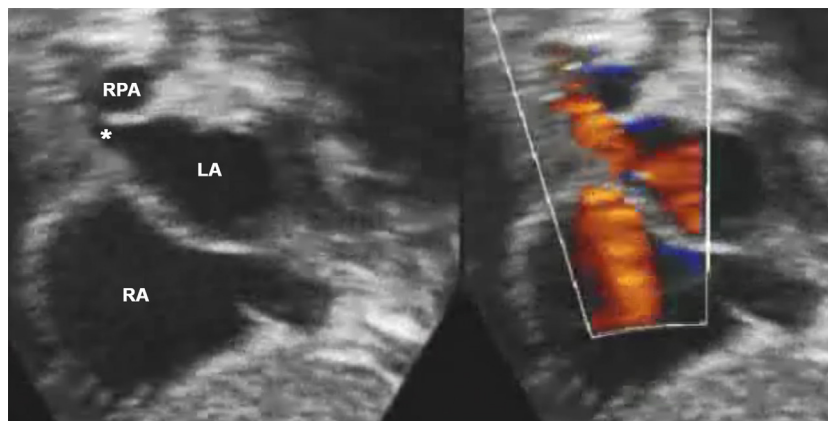


**Figure 5** Subcostal sagittal (short-axis) view: right upper pulmonary vein (*asterisk*) coursing inferior to the right pulmonary artery (RPA) and posterior to the superior vena cava before draining into the left atrium (LA). *RA*, Right atrium.

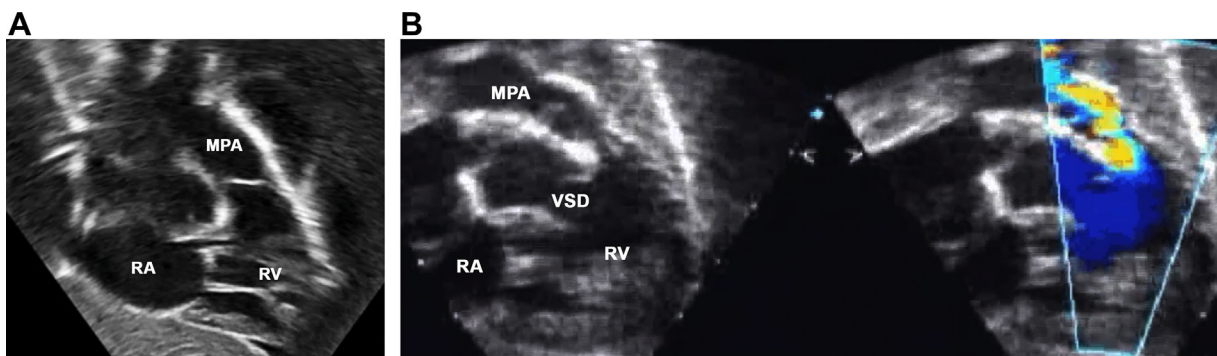


**Figure 6** Subcostal right anterior oblique view with counterclockwise rotation of the transducer from the subcostal coronal view for simultaneous visualization of the right ventricular (RV) inflow and outflow tracts: **(A)** normal heart with an unobstructed RV outflow tract and **(B)** tetralogy of Fallot with anterior deviation of the conal septum resulting in a ventricular septal defect (VSD) and narrow RV outflow tract; color mapping reveals an unrestrictive VSD and subvalvar pulmonary stenosis with turbulent flow along the narrow RV outflow tract. *MPA*, Main pulmonary artery; *RA*, right atrium.

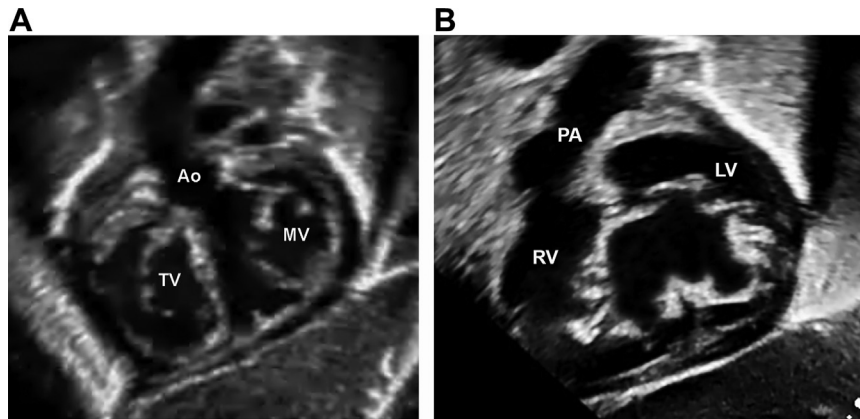


**Figure 7** Subcostal left anterior oblique view with clockwise rotation of the transducer from the subcostal coronal view for en face visualization of the atrioventricular (AV) junction: **(A)** normal heart with separate tricuspid valve (TV) and mitral valve (MV) orifices and an unobstructed left ventricular (LV) outflow tract and **(B)** AV septal defect with an en face view of the common AV valve and an unobstructed right ventricular (RV) outflow tract. Ao, Aorta; PA, pulmonary artery.

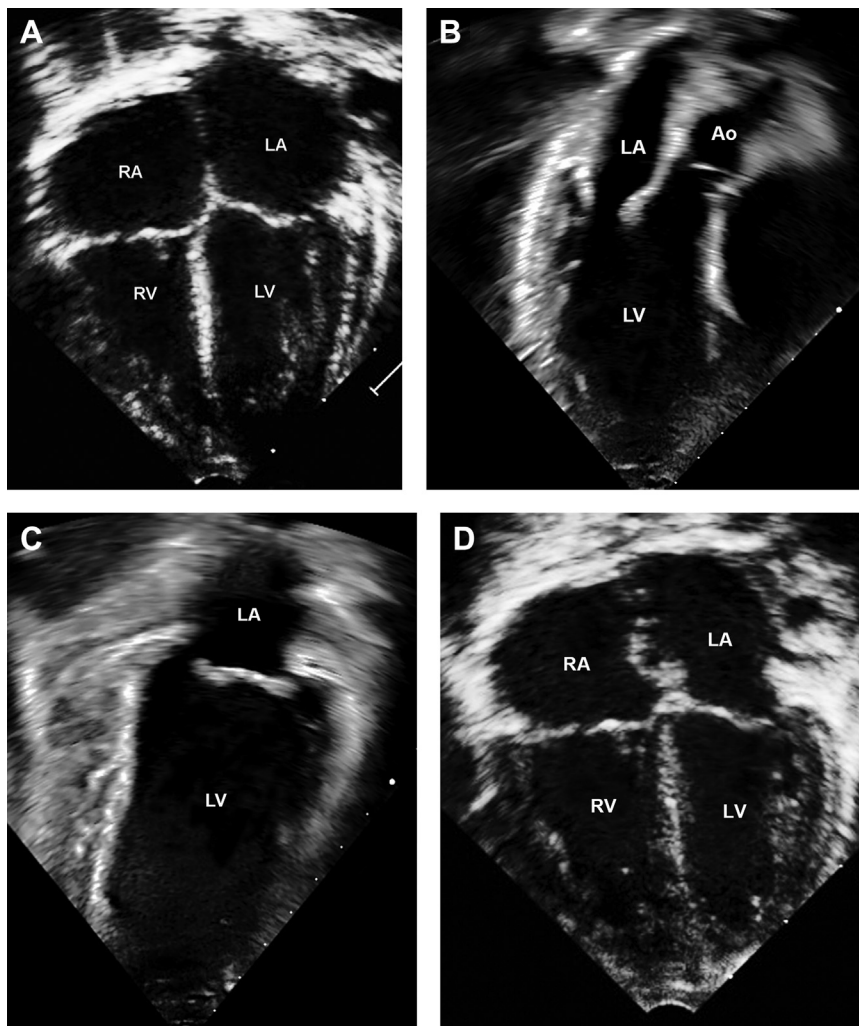


**Figure 8** Apical views: **(A)** apical four-chamber view, **(B)** apical three-chamber view, **(C)** apical two-chamber view, and **(D)** right ventricular (RV)-focused apical four-chamber view with movement of the probe more medially from the standard apical four-chamber view. Reproduced with permission from Lopez *et al.*<sup>2</sup> Ao, Aorta; LA, left atrium; LV, left ventricle; RA, right atrium.

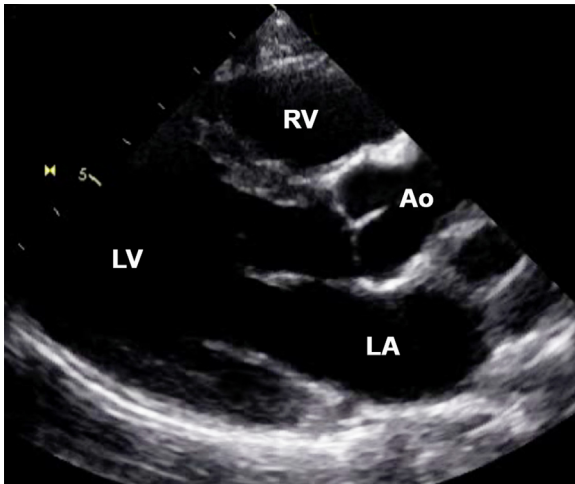


**Figure 9** Parasternal long-axis view: reference image showing the left atrium (LA), left ventricle (LV), proximal aorta (Ao), and right ventricle (RV) as well as the fibrous continuity between the MV and AoV.

ventricular diastolic dysfunction, so these should be excluded when atrial dilation is present.

Quantification of RA size is not standard in pediatric TTE, although the 2010 guidelines suggested the use of major- and minor-axis lengths from apical four-chamber views.<sup>2</sup> Normal values for RA areas have been published.<sup>58</sup> For the LA, some centers use the anteroposterior LA diameter-to-aortic root diameter ratio obtained by M-mode or 2DE to assess the hemodynamic significance of a patent ductus arteriosus in premature infants, although this ratio correlates poorly with LA volumes and is not included in the 2011 ASE guidelines for targeted neonatal TTE.<sup>59</sup> Calculating LA volumes from LA areas or area and length measurements obtained in apical four-chamber and two-chamber views at end-systole just before left AV valve opening has become standard practice in many centers (Figure 21), providing useful information about diastolic function and ventricular filling pressures.<sup>2</sup> A >5-mm difference in LA lengths measured in four-chamber and two-chamber views invalidates the LA volume calculation.<sup>29</sup> Normal 2DE reference values for LA volumes in children have been published.<sup>60</sup> LA strain as a measure of LA function may be used to evaluate LV diastolic function,<sup>51,52</sup> and

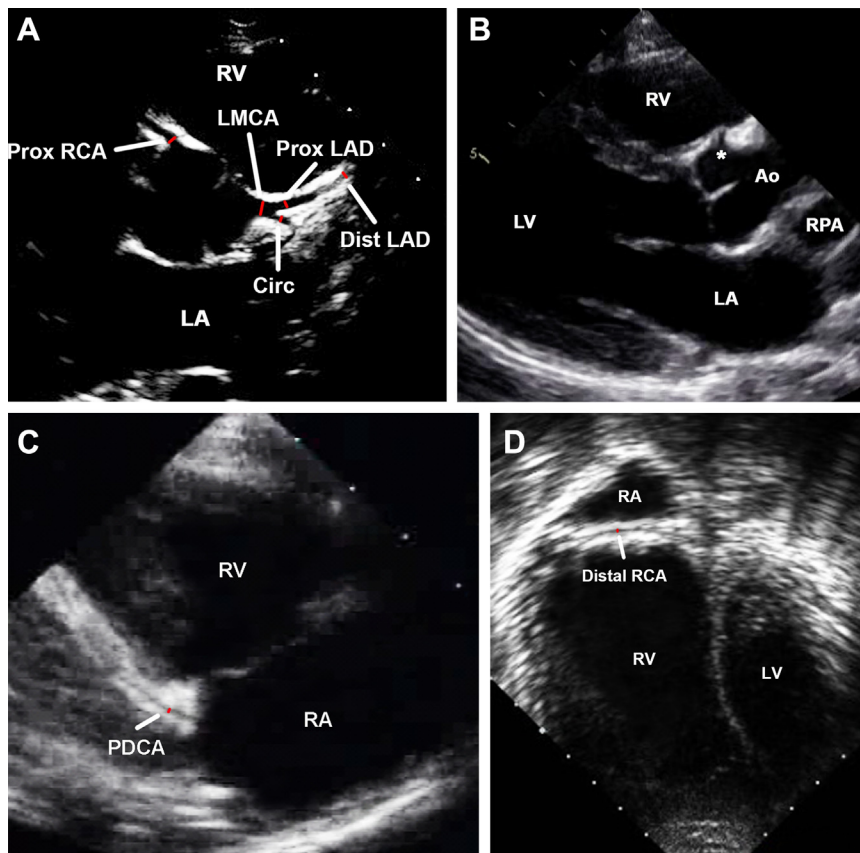


**Figure 10** Views to evaluate the coronary artery (CA): **(A)** parasternal short-axis view showing the left main CA (LMCA) and proximal right CA (Prox RCA) originating from the aortic root with the LMCA supplying the left anterior descending CA (LAD), with proximal (Prox LAD) and distal (Dist LAD) regions shown, as well as the circumflex CA (Circ); **(B)** parasternal long-axis view showing the origin of the right CA (*asterisk*) from the anterior aspect of the aortic root; **(C)** modified parasternal long-axis view with rightward and posterior-inferior tilting of the transducer showing the posterior descending CA (PDCA) coursing along the posterior interventricular groove; and **(D)** modified apical four-chamber view with posterior tilting showing the distal RCA coursing along the right-sided posterior AV groove. Reproduced with permission from Lopez *et al.*<sup>2</sup> Ao, Aorta; LA, left atrium; LV, left ventricle; RA, right atrium; RPA, right PA; RV, right ventricle.

**Table 11** Protocol for patients with dextrocardia

| View                                 | Transducer indicator direction |
|--------------------------------------|--------------------------------|
| Subcostal coronal (long-axis) view   | Patient's left side            |
| Subcostal sagittal (short-axis) view | Patient's lower extremity      |
| Apical view                          | Patient's left side            |
| Parasternal long-axis view           | Patient's left shoulder        |
| Parasternal short-axis view          | Patient's left hip             |
| Suprasternal long-axis view          | Patient's head                 |
| Suprasternal short-axis view         | Patient's left side            |

3DE has been used to measure LA volumes and strain in healthy children with normal reference values.<sup>61</sup>

The atrial septum should be evaluated in all initial pediatric TTE studies.<sup>28</sup> A secundum atrial septal defect or sinus venosus defect should be suspected when RA or RV dilation is seen. Subcostal and right parasternal views provide the best evaluation of the atrial septum because it is perpendicular to the ultrasound beam in these views (Figures 4 and 11). Color mapping can

confirm interatrial shunting across a patent foramen ovale or atrial septal defect, and PW Doppler interrogation can characterize the direction of flow throughout the cardiac cycle. The size of a secundum atrial septal defect should be measured in orthogonal planes along with the sizes of the rims at the superior, inferior, anterior, and posterior margins of the defect to determine if device closure is feasible. Three-dimensional echocardiography can be helpful in characterizing the shape and size of a defect, and evaluation of the spatial relationship of a defect with the systemic and pulmonary veins and with the AV valves can help with planning optimal treatment strategies.

### Key Points and Recommendations

- The atrial septum should be evaluated in subcostal or right parasternal views.
- When possible, LA volumes should be measured, particularly when there is MV dysfunction, LV volume overload or hypertrophy, or suspected LV diastolic dysfunction.

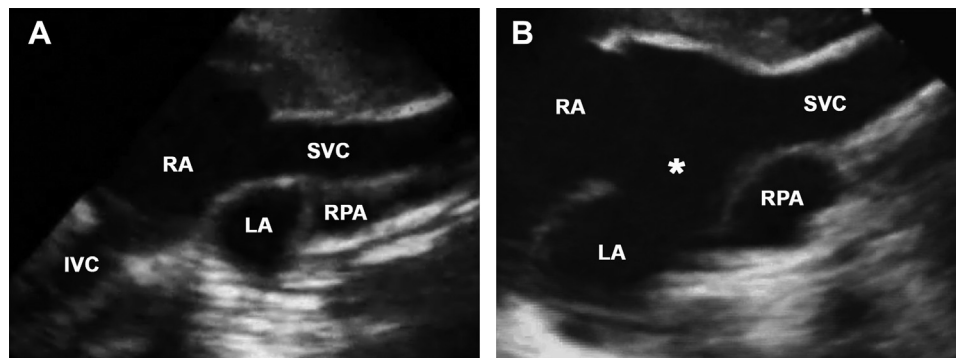


**Figure 11** Right parasternal long-axis view: **(A)** bicaval reference view showing connection of the superior vena cava (SVC) and inferior vena cava (IVC) to the right atrium (RA) with a nearly perpendicular orientation of the atrial septum relative to the ultrasound beam and **(B)** magnified image of a superior sinus venosus defect (asterisk) with relationship of the SVC to both the RA and left atrium (LA). RPA, Right pulmonary artery.

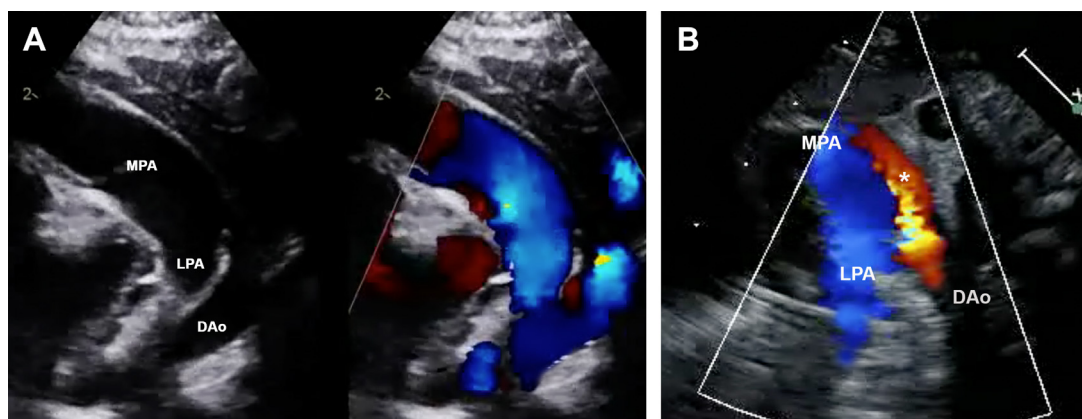


**Figure 12** High left parasternal sagittal (ductal) view: **(A)** normal heart with no ductal connection between the distal main pulmonary artery (MPA) and the proximal descending aorta (DAo) and **(B)** image with color mapping showing a small patent ductus arteriosus (asterisk) with flow from the proximal DAo to the distal MPA. LPA, Left PA.

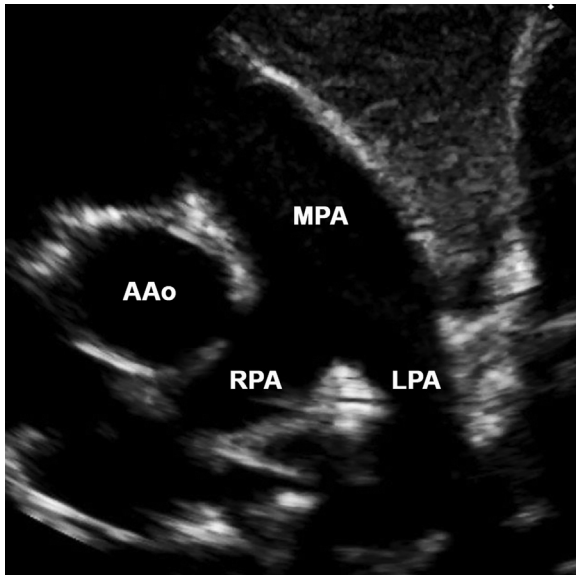


**Figure 13** High left parasternal transverse view: main pulmonary artery (MPA) bifurcating into the proximal right pulmonary artery (RPA) and left pulmonary artery (LPA). AAo, Ascending aorta.

### AV Valves

The AV valve apparatus includes the annulus, leaflets, papillary muscles, and chordae tendineae, all of which should be characterized during TTE.<sup>1</sup> There is more variability among the components of the tricuspid valve (TV) than the MV.<sup>62</sup> Morphologic abnormalities can occur at the valvar and subvalvar level (Table 14). Morphometric assessment of transverse annular diameters has been described previously,<sup>2</sup> and standard practice involves measurements in diastole at the frame after maximum leaflet excursion, from inner edge to inner edge at the hinge points of the leaflet attachments in apical and parasternal views (Figure 22). AV valve area is not routinely measured in children because of the paucity of normal data and validation of its value.<sup>63</sup> The subcostal left ante-

rior oblique view is frequently used in patients with a complete AV septal defect for an en face evaluation of the common AV valve and its relationship with the ventricular septum to determine the degree of balance (Figure 7).<sup>64</sup>

When there is AV valve stenosis, CW Doppler interrogation should measure the velocity time integral to calculate the mean pressure gradient across the valve. Other methods from the adult guidelines include pressure half-time and effective orifice area, although these have limited use in children.<sup>2</sup> Faster heart rates in children decrease the diastolic filling time and can increase the mean gradient across stenotic valves, necessitating the documentation of heart rates.<sup>63</sup> Other potential confounders when assessing AV valve stenosis include suboptimal angle of interrogation, AV valve regurgitation, CHD with increased flow across the AV valve (ventricular septal defect or patent ductus arteriosus for the MV and atrial septal defect for the TV), and potential atrial decompression or “pop-off” via an atrial septal defect. RV and PA systolic pressures should be assessed when there is MV stenosis. Recommendations from adult guidelines for quantitative and semi-quantitative evaluation of AV valve regurgitation include effective regurgitant area, vena contracta, and regurgitant fraction and volume. The presence of multiple regurgitant jets, inconsistent definitions of severity, and poor reproducibility<sup>65</sup> have limited their use in children. Instead, most pediatric centers assess AV valve regurgitation severity by (1) using color mapping for a qualitative assessment of the regurgitant jet(s), (2) quantifying associated atrial and/or ventricular dilation if present, and (3) evaluating for systolic flow reversal in the systemic or pulmonary veins.<sup>63</sup>

Various studies showing the value of 3DE in characterizing AV valve morphology and function have been published.<sup>66,67</sup> The 2017 3DE in CHD guidelines highlight the ability of 3DE to assess leaflet morphology, chordal support, and number and location of regurgitant jets by providing multiple views of the AV valves, including en face views from the atrial or ventricular aspect (Figure 23).<sup>6</sup> In addition, the document outlines the best views to use during the 3DE evaluation of specific AV valvar abnormalities such as Ebstein anomaly of the TV, MV prolapse, parachute MV, double-orifice MV, and AV septal defect. The use of 3DE to quantify AV valve regurgitation has not yet been validated in children.

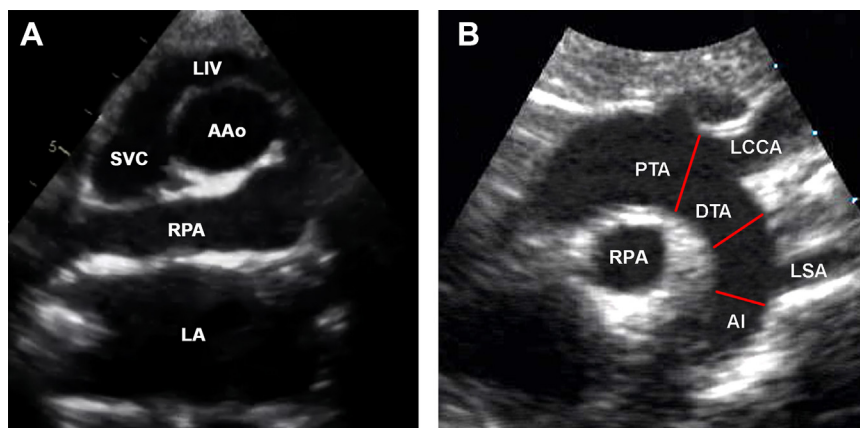


**Figure 14** Suprasternal views: (A) short-axis reference image showing the ascending aorta (AAo) in cross-section with right pulmonary artery (RPA) coursing posteriorly and the left innominate vein (LIV) coursing anteriorly before draining into the superior vena cava (SVC) and (B) long-axis reference image showing diameter measurement locations for the proximal transverse aortic arch (PTA), distal transverse aortic arch (DTA), and aortic isthmus (AI). Reproduced with permission from Lopez *et al.*<sup>2</sup> LA, Left atrium; LCCA, left common carotid artery; LSA, left subclavian artery.

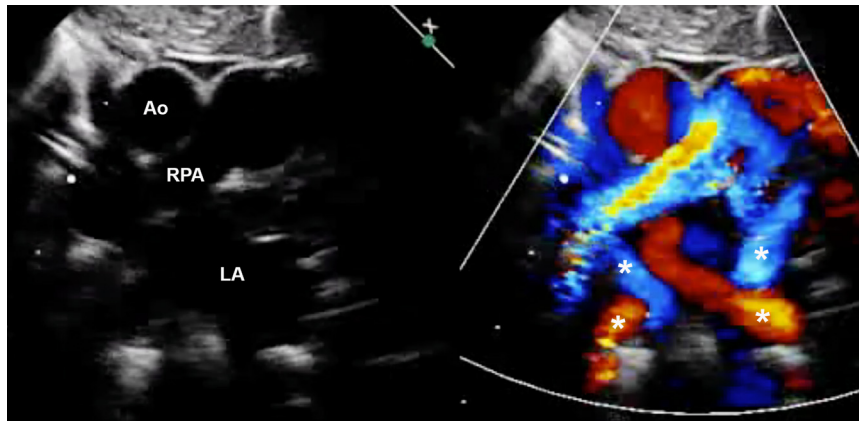


**Figure 15** Suprasternal short-axis (“crab”) view: inferior angulation with color-compare showing four pulmonary veins (asterisk) draining into the left atrium (LA). Ao, Aorta; RPA, right pulmonary artery.

## Key Points and Recommendations

- AV valve morphology and function should be evaluated in multiple views.
- Assessment of AV valve stenosis may not be accurate in children with faster heart rates or intracardiac shunts.
- Quantitative Doppler assessment of the severity of AV valve stenosis should be performed, recognizing the limitations in children.
- Quantitative assessment of the severity of AV valve regurgitation is limited in children, so qualitative assessment or other indirect surrogates of severity should be used.
- Three-dimensional echocardiography may be useful in the evaluation of AV valve morphology in targeted populations.

## Right Ventricle

The right ventricle is difficult to evaluate by TTE because of its complex geometry, trabeculations, and retrosternal position. Understanding RV anatomy requires sweeps in subcostal, apical, and parasternal views. Nonstandard views that focus on the right ventricle include modified apical four-chamber and three-chamber RV views located more medially on the chest (Figure 8D) and the subcostal right anterior oblique view (Figure 6A).<sup>68</sup> Abnormal RV geometry in various CHDs can affect RV pump function.<sup>69</sup> Multiple measurements have been used to assess RV size and function, all with significant limitations and suboptimal intraobserver and interobserver reliability. Consequently, comprehensive evaluation should (1) include a subjective assessment to provide context for the interpretation, (2) not be limited to a single parameter, and (3) account for the full range of abnormal loading conditions that contribute to measurement variability (Table 15).

**Measures of RV Size.** RV size can help predict outcomes, including the need for interventions like PV replacement in patients with pulmonary regurgitation and associated RV volume overload.<sup>70</sup> Compared with RV volumes derived from cardiac MRI, 2DE linear RV measurements exhibit weak correlation, 2DE areas exhibit moderate correlation, and 3DE volumes exhibit good correlation.<sup>71</sup> RV areas and volumes should be measured during both diastole and systole: end-diastole occurs when the TV closes and end-systole occurs at the frame just before the TV opens. Linear measurements (RV basal and midcavity

minor-axis diameters and RV major-axis length) are generally performed in apical four-chamber views at end-diastole, taking care not to foreshorten the right ventricle (Figures 24A and B).<sup>2</sup> The RV apical minor-axis diameter can be helpful because apical remodeling correlates with RV dysfunction and with clinical outcomes in several clinical scenarios (Figure 24A).<sup>72,73</sup> RV areas should also be obtained in apical four-chamber views (Figure 24C).<sup>2</sup> Although RV linear and area measurements are suboptimal estimates of RV volumes, they may be useful for serial evaluations of RV size and may help signal the need for cardiac MRI.<sup>74</sup> Multiple 3DE methods to measure RV volumes have been used, and fully automated methods are now available. Nevertheless, RV evaluation by 3DE is still not routinely done in children, mostly because (1) 3DE-derived volumes tend to underestimate MRI-derived volumes,<sup>75</sup> (2) there is a paucity of normal pediatric reference values, (3) application of 3DE RV algorithms have not yet been fully validated for the abnormally shaped RV in CHD, and (4) incorporating 3DE into clinical work flow can be challenging.<sup>6</sup>

## Two-Dimensional Echocardiographic and 3DE Measures of RV Systolic Function.

Because of the complex 3D shape of the right ventricle, 2DE measures of RV function that use apical four-chamber views, namely, tricuspid annular plane systolic excursion (TAPSE) and fractional area change (FAC), do not account for the RV outflow tract contribution to performance.<sup>76</sup> TAPSE involves M-mode evaluation of systolic longitudinal displacement of the lateral tricuspid annulus in the apical four-chamber view to quantify RV longitudinal systolic function. Color M-mode improves measurement reliability by precisely defining peak displacement (Figure 25). Normal reference values and Z scores have been published.<sup>77</sup> TAPSE correlates well with RV function and abnormal loading conditions, although it is more useful with RV pressure overload than RV volume overload, which can cause passive rocking of the TV annulus.<sup>78</sup> In children with pulmonary hypertension, TAPSE correlates well with RV work, reflects adequacy of RV adaptation to pressure overload,<sup>79</sup> and predicts adverse outcomes.<sup>80</sup> TAPSE does have several limitations: (1) it does not reflect apical function, which may be reduced when basal function is normal; (2) it does not measure the RV radial or circumferential systolic function, which in some scenarios may increase as longitudinal function decreases; (3) it does not always correlate with tissue Doppler velocities because of sampling variability, translational motion, segment-to-segment interactions, and regional differences in RV longitudinal and radial function at the base; and (4) it does not account for the RV outflow tract.

**Table 12** Comparison of commonly used Z score models<sup>19</sup>

| Z score model                 | PHN <sup>20</sup>  | Boston <sup>21</sup>  | Italy <sup>22</sup>   | Detroit <sup>23</sup>  |
|-------------------------------|--|---|---|--|
| Reference                     | Lopez <i>et al.</i> (2017) <sup>20</sup>   | Boston Z scores*  | Cantinotti <i>et al.</i> (2017) <sup>22</sup>   | Pettersen <i>et al.</i> (2008) <sup>23</sup>   |
| Model regression <sup>†</sup> | $y = m \times BSA^\alpha$  | $y = m \times BSA^\alpha$ ( $y = \beta + m \times BSA^\alpha$ for the CHAs)   | $\ln(y) = \beta + [m \times \ln(BSA)]$  | $\ln(y) = \beta + (m_1 \times BSA) + (m_2 \times BSA^2) + (m_3 \times BSA^3)$  |
| Data source                   | 19 centers   | 1 center  | 1 center  | 1 center   |
| Sample size                   | 3,215  | >2,000  | 1,151   | 782  |
| Study population              | <ol style="list-style-type: none"> <li>1. Weight-for-length Z &lt; 2 if &lt;2 y old</li> <li>2. BMI &lt; 95th percentile if ≥2 y old</li> <li>3. Gestational age ≥ 37 wk</li> <li>4. No structural or CHD</li> <li>5. No systemic disorder with cardiovascular manifestations</li> <li>6. No family history of left heart disease or cardiomyopathy</li> </ol> | <ol style="list-style-type: none"> <li>1. Weight &gt; 2.5 kg</li> <li>2. BSA &gt; 0.18 m<sup>2</sup></li> <li>3. -2 &gt; BMI Z &gt; 2</li> <li>4. No premature babies</li> <li>5. No structural or CHD</li> <li>6. No systemic disorder with cardiovascular manifestations</li> <li>7. No family history of left heart disease or cardiomyopathy</li> </ol> | <ol style="list-style-type: none"> <li>1. Weight-for-length Z &lt; 2 if &lt;2 y old</li> <li>2. BMI &lt; 95th percentile if ≥2 y old</li> <li>3. Premature babies included</li> <li>4. No structural or CHD</li> <li>5. No systemic disorder with cardiovascular manifestations</li> <li>6. No family history of genetic cardiac disease</li> </ol> | <ol style="list-style-type: none"> <li>1. No obese subjects</li> <li>2. BSA &lt; 2 m<sup>2</sup></li> <li>3. No reference to gestational age or BMI</li> <li>4. No structural or CHD</li> <li>5. No systemic disorder with cardiovascular manifestations</li> <li>6. No family history of genetic cardiac disease</li> </ol> |
| Race data                     | Multiracial  | Not reported  | Caucasian   | Not reported   |
| Observers                     | 2  | Multiple  | 1   | Multiple   |

BMI, Body mass index; BSA, body surface area; CHD, congenital heart disease.

\*The original publication from Boston involved only 496 children (18), but the regression equations used for comparison in this study were based on data from >2,000 children with variable sample sizes for each parameter.

<sup>†</sup>y = measurement value; β = intercept; m, m<sub>1</sub>, m<sub>2</sub>, and m<sub>3</sub> = slope values.

FAC is calculated as the difference between RV diastolic and systolic areas divided by the diastolic area. Although its reproducibility is limited by trabeculations that complicate endocardial definition, FAC provides information about RV longitudinal and radial function at the base and apex, and it accounts for translational motion of the right ventricle. Finally, RVEF can be calculated from 3DE RV volumes, and 3DE methods to measure RV size and function are better than 2DE methods compared with MRI (Figure 26).<sup>81</sup> When feasible, 3DE assessment of RVEF may be useful in select scenarios, including pulmonary hypertension and repaired tetralogy of Fallot.<sup>6</sup>

**RV Doppler Indices.** The peak tricuspid regurgitation jet velocity estimates RV systolic pressure and is used routinely in clinical practice. The systolic-to-diastolic duration ratio calculated from tricuspid regurgitation duration compared with the rest of the cardiac cycle has been used to evaluate RV function. It reflects adverse RV-LV interactions with RV pressure overload and predicts outcomes in patients with pulmonary hypertension, cardiomyopathy, and single ventricle CHD.<sup>82</sup> TDI evaluation of peak systolic velocity (s') at the lateral TV annulus provides information about RV longitudinal systolic function. The myocardial performance index (MPI), calculated as the sum of isovolumic contraction and relaxation times divided by ejection time measured by spectral Doppler or TDI evaluation, is another index of combined RV systolic and diastolic function. Isovolumic times are short or absent when pulmonary vascular impedance is low, so RV MPI is highly variable and not useful in the normal RV. However, isovolumic times increase when abnormal loading conditions negatively affect RV function. Consequently, RV MPI may be less variable and more useful in the setting of RV pressure overload, as seen in pulmonary hypertension and systemic RVs in biventricular circulation (such as congenitally corrected transposition of the great arteries).<sup>83</sup>

**STE Assessment of RV Mechanics.** RV GLS may predict clinical outcomes in patients with pulmonary hypertension and repaired tetralogy of Fallot.<sup>84,85</sup> RV and single ventricular GLS is typically measured in a single apical view with relatively good reproducibility using a single ultrasound platform.<sup>86,87</sup> RV GLS is usually reported as the average of basal, mid, and apical lateral wall segments. Because the septum is shared by both ventricles and is important to RV ejection, the average of three lateral wall and three septal segments may be useful (Figure 27).

**Measures of RV Diastolic Function.** RV diastolic function is not routinely evaluated in pediatric TTE. As with RV systolic function, multiple parameters should be considered when evaluating RV diastolic function, always in the context of the clinical scenario. TV inflow velocities during early filling (E wave) and atrial contraction (A wave) as well as the E/A ratio have been used to evaluate RV relaxation and filling. TDI evaluation of peak early diastolic velocity (e') at the lateral TV annulus is another measure of RV diastolic function that may predict clinical outcomes (the peak late diastolic velocity or a' has not been linked to clinical outcomes). TV E/e' ratio can also be used to evaluate RV diastolic function, but it does not reliably reflect RV filling pressures in children.<sup>88</sup> In the absence of significant TV dysfunction, qualitative assessment of RA size may reflect RV filling pressures. Surrogates of RA pressure, such as hepatic vein A-wave reversal, may help identify decreased RV compliance. Antegrade flow across the PV at end-diastole is also associated with restrictive RV physiology, although its clinical significance has not been fully defined.<sup>89</sup>

**RV-LV Interactions.** RV-LV interactions occur because of shared myocardial fibers, the shared interventricular septum, and the globally enclosing pericardium.<sup>90</sup> They are important in the setting of RV pressure and volume overload, as the interactions can lead to decreased LV filling and output with abnormal RV loading conditions.

**Table 13** Suggested components of an agitated saline contrast and UEA protocol

| Agitated saline contrast study   |
|--|
| <b>Appropriate indication</b> <ul style="list-style-type: none"> <li>• Possible intracardiac shunt</li> <li>• Possible intrapulmonary shunt</li> <li>• Possible unroofed coronary sinus</li> </ul>   |
| <b>Location of intravenous site for contrast injection</b> <ul style="list-style-type: none"> <li>• Right antecubital vein if right SVC</li> <li>• Left antecubital vein if left SVC draining to the coronary sinus</li> <li>• Bilateral antecubital veins to evaluate bilateral SVCs <math>\pm</math> connecting vein</li> </ul>  |
| <b>Appropriate transthoracic echocardiographic view</b> <ul style="list-style-type: none"> <li>• Apical four-chamber view</li> <li>• Subcostal coronal view</li> </ul>   |
| <b>Harmonic imaging to improve visualization of contrast</b>   |
| <b>Contrast preparation and injection</b> <ul style="list-style-type: none"> <li>• Two 10-mL syringes connected by a three-way stopcock, one syringe filled with normal saline + 0.5-1 mL air <math>\pm</math> 1 mL blood from patient, agitated by passing mixture from one syringe to the other</li> <li>• Rapid injection of mixture while acquiring a long image clip (up to 10 sec)</li> <li>• Full contrast opacification of the right atrium and right ventricle</li> </ul> |
| <b>Testing for intracardiac (interatrial) shunt</b> <ul style="list-style-type: none"> <li>• Likely present if contrast appears in LA within three to six cardiac cycles after RA opacification</li> <li>• Valsalva maneuver or gentle pressure on abdomen to increase RA pressure as confirmed by leftward shift of atrial septum helpful if initial test negative</li> </ul>   |
| <b>Testing for intrapulmonary shunt</b> <ul style="list-style-type: none"> <li>• Likely present if contrast appears in LA later than six cardiac cycles after RA opacification</li> </ul>  |
| <b>Testing for unroofed coronary sinus</b> <ul style="list-style-type: none"> <li>• Agitated saline contrast injection into a left superior systemic vein</li> <li>• Present if contrast appears in coronary sinus then simultaneously in RA and LA</li> </ul>   |
| UEA study  |
| <b>Approved pediatric indication (Lumason)</b> <ul style="list-style-type: none"> <li>• LV cavity opacification</li> </ul>   |
| <b>Off-label indications</b> <ul style="list-style-type: none"> <li>• Intracardiac mass</li> <li>• Apical hypertrophic cardiomyopathy</li> <li>• LV noncompaction</li> <li>• Differences in myocardial perfusion at rest or with stress</li> </ul>   |

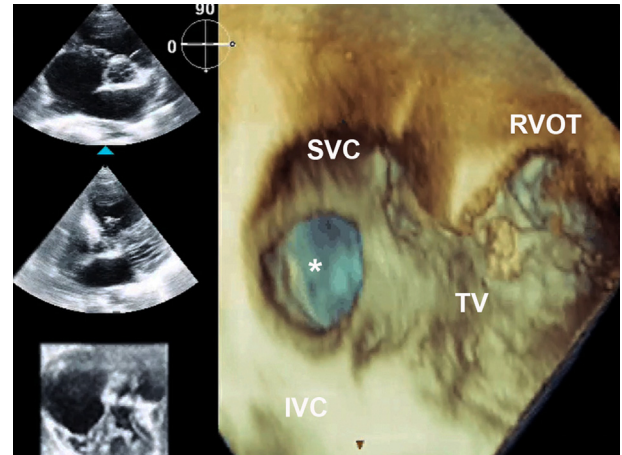


**Figure 16** Three-dimensional echocardiography with multiplanar reconstruction: secundum atrial septal defect (*asterisk*) visualized from the right atrial aspect. IVC, inferior vena cava; RVOT, right ventricular outflow; SVC, superior vena cava; TV, tricuspid valve.

pressure and strain) and other similar parameters such as constructive and wasted myocardial work can inform on the mechanisms of RV dysfunction and may provide a more comprehensive and sensitive assessment of RV function than strain alone.<sup>92</sup> Three-dimensional echocardiography, 3D strain evaluation, and artificial intelligence have been used together for a more extensive regional assessment of the RV base, apex, and outflow tract.<sup>56</sup> Diastolic strain rates have been shown to correlate with RV filling pressures.<sup>93</sup> Ultrafast ultrasound techniques may eventually provide information on intracavitary flow patterns, myocardial perfusion, and tissue stiffness.<sup>94</sup>

## Key Points and Recommendations

- Most RV systolic functional parameters do not account for the contribution of the RV outflow tract.
- RV systolic function should be evaluated by a combination of qualitative assessment and quantitative parameters.
- TAPSE and FAC are useful indices of RV systolic function.
- Three-dimensional echocardiographic measurements of RV volumes and EF as well as longitudinal strain analysis may be performed when feasible in certain conditions.

## Left Ventricle and Ventricular Septum

In normal hearts, the left ventricle is usually seen as a muscular bullet shape in subcostal coronal, apical, and parasternal long-axis views and as a muscular circular structure in subcostal sagittal and parasternal short-axis views. Assessment of LV size and global and regional performance is a crucial component of a complete pediatric TTE. This can be challenging in pediatrics because of the wide variability of LV shapes and sizes in children, especially in the setting of CHD. Ventricular dysfunction is common in patients with acquired, genetic, or CHD, presenting as primary or secondary cardiomyopathy, often in the setting of myocarditis, other inflammatory processes, musculoskeletal disease, chemotherapy, or prior cardiac surgery. Serial measurements are essential to evaluate progressive dysfunction, monitor response to therapy, or identify new or recurrent complications of CHD.

**Two-Dimensional Echocardiographic and M-Mode Measures of LV Size.** Different methods to measure LV size have

Parameters to evaluate RV-LV interactions in the setting of RV pressure overload include systolic-to-diastolic duration ratio, septal curvature, early diastolic leftward septal displacement, LV eccentricity index, and RV-to-LV diameter ratio at end-systole in parasternal short-axis views.<sup>91</sup> When there is constrictive or tamponade physiology, RV-LV interactions are manifested as exaggerated respiratory variation with increased RV filling during inspiration and increased LV filling with expiration.

**Future Directions.** New modalities to evaluate the right ventricle in various clinical scenarios are being studied and validated in children. For example, measures of RV electromechanical dyssynchrony may be useful because it can contribute to RV remodeling and dysfunction in patients with repaired tetralogy of Fallot and other CHDs.<sup>37</sup> RV global and regional myocardial work (the product of

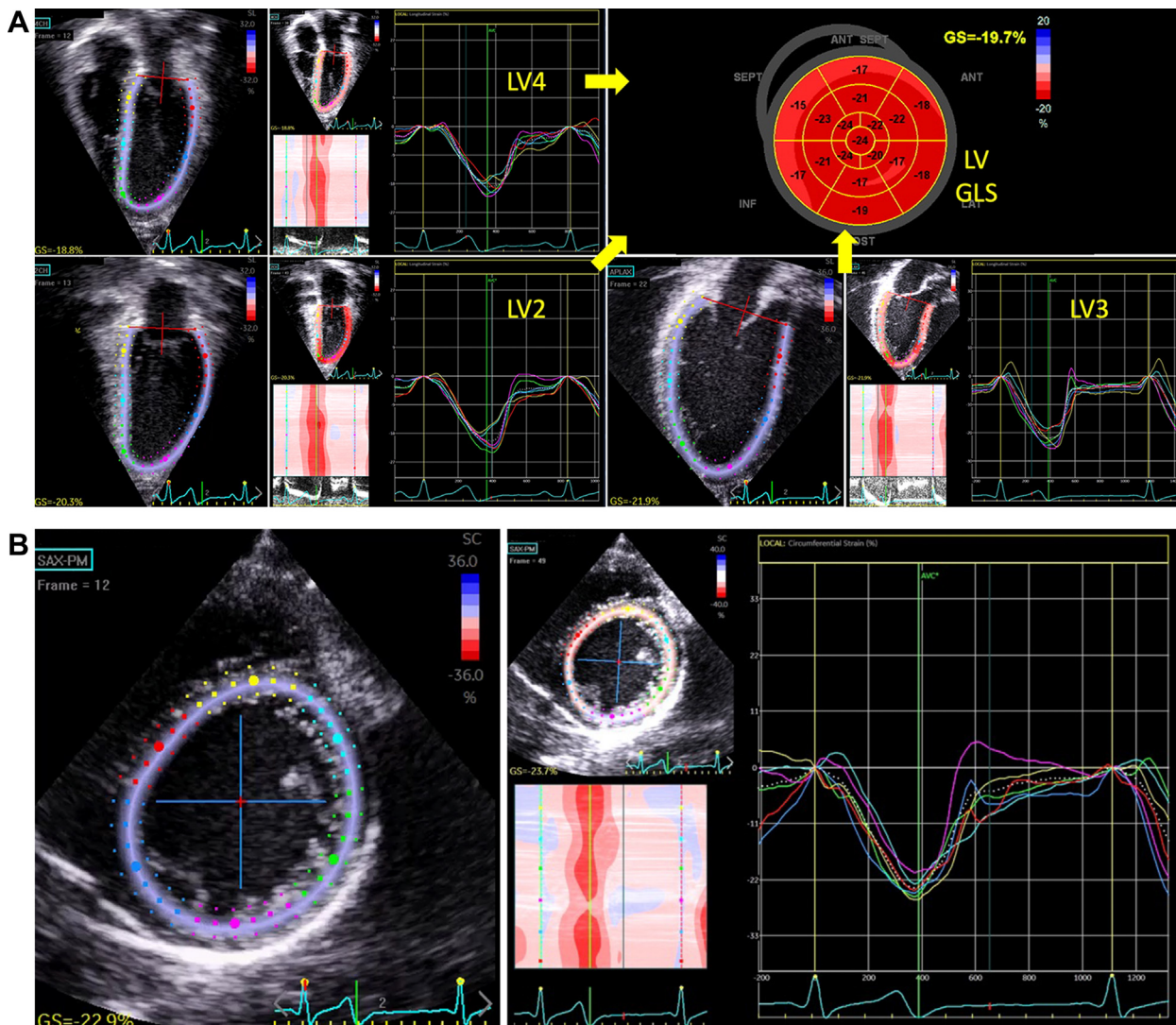


**Figure 17** Two-dimensional strain echocardiography: (A) upper panels showing normal strain values for left ventricular (LV) global longitudinal strain (GLS) from the apical four-chamber (LV4), apical two-chamber (LV2), and apical three-chamber (LV3) views that are then combined to form the bull's-eye image on the upper right corner; (B) lower panels showing normal strain curves for LV circumferential strain from the parasternal short-axis view at the level of the papillary muscles.

been described, each with advantages and weaknesses (Table 16).<sup>2,35</sup> Two-dimensional echocardiographic LV sizes should be measured during (1) end-diastole at the frame with maximum chamber luminal area or when the MV closes and (2) end-systole at the frame with minimum area or just before the MV opens. Parasternal short- or long-axis views are usually used to measure septal and posterior wall thickness and internal diameter of the LV short axis from septum to free wall; parasternal short-axis views are usually used to measure LV areas along the short-axis plane; and apical views are usually used to measure LV areas along the long-axis plane and LV long-axis lengths from base to apex. The blood-endocardium interface should be well visualized in these views. Although the ASE guidelines for adult TTE recommend LV internal diameter measurements in parasternal long-axis views to ensure that the measurements are perpendicular to the LV long axis,<sup>35</sup> short-axis views are more useful in children, as the LV short axis is not always circular. This is seen particularly in heart diseases with abnormal loading conditions for the right ventricle,

such as atrial septal defects, pulmonary regurgitation, and pulmonary hypertension.

When available, short-axis measurements should be obtained at the level of the MV leaflet tips in young patients and at the papillary muscles in older patients. The LV short-axis diameter is frequently used as a surrogate for LV size, but linear measurements in one dimension may misrepresent an abnormally shaped chamber; in fact, the internal diameter is only representative of LV size when the LV short-axis geometry is circular (Figure 28A). Wall thickness should be measured at end-diastole and end-systole, making sure not to include RV trabeculations and muscle bundles in the septal thickness measurement. This is especially true for patients with LV hypertrophy, often with variable and asymmetric thickening of LV wall segments (Figures 28B). Relative wall thickness, calculated as the sum of end-diastolic septal and posterior wall thickness divided by the end-diastolic dimension, can be used to assess for LV hypertrophy. Careful attention to measurement location on prior studies can

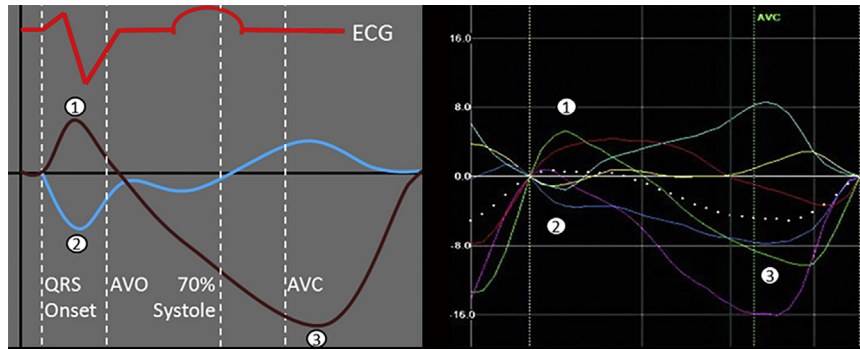


**Figure 18** Electromechanical dyssynchrony: the three classic pattern dyssynchrony (CPD) criteria are labeled numerically in both panels: (1) early stretch in at least one segment with delayed activation, (2) early contraction termination in a septal wall segment with peak contraction occurring in the first 70% of the systolic ejection phase, and (3) early stretch of segments that must actively contract with late postsystolic peak strain. In the *left panel*, strain analysis begins at the QRS onset with a simplified pair of representative septal (*blue*) and lateral wall (*brown*) curves. The *right panel* reveals CPD pattern in an infant with dilated cardiomyopathy and left bundle branch block on electrocardiography. Reproduced with permission from Forsha *et al.*<sup>45</sup> AVC, AoV closure; AVO, AoV opening.

ensure accurate serial measurements for comparison. LV diameters and wall thickness can be measured by 2DE or M-mode. Although the 2010 quantification guidelines recommended only 2DE for these measurements,<sup>2</sup> many centers use M-mode routinely in clinical prac-

tice, partly because of familiarity after decades of use. In addition, it provides greater temporal resolution than 2DE in patients with faster heart rates, allowing better characterization of wall motion to assess function, electromechanical dyssynchrony, and interventricular interactions.<sup>95</sup> Careful use of the QRS onset on the electrocardiogram (rather than the point of maximal diameter) to time end-diastolic M-mode measurements may increase reproducibility and decrease variability. Proponents of 2DE for these measurements point to the following facts to justify their approach: (1) current ultrasound systems exhibit excellent spatial resolution, (2) 2DE can guarantee that the measurements are performed along the true minor axis of the left ventricle, and (3) M-mode cannot account for the frequent lateral motion of the heart during the respiratory cycle seen in children.<sup>96</sup> It is important to note that the PHN Z scores for these measurements were obtained by 2DE and not M-mode, so the PHN model should not be used for M-mode measurements.

LV volumes can be calculated using various methodologies as described in the 2010 quantification guidelines.<sup>2</sup> The modified Simpson biplane method (method of disks) uses the summation of disks approach by calculating LV volumes from LV long-axis areas obtained in apical four-chamber and two-chamber views (Figures 8A and C, and 29). The bullet (5/6 area-length) method uses measurements of short-axis areas and long-axis lengths to estimate LV volumes (Figure 30). LV mass can be estimated by subtracting endocardial volume from epicardial volume and multiplying the difference by the density of LV muscle. Abnormal LV mass Z scores  $\geq 2$  represent LV hypertrophy, which can then be divided into eccentric vs concentric hypertrophy: the former represents normal mass-to-volume ratio (Z score  $< 2$ ) as seen in the setting of LV volume overload lesions like a ventricular septal defect, and the latter represents elevated mass-to-volume ratio (Z score  $\geq 2$ ) as seen in the setting of LV pressure overload lesions like aortic stenosis or systemic hypertension.

### Two-Dimensional Echocardiographic and M-Mode Measures of LV Function.

All 2DE and M-mode methods to measure LV systolic function are subject to errors in accuracy and reproducibility. Qualitative visual inspection is often the first method used, but it relies on operator skill and interpreter experience and is prone to significant interobserver and interstudy variability.<sup>97</sup> Standard quantitative methods include SF from linear measurements and EF from LV volumetric measurements. SF is easily and effectively measured in parasternal short-axis views using 2DE or M-mode, but

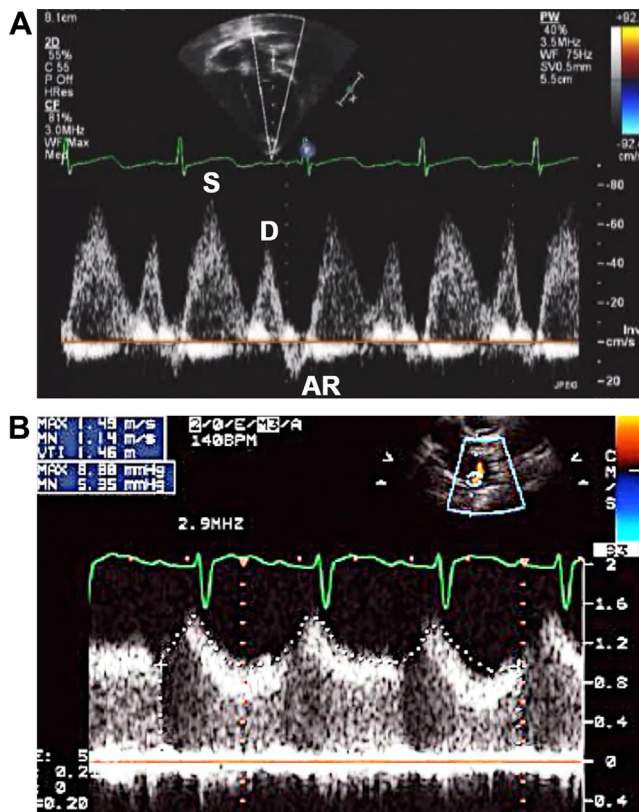


**Figure 19** Pulmonary vein Doppler flow patterns: (A) normal Doppler flow pattern obtained from an apical view showing antegrade flow during ventricular systole (S) and diastole (D) and intermittent flow reversal during atrial contraction (AR) with low-velocity and phasic flow that returns to baseline and (B) abnormal Doppler flow pattern obtained from a parasternal view showing nonphasic flow with relatively high velocity and no return to baseline suggestive of pulmonary vein stenosis. Reproduced with permission from Lopez *et al.*<sup>2</sup>

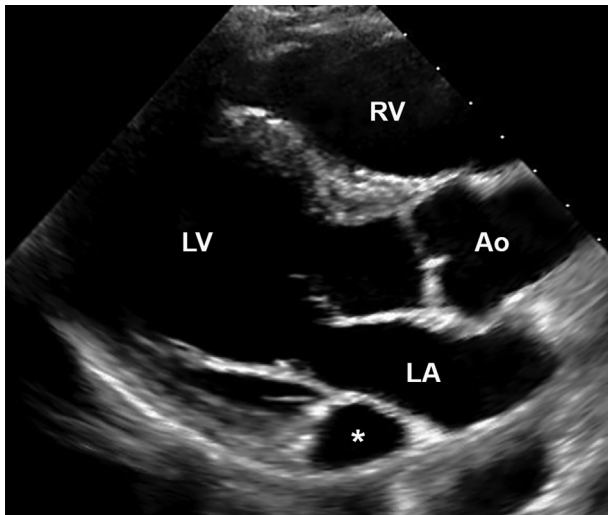


**Figure 20** Parasternal long-axis view: dilated coronary sinus (*asterisk*) coursing along the posterior left atrioventricular groove suggestive of a persistent left SVC. Ao, Aorta; LA, left atrium; LV, left ventricle; RV, right ventricle.

it (1) does not account for longitudinal shortening, (2) should not be measured in the setting of regional wall motion abnormalities (such as paradoxical septal motion), and (3) should not be used when the left ventricle has an abnormal shape or noncircular geometry in the short-axis views (as seen with RV pressure or volume overload). Despite their popularity, there are challenges with these functional indices.<sup>96</sup> Among the 3215 normal children in the PHN Echo Z-Score Project, 17% were found to have an abnormally low SF (<25%) and/or EF (<50%) after the calculations were made from blinded measurements, despite the fact that all subjects were thought to have qualitatively normal LV systolic function at both the local institution and at the PHN core laboratory. The authors speculated that this significant variability in LV functional indices is likely minimized in daily clinical practice by manipulation of the measurements to match the subjective qualitative assessment. Advances in artificial intelligence have allowed automated measurements of LV size from multiple views,

possibly mitigating the challenges associated with the known variability of these functional indices.

**Other Measures of LV Size and Systolic Function.** The use of 3DE to measure LV volumes and EF in children has gained popularity because of its lack of dependence on geometric assumptions, improvements in 3DE transducer technology, and semiautomated analysis software now available on many platforms. Several pediatric studies have shown that 3DE measurements of LV volumes and EF have better reproducibility and correlate better with cardiac MRI measurements than M-mode and 2DE measurements.<sup>98,99</sup> The ASE guidelines document on 3DE in CHD summarizes the various modes of image acquisition and semiautomated endocardial tracking that are used to measure LV volumes and EF.<sup>6</sup> There are, however, limitations associated with 3DE, and these include lower temporal resolution, challenges with imaging the entire LV using a single transducer position, and lack of validation of 3DE assessment of LV mass and dyssynchrony.

TDI measurement of velocity at the lateral and septal aspects of the MV annulus ( $s'$ ) is a measure of LV systolic function that is independent of geometry, although it has variable utility in pediatrics. As for the right ventricle, MPI is a geometrically independent measure of combined LV systolic and diastolic function. As with the right ventricle, LV global dysfunction results in prolongation of the isovolumic times, resulting in increased LV MPI. However, significant measurement variability of isovolumic times and the inability to determine which component is abnormal have precluded the routine use of this parameter at many pediatric centers. LV GLS provides early detection of myocardial dysfunction before abnormal changes in SF or EF.<sup>36</sup> It can be measured in apical four-, three-, and two-chamber views with good reproducibility when using a single ultrasound platform, using the average value to assess LV function (Figure 17).<sup>35,42,43</sup> Because circumferential deformation appears to compensate for decreased longitudinal function in patients with LV pressure overload, global circumferential strain may have additive value in these patients.<sup>100</sup> Evaluation of LV peak segmental strain is recommended in some guidelines for adult patients, but its reproducibility is poor in children. However, regional pattern analysis to identify electromechanical dyssynchrony and discoordination may be helpful in children with pacemakers or in candidates for cardiac resynchronization therapy. This can be done by looking for patterns of abnormal LV contraction timing in LV longitudinal strain curves.<sup>45,46</sup>

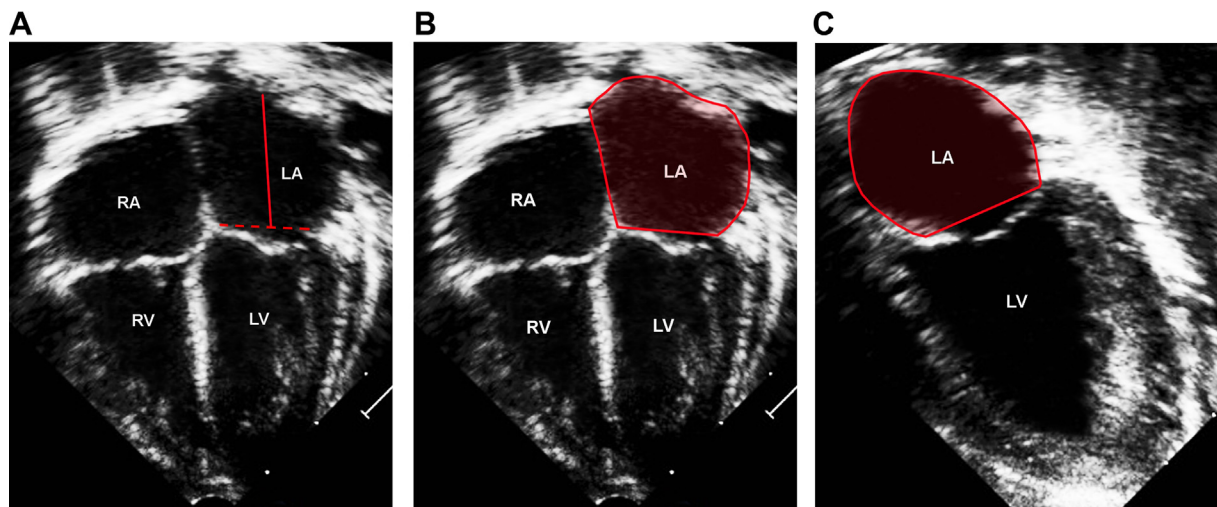


**Figure 21** Left atrial (LA) volumes calculated from LA length and area measurements at ventricular end-systole: (A) LA major-axis length from the apical four-chamber view, (B) LA area from the apical four-chamber view, and (C) LA area from the apical two-chamber view. Reproduced with permission from Lopez *et al.*<sup>2</sup> LV, Left ventricle; RA, right atrium; RV, right ventricle.

**Table 14** Morphologic abnormalities of the AV valves

|  |
|--|
| Valvar disease   |
| • Anomalous cleft  |
| • Double orifice   |
| • Leaflet perforation or fenestration                        |
| • Diminutive or absent leaflet                               |
| • Displaced leaflet  |
| • Myxomatous changes   |
| • Intravalvar or supervalvar ring or membrane                |
| • Associated thrombus or vegetation                          |
| Subvalvar disease  |
| • Single papillary muscle group (parachute deformity)        |
| • Closely-spaced papillary muscle groups (parachute variant) |
| • Muscularized (absent) chordae (arcade)                     |
| • Shortened chordae (tethered leaflet)                       |
| • Elongated chordae (prolapse)                               |
| • Secondary disruption of chordae (flail leaflet)            |

**Measures of LV Diastolic Function.** In contrast to adult TTE studies, diastolic functional assessment is not routine during pediatric TTE.<sup>101</sup> High heart rates and poor cooperation in children have resulted in significant measurement variability with few published normal reference values. Nevertheless, diastolic dysfunction occurs in children with various CHDs (such as LV outflow tract obstruction, endocardial fibroelastosis, and single ventricles) and with cardiomyopathy or myocarditis. The most common measurements include MV inflow E and A wave velocities from apical four-chamber views and the E/A ratio, although these parameters are frequently not helpful in isolation. TDI measurement of peak early diastolic velocity ( $e'$ ) at the lateral and septal MV annulus and the E/ $e'$  ratio have been used, but E/ $e'$  has not reliably correlated with LV filling pressures in children. With normal diastolic function, PW Doppler interrogation of the pulmonary veins in apical and parasternal views should reveal the characteristic phasic flow patterns with antegrade flow in systole (S wave) and early diastole (D wave) and reversal during atrial contraction (A wave). Prominent A-wave reversal has predicted significant diastolic dysfunction in adults, but this has not been validated in children. Lastly, LA size and PA systolic pressures also reflect LV filling pressures and diastolic function.

**Future Directions.** More accurate and reproducible indices of LV systolic function are needed, especially given the challenges highlighted by the PHN Echo Z-Score Project as it relates to SF and EF.<sup>96</sup> Advances in transducer technology and image processing as well as newer and

better artificial intelligence algorithms may provide solutions to these problems by providing more accurate data and minimizing the effects of human error. Newer modalities may provide early recognition of the vulnerable LV before the development of abnormalities in SF or EF, potentially allowing earlier treatment and improving outcomes.

**Ventricular Septum.** The ventricular septum is shared by both ventricles and should be evaluated in all initial pediatric TTE studies. It should have a rounded contour throughout the cardiac cycle when viewed in a subcostal sagittal or parasternal short-axis view. Abnormalities of ventricular septal shape and motion include (1) flattening during diastole, systole, or the entire cardiac cycle, (2) systolic bowing into the LV chamber, (3) paradoxical motion, (4) hypokinesis, and (5) dyskinesis. Color mapping in subcostal, apical, and parasternal sweeps should be performed to exclude a ventricular septal defect. Because more than one defect can occur, the location and size of each ventricular septal defect should be evaluated along with their spatial relationship to surrounding structures, including the AV valves and semilunar valves. Both PW and CW Doppler interrogation should be performed in a view where the flow is coaxial to the ultrasound beam and should evaluate the direction of flow and the degree of restriction across a defect. Classification of ventricular septal defects has been fraught with controversy, although a recent consensus document attempts to harmonize the various nomenclature systems into one that combines the important features of each approach.<sup>102</sup>

### Key Points and Recommendations

- LV short-axis linear measurements by 2DE or M-mode are limited when the LV cross-sectional shape is not circular or when there is abnormal regional wall motion.
- LV assessment should be performed in all TTE studies, including 2DE and Doppler echocardiography to measure LV size, mechanics, and systolic and diastolic function.
- The evaluation may also include a combination of M-mode, 3DE, and STE.
- Two-dimensional echocardiographic and 3DE volumetric measurements and STE are preferable to 2DE or M-mode linear measurements in the setting of abnormal LV shape or regional wall motion abnormalities.

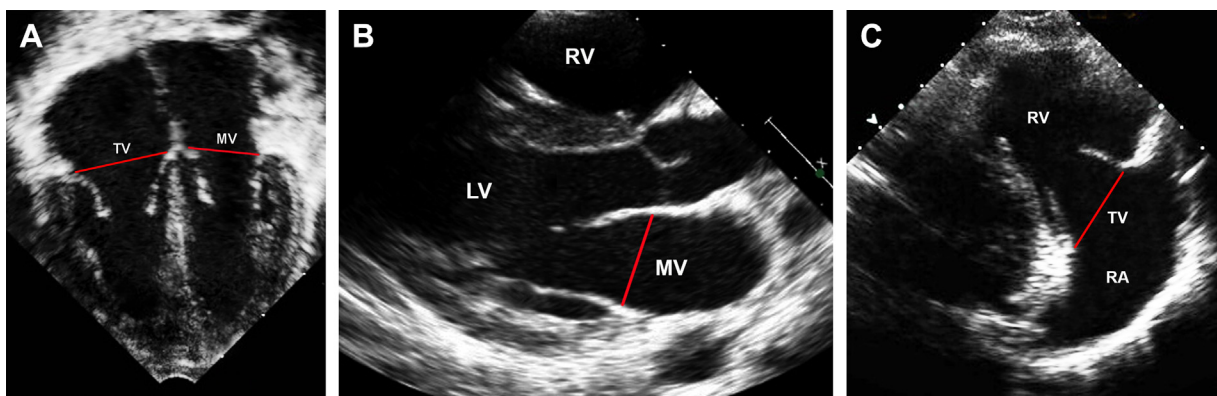


**Figure 22** Tricuspid valve (TV) and mitral valve (MV) annular diameter measurements in diastole at the frame after maximum leaflet excursion: (A) TV and MV transverse diameters from the apical four-chamber view, (B) MV anteroposterior diameter from the parasternal long-axis view, and (C) TV anteroposterior diameter in the parasternal long-axis view with rightward and posteroinferior tilting. Reproduced with permission from Lopez et al.<sup>2</sup> LV, Left ventricle; RA, right atrium; RV, right ventricle.

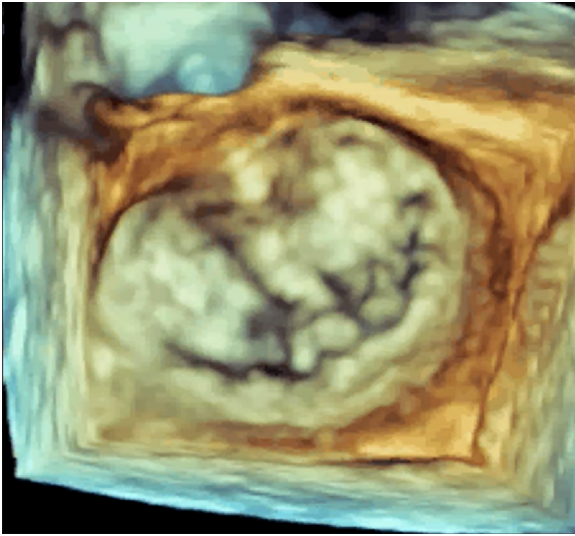


**Figure 23** Three-dimensional echocardiography: en face image of the mitral valve from the left atrial aspect.

### Ventricular Outflow Tracts and Semilunar Valves

**RV Outflow Tract and PV.** The RV outflow tract is a geometrically complex muscular structure composed of the subpulmonary conus or infundibulum, anterior RV free wall, crest of the ventricular septum, papillary muscle of the conus, and PV.<sup>103</sup> Outflow tract obstruction can result from abnormal development of any component. Imaging the RV outflow tract can be performed in subcostal views, modified apical views with anterior tilting, and parasternal long-axis and short-axis views with the RV outflow tract oriented along the axial direction. Its relationship with the TV and ventricular septum is well seen in subcostal sweeps, although a single-plane image clip with counterclockwise rotation from the subcostal coronal view (right anterior oblique view) is particularly useful when there is conal malalignment as seen in tetralogy of Fallot (Figure 6B). Subcostal and parasternal views can usually demonstrate the anterior aspect of the RV outflow tract, and subcostal and modified apical views with anterior tilting provide the best angle for Doppler interrogation.<sup>1</sup> Color mapping in these views should evaluate for obstruction, ventricular septal defects that can be confused with RV outflow tract obstruction, and coronary-cameral fistulae.<sup>29</sup> When possible, 3DE allows good visualization of a complex RV outflow tract.<sup>6</sup> Measurement of the RV outflow tract diameter may be performed from inner edge to inner edge at end-diastole. The proximal RV outflow tract diameter from the anterior free wall to the aortic root is best measured along the axial direction in parasternal short-axis views,<sup>35</sup> whereas the distal RV outflow tract diameter is best measured just proximal to the PV in parasternal long-axis views.<sup>2</sup>

The PV is evaluated in similar views as the RV outflow tract, although valvar morphology is best assessed in parasternal views. The PV annular diameter should be measured from inner edge to inner edge during maximal valve opening in early to mid-systole in parasternal long-axis views (Figure 31A).<sup>2,20</sup> En face imaging of the PV is sometimes possible with a high left parasternal view, but this is dependent largely on cardiac position and thoracic configuration. Color mapping should be performed in multiple views to evaluate for obstruction and regurgitation. PW Doppler interrogation should be performed below, at, and above the valve to detect dynamic or multiple levels of obstruction, recog-

nizing that the dominant resistor in a series of obstructions will confound the degree of obstruction measured at other levels.<sup>2</sup> CW Doppler interrogation should measure peak velocities of stenotic and regurgitant jets, making sure to identify on the report the view(s) from which the velocities were measured. Doppler evaluation along the RV outflow tract and PV may be confounded by (1) the presence of a large shunt equalizing pulmonary and systemic systolic pressures, (2) the normally elevated PA pressures in the neonatal period, (3) severe tricuspid regurgitation, or (4) low cardiac output secondary to severe RV dysfunction. Assessment of the degree of PV stenosis in these settings should be based more on annular size and leaflet morphology.<sup>2</sup>

**LV Outflow Tract and AoV.** The LV outflow tract represents the area below the AoV whose boundaries include the ventricular septum and anterior MV leaflet. The absence of a muscular subaortic conus in the normal heart results in fibrous continuity between the AoV and MV, distinguishing the LV outflow tract from the RV outflow tract with its circumferential muscular sleeve below the PV. The LV outflow tract is typically considered to be circular in shape even though it is often more elliptical,<sup>2</sup> and it is best measured in mid-systole in parasternal long-axis views along the axial direction approximately 3 to 10 mm below the AoV annulus.<sup>29</sup> Modified parasternal long-axis views may be necessary in patients with a sigmoid septum or variations in AoV alignment with the left ventricle. The AoV annulus is defined by 2DE as the virtual ring connecting the basal extension of each AoV leaflet, although each leaflet is attached within the aortic root in a 3D semilunar fashion from the ventriculoarterial junction up to the sinotubular junction. Consequently, the AoV annulus is more of a virtual diagnostic construct rather than a true anatomic entity (Figure 31B).<sup>35</sup> Nevertheless, it is measured along the axial direction in the same parasternal long-axis view as the LV outflow tract, from inner edge to inner edge at the leaflet hinge points during maximal valve opening in early to mid-systole. AoV morphology is best evaluated in parasternal short-axis views where all three leaflets can be seen simultaneously (Figure 32). Minor tilting of the transducer with short sweeps through the full depth of the valve may be necessary to assess for leaflet asymmetry or partial or complete commissural fusion (as in a bicuspid AoV). Three-dimensional echocardiography can be used to evaluate AoV morphology and for en face measurement of the annulus, especially when the 2DE source images are good. Image compounding or frame reordering, although not yet standard, may provide better leaflet visualization in smaller children and in patients with higher heart rates.<sup>34</sup>

Doppler interrogation of the LV outflow tract and AoV should be performed in subcostal coronal, apical three-chamber, right parasternal, and suprasternal long-axis views, optimizing alignment with the direction of flow. Color mapping should evaluate for dynamic midcavity obstruction as well as subvalvar, valvar, and supra-valvar aortic stenosis, using a high color velocity range that displays aliasing only when there is significantly increased flow velocity. PW Doppler interrogation should be performed at all these areas before CW Doppler interrogation to measure the maximum instantaneous pressure gradient along the entire outflow tract.<sup>29</sup> PW Doppler interrogation below the AoV should position the sample volume in the same area where the LV outflow tract diameter was measured. If MV regurgitation is present, the LV outflow tract gradient may be estimated from the difference between the maximum instantaneous retrograde gradient across the MV plus an assumed LA pressure and a systolic blood pressure measured simultaneously from an upper extremity. However, the accuracy of this approach may be limited by the inherent increase in measurement error with the higher velocities of MV regurgitant jets.

**Table 15** Evaluation of RV size, function, and hemodynamics

| Measurement                                       | Modality/view                                 | Timing/calculation                | Utility                         | Strengths  | Weaknesses   |
|---|---|-----------------------------------|---------------------------------|--|--|
| Guidelines (should be performed)                  |   |                                   |                                 |  |  |
| Subjective assessment                             | 2DE: subcostal, apical, and parasternal views | Throughout cardiac cycle          | RV size and function            | <ul style="list-style-type: none"> <li>• Quick and simple</li> <li>• Provides context for other measurements</li> </ul>  | <ul style="list-style-type: none"> <li>• Depends on good blood-endocardium border</li> <li>• Poor reproducibility</li> <li>• Regional functional abnormalities can limit accuracy</li> <li>• Correlates poorly with MRI-derived EF</li> </ul>  |
| TR jet peak velocity                              | CW: apical or parasternal views               | Systole                           | RV systolic pressure estimation | <ul style="list-style-type: none"> <li>• Noninvasive method to estimate PA systolic pressures</li> </ul>   | <ul style="list-style-type: none"> <li>• Depends on alignment</li> <li>• Incomplete spectral envelope can limit accuracy</li> <li>• Assumed or estimated RA pressure</li> </ul>  |
| EDA   | 2DE: apical four-chamber view                 | Maximum area at end-diastole      | RV size                         | <ul style="list-style-type: none"> <li>• Used for FAC calculation</li> </ul>   | <ul style="list-style-type: none"> <li>• Depends on good blood-endocardium border</li> <li>• Difficult to visualize RV lateral wall</li> <li>• Depends on distinct apical endocardium</li> <li>• Foreshortening can limit accuracy</li> <li>• Depends on loading conditions</li> </ul> |
| ESA   | 2DE: apical four-chamber view                 | Minimum area at end-systole       | RV size                         | <ul style="list-style-type: none"> <li>• Used for FAC calculation</li> </ul>   | <ul style="list-style-type: none"> <li>• Depends on good blood-endocardium border</li> <li>• Difficult to visualize RV lateral wall</li> <li>• Depends on distinct apical endocardium</li> <li>• Foreshortening can limit accuracy</li> </ul>  |
| FAC   | 2DE: apical four-chamber view                 | $(EDA - ESA) / EDA \times 100\%$  | RV systolic function            | <ul style="list-style-type: none"> <li>• Normal data available</li> <li>• Correlates modestly with MRI-derived EF</li> <li>• Accounts for longitudinal and radial RV shortening</li> </ul> | <ul style="list-style-type: none"> <li>• Same as above</li> </ul>  |
| TAPSE   | M-mode: apical four-chamber view              | Systole                           | RV systolic function            | <ul style="list-style-type: none"> <li>• Correlates modestly with MRI-derived EF</li> <li>• Quick and simple</li> <li>• Good temporal resolution</li> </ul>                                | <ul style="list-style-type: none"> <li>• Normal values not adjusted for body size</li> <li>• Not validated in children with CHD</li> <li>• Depends on loading conditions</li> </ul>  |
| Peak TV inflow velocity in early diastole (E)     | PW: apical four-chamber view                  | Early diastole                    | RV diastolic function           | <ul style="list-style-type: none"> <li>• Quick and simple</li> <li>• No geometric assumptions</li> </ul>   | <ul style="list-style-type: none"> <li>• Respiratory variation necessitates averaging over five cardiac cycles</li> <li>• Fast heart rates can limit accuracy</li> </ul>   |
| Peak TV inflow velocity at atrial contraction (A) | PW: apical four-chamber view                  | Atrial contraction                | RV diastolic function           | <ul style="list-style-type: none"> <li>• Same as above</li> </ul>  | <ul style="list-style-type: none"> <li>• Same as above</li> </ul>  |
| Recommendations (may be performed)                |   |                                   |                                 |  |  |
| End-diastolic basal diameter                      | 2DE: apical four-chamber view                 | Maximum dimension at end-diastole | RV size                         | <ul style="list-style-type: none"> <li>• Normal data available</li> </ul>  | <ul style="list-style-type: none"> <li>• Depends on good blood-endocardium border</li> <li>• Difficult to visualize RV lateral wall</li> <li>• Correlates poorly with MRI-derived RV volume</li> </ul>   |

(Continued)

**Table 15** (Continued)

| Measurement                                     | Modality/view                            | Timing/calculation                | Utility               | Strengths  | Weaknesses  |
|---|--|-----------------------------------|-----------------------|--|---|
| End-diastolic midcavity diameter                | 2DE: apical four-chamber view            | Maximum dimension at end-diastole | RV size               | <ul style="list-style-type: none"> <li>• Normal data available</li> </ul>  | <ul style="list-style-type: none"> <li>• Same as above</li> </ul>   |
| End-diastolic apical-cavity diameter            | 2DE: apical four-chamber view            | Maximum dimension at end-diastole | RV size               | <ul style="list-style-type: none"> <li>• Related to apical remodeling in pulmonary hypertension, hypoplastic left heart syndrome, and other CHD</li> </ul> | <ul style="list-style-type: none"> <li>• Depends on distinct apical endocardium</li> <li>• Paucity of normal data</li> </ul>  |
| End-diastolic length                            | 2DE: apical four-chamber view            | Maximum dimension at end-diastole | RV size               | <ul style="list-style-type: none"> <li>• Normal data available</li> </ul>  | <ul style="list-style-type: none"> <li>• Depends on good blood-endocardium border</li> <li>• Depends on distinct apical endocardium</li> <li>• Foreshortening can limit accuracy</li> <li>• Correlates poorly with MRI-derived RV volume</li> </ul>   |
| EDV by 3DE                                      | 3DE: apical or subcostal views           | Maximum volume at end-diastole    | RV size               | <ul style="list-style-type: none"> <li>• Normal data available</li> </ul>  | <ul style="list-style-type: none"> <li>• 3DE volume calculation software needed</li> <li>• Lower temporal resolution</li> <li>• Depends on good blood-endocardium border</li> <li>• Difficult to visualize RV lateral wall</li> <li>• Depends on distinct apical endocardium</li> <li>• Foreshortening can limit accuracy</li> <li>• Usually underestimates MRI-derived RV volume (agreement is worse with dilated ventricles)</li> </ul> |
| ESV by 3DE                                      | 3DE: apical or subcostal views           | Minimum volume at end-systole     | RV size               | <ul style="list-style-type: none"> <li>• Normal data available</li> </ul>  | <ul style="list-style-type: none"> <li>• Same as above</li> </ul>   |
| RVEF by 3DE                                     | 3DE: apical or subcostal views           | $(EDV - ESV) / EDV \times 100\%$  | RV systolic function  | <ul style="list-style-type: none"> <li>• Normal data available</li> </ul>  | <ul style="list-style-type: none"> <li>• Lower temporal resolution for single-beat acquisition</li> <li>• Depends on good blood-endocardium border</li> <li>• Difficult to visualize RV lateral wall</li> <li>• Depends on distinct apical endocardium</li> <li>• Foreshortening can limit accuracy</li> <li>• Depends on loading conditions</li> <li>• Variable agreement with MRI-derived EF depending on CHD</li> </ul>                |
| Peak TV annular velocity in systole (s')        | Tissue Doppler: apical four-chamber view | Systole                           | RV systolic function  | <ul style="list-style-type: none"> <li>• Good temporal resolution</li> <li>• Normal data available</li> </ul>  | <ul style="list-style-type: none"> <li>• Depends on alignment</li> <li>• Depends on loading conditions</li> <li>• Not useful when regional functional abnormalities are present</li> </ul>  |
| Peak TV annular velocity in early diastole (e') | Tissue Doppler: apical four-chamber view | Early diastole                    | RV diastolic function | <ul style="list-style-type: none"> <li>• Same as above</li> </ul>  | <ul style="list-style-type: none"> <li>• Same as above</li> </ul>   |

(Continued)

Table 15 (Continued)

| Measurement   | Modality/view  | Timing/calculation   | Utility                                      | Strengths  | Weaknesses   |
|---|--|--|--|--|--|
| Peak TV annular velocity at atrial contraction (a') | Tissue Doppler: apical four-chamber view   | Atrial contraction   | RV diastolic function                        | <ul style="list-style-type: none"> <li>• Same as above</li> </ul>  | <ul style="list-style-type: none"> <li>• Same as above</li> </ul>  |
| RV free wall longitudinal strain                    | STE: apical four-chamber view  | Systole  | RV systolic function                         | <ul style="list-style-type: none"> <li>• Useful in pulmonary hypertension, repaired tetralogy of Fallot, and systemic RV</li> <li>• No geometric assumptions</li> </ul>  | <ul style="list-style-type: none"> <li>• STE software needed</li> <li>• Requires good 2DE images</li> <li>• Intervendor variability</li> <li>• Limited pediatric experience</li> </ul>   |
| RV GLS (including septum)                           | STE: apical four-chamber view  | Systole  | RV systolic function                         | <ul style="list-style-type: none"> <li>• Useful in pulmonary hypertension, repaired tetralogy of Fallot, and systemic RV</li> <li>• No geometric assumptions</li> <li>• Includes contribution of ventricular septum</li> </ul> | <ul style="list-style-type: none"> <li>• STE software needed</li> <li>• Requires good 2DE images</li> <li>• Intervendor variability</li> <li>• Limited pediatric experience</li> <li>• Ventricular septum included in both LV and RV evaluation</li> </ul>                                 |
| MPI   | PW, CW, or tissue Doppler: apical and parasternal views at RV inflow and outflow | (IVCT + IVRT)/ET   | Combined RV systolic and diastolic function  | <ul style="list-style-type: none"> <li>• Normal data available</li> <li>• Useful in pulmonary hypertension</li> </ul>  | <ul style="list-style-type: none"> <li>• Not valid for normal RV</li> <li>• Needs two separate images for PW/CW assessment</li> <li>• Needs similar heart rate in both images</li> <li>• No information regarding individual contributions of systolic or diastolic dysfunction</li> </ul> |
| Systolic-to-diastolic duration ratio (S/D ratio)    | CW of tricuspid regurgitation jet: apical or parasternal views                   | Duration of tricuspid regurgitation divided by duration of rest of cardiac cycle | RV global function and RV-LV interactions    | <ul style="list-style-type: none"> <li>• Quick and simple</li> <li>• Normal data available</li> <li>• Useful in pulmonary hypertension</li> </ul>  | <ul style="list-style-type: none"> <li>• Depends on presence of tricuspid regurgitation</li> <li>• Affected by heart rate</li> </ul>   |
| RV/LV diameter ratio                                | 2DE: parasternal view  | Systole  | RV loading conditions and RV-LV interactions | <ul style="list-style-type: none"> <li>• Quick and simple</li> <li>• Normal data available</li> </ul>  | <ul style="list-style-type: none"> <li>• No validation in children</li> </ul>  |
| IVA   | Tissue Doppler: apical four-chamber view   | TV peak isovolumic annular velocity divided by time to peak velocity             | RV systolic function                         |  | <ul style="list-style-type: none"> <li>• Depends on alignment</li> <li>• High measurement variability</li> </ul>   |
| IVCT  | Tissue Doppler: apical four-chamber view   | Time from end of a' wave to beginning of s' wave                                 | RV diastolic function                        |  | <ul style="list-style-type: none"> <li>• Depends on alignment</li> <li>• High measurement variability</li> <li>• Normally very short or absent when pulmonary vascular impedance is low</li> </ul>   |
| IVRT  | Tissue Doppler: apical four-chamber view   | Time from end of s' wave to beginning of e' wave                                 | RV diastolic function                        |  | <ul style="list-style-type: none"> <li>• Same as above</li> </ul>  |

EDA, end-diastolic area; EDV, end-diastolic volume; ESA, end-systolic area; ESV, end-systolic volume; ET, ejection time; IVA, isovolumic acceleration; IVCT, isovolumic contraction time; IVRT, isovolumic relaxation time; STE, speckle-tracking echocardiography; TR, tricuspid regurgitation.

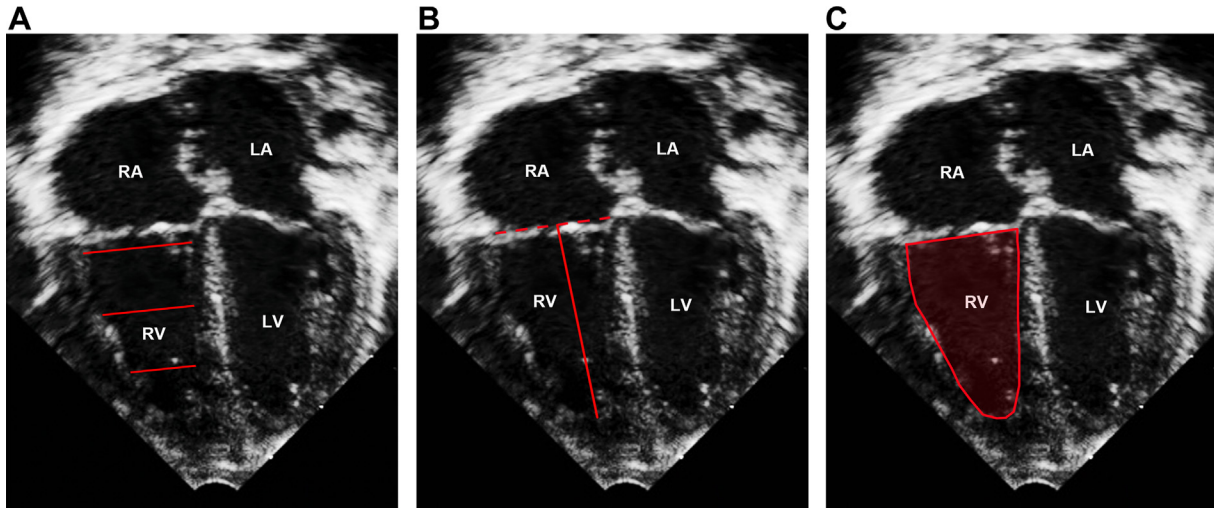


**Figure 24** Right ventricular (RV) measurements from the RV-focused apical four-chamber view at end-diastole: **(A)** RV basal, mid-cavity, and apical diameters; **(B)** RV length; and **(C)** RV area (RV ventricular FAC is calculated as [RV diastolic area—RV systolic area]/diastolic area). Reproduced with permission from Lopez *et al.*<sup>2</sup> LA, Left atrium; LV, left ventricle; RA, right atrium.

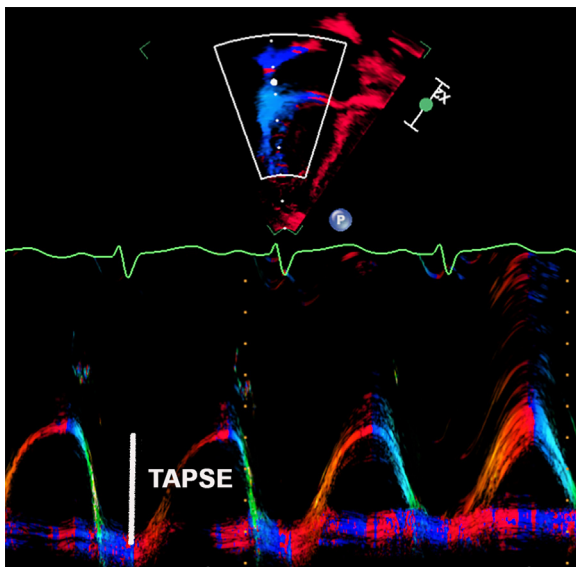


**Figure 25** Color M-mode in the right ventricular-focused apical four-chamber view: Tricuspid annular plane systolic excursion (TAPSE) at the lateral tricuspid valve annulus.

When there is AoV stenosis or regurgitation, it is important to optimize transducer alignment since the stenotic or regurgitant jet may be eccentric. The nonimaging CW Doppler transducer is an important component of adult TTE protocols, although its use in children may be limited by excessive noise during evaluation of high velocities. Quantification of the severity of AoV regurgitation in adults frequently involves the pressure half-time or slope of the spectral Doppler tracing, but their use has not been validated in children.<sup>2</sup> Evaluation of severity in pediatrics usually involves qualitative assessment of the regurgitant jet and indirect indices such as diastolic flow reversal in the aorta and LV dilation.

Doppler evaluation of AoV stenosis should include both maximum instantaneous and mean gradients from multiple views. Gradients measured in apical views tend to be lower than those in right parasternal views,<sup>104</sup> highlighting the importance of documenting the view from which the maximum gradient was measured in the report.

Quantification of AoV stenosis severity can be complicated in children because (1) Doppler-derived maximum instantaneous gradients are fundamentally different from catheterization-derived peak-to-peak gradients, the latter having provided data for the natural history studies<sup>105</sup>; (2) different physiologic states lead to variable AoV gradients in the same patient; (3) pressure recovery contributes to differences in gradients measured by TTE and by catheterization, and its effects are greater in small children than adults and with mild compared with severe stenosis<sup>106</sup>; (4) LV dysfunction with an associated decrease in cardiac output can result in lower gradients despite significant stenosis; and (5) the measured pressure gradients in neonates may not be as high as in older children and adults when there is significant stenosis. In the last two scenarios, AoV stenosis severity may be better evaluated by careful examination of AoV morphology and calculation of AoV annular diameter Z score than by the measured gradient across the valve.<sup>2</sup> Although pressure recovery can be calculated from TTE data, the paucity of validation studies in children has precluded its routine use. AoV area can also be calculated from the continuity equation and from planimetry using en face 2DE and 3DE images, but significant measurement variability due to minor variations in imaging plane, limited temporal resolution, and random measurement error has precluded routine use of this parameter to evaluate AoV stenosis in children.

### Key Points and Recommendations

- The RV outflow tract should be evaluated in subcostal, apical, and parasternal views, noting the view used when measuring gradients.
- The LV outflow tract should be evaluated in apical, right parasternal, and suprasternal views, noting the view used when measuring gradients.
- The AoV “annulus” is more of a virtual diagnostic construct than a true anatomic entity because of the semilunar attachments of the AoV leaflets.
- The LV outflow tract and PV and AoV annular diameters should be measured in parasternal long-axis views.
- AoV morphology is best evaluated with en face 2DE and 3DE images in parasternal short-axis views.

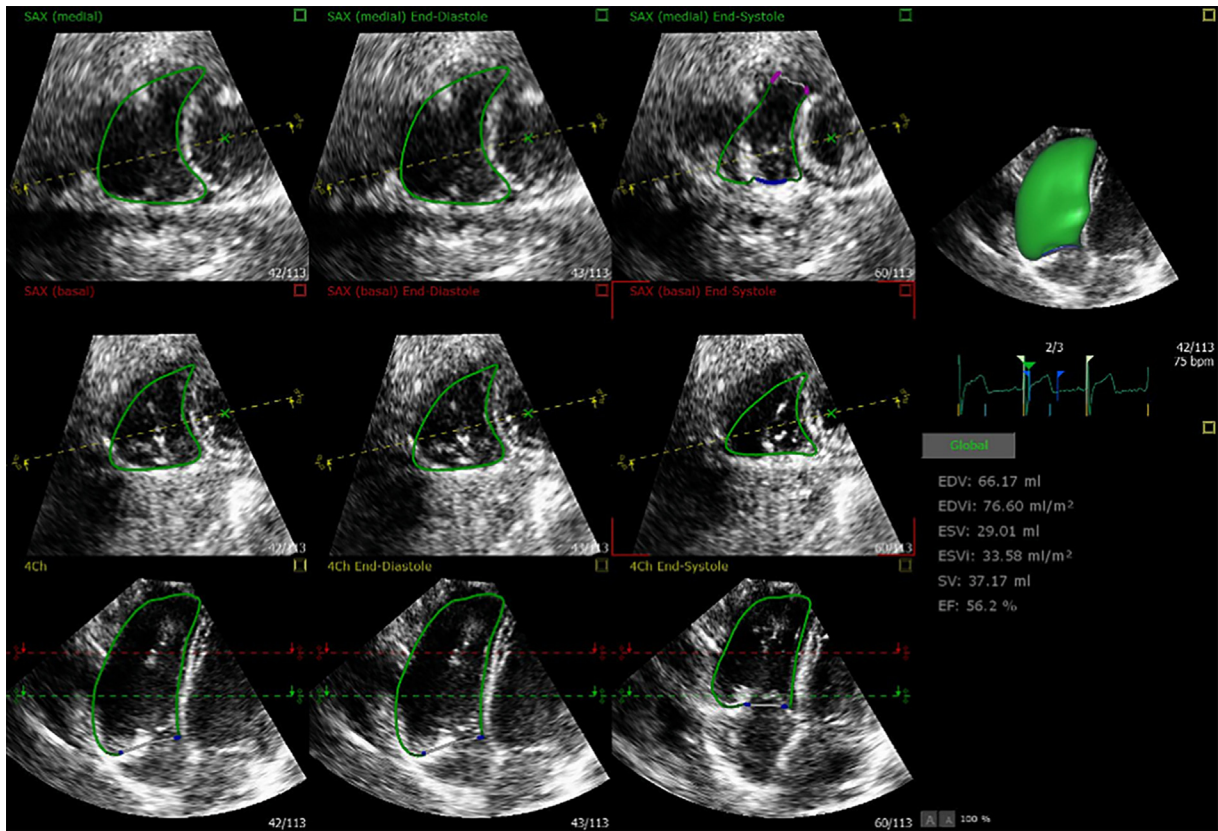


**Figure 26** Three-dimensional echocardiography: measurements of right ventricular volumes and calculation of right ventricular ejection fraction.

**Great Arteries and Their Proximal Branches**

**PAs.** The main PA courses anteriorly and superiorly from the right ventricle to the left of and anterior to the aorta before bifurcating into branch PAs. PA anatomy, size, and flow should be evaluated in pediatric TTE. PA stenosis or hypoplasia is often seen with tetralogy

of Fallot as well as genetic conditions like Williams or Alagille syndrome. Conversely, PA dilation is seen with isolated PV stenosis or “absent” PV, possibly because abnormal eccentric flow across the PV can lead to vessel wall weakness, as demonstrated by MRI studies in patients with a bicuspid PV.<sup>107</sup> PA dilation also results from significant left-to-right shunts with increased pulmonary blood flow (atrial



**Figure 27** Two-dimensional strain echocardiography: right ventricular (RV) global longitudinal strain (GLS) obtained from the RV-focused apical four-chamber view (although RV GLS is usually reported as the average of basal, mid, and apical lateral wall segments, including three septal segments as well may be useful as the septum contributes to RV ejection).

**Table 16** Evaluation of LV size and function

| Measurement                      | Modality/view   | Timing/calculation                    | Utility              | Strengths  | Weaknesses  |
|----------------------------------|---|---------------------------------------|----------------------|--|---|
| Guidelines (should be performed) |   |                                       |                      |  |   |
| Subjective assessment            | 2DE: subcostal, apical, and parasternal views                       | Throughout cardiac cycle              | LV size and function | <ul style="list-style-type: none"> <li>• Quick and simple</li> <li>• Provides context for other measurements</li> </ul>  | <ul style="list-style-type: none"> <li>• Depends on good blood-endocardium border</li> <li>• Regional functional abnormalities can limit accuracy</li> </ul>  |
| EDD                              | 2DE or M-mode: parasternal short-axis                               | Maximum diameter at end-diastole      | LV size              | <ul style="list-style-type: none"> <li>• Quick and simple</li> <li>• Used for SF calculation</li> <li>• 2DE: adjustable alignment to measure largest diameter that bisects both septum and posterior wall</li> <li>• M-mode: better temporal resolution</li> <li>• Normal data available</li> </ul>                        | <ul style="list-style-type: none"> <li>• Depends on good blood-endocardium border</li> <li>• Inappropriate for abnormal LV shape or regional functional abnormalities</li> <li>• M-mode: cannot correct for lateral cardiac motion during respiratory cycle</li> </ul>  |
| ESD                              | 2DE or M-mode: parasternal short-axis                               | Minimum diameter at end-systole       | LV size              | <ul style="list-style-type: none"> <li>• Same as above</li> </ul>  | <ul style="list-style-type: none"> <li>• Same as above</li> </ul>   |
| EDST                             | 2DE or M-mode: parasternal short-axis                               | Maximum diameter at end-diastole      | LV size              | <ul style="list-style-type: none"> <li>• Quick and simple</li> <li>• Used for RWT calculation</li> <li>• 2DE: adjustable alignment to measure along the axis of the largest diameter that bisects both septum and posterior wall</li> <li>• M-mode: better temporal resolution</li> <li>• Normal data available</li> </ul> | <ul style="list-style-type: none"> <li>• Same as above</li> </ul>   |
| EDPWT                            | 2DE or M-mode: parasternal short-axis                               | Maximum diameter at end-diastole      | LV size              | <ul style="list-style-type: none"> <li>• Same as above</li> </ul>  | <ul style="list-style-type: none"> <li>• Same as above</li> </ul>   |
| SF                               | 2DE or M-mode: parasternal short-axis                               | $(EDD - ESD)/EDD \times 100\%$        | LV systolic function | <ul style="list-style-type: none"> <li>• Quick and simple</li> <li>• Normal data available</li> <li>• Correlates well with MRI-derived EF</li> </ul>   | <ul style="list-style-type: none"> <li>• Depends on good blood-endocardium border</li> <li>• Measures only radial function and does not account for longitudinal function</li> <li>• Inappropriate for abnormal LV shape or regional functional abnormalities</li> <li>• Depends on loading conditions</li> </ul> |
| EDA                              | 2DE: parasternal short-axis or subcostal sagittal (short-axis) view | Maximum area at end-diastole          | LV size              | <ul style="list-style-type: none"> <li>• Used for LV volume and mass calculation</li> <li>• Appropriate for abnormal LV shape</li> </ul>   | <ul style="list-style-type: none"> <li>• Depends on good blood-endocardium border</li> </ul>  |
| EDA <sub>epi</sub>               | 2DE: parasternal short-axis or subcostal sagittal (short-axis) view | Maximum area at end-diastole          | LV size              | <ul style="list-style-type: none"> <li>• Used for LV volume and mass calculation</li> <li>• Appropriate for abnormal LV shape</li> </ul>   | <ul style="list-style-type: none"> <li>• Depends on good display of epicardium</li> <li>• Sector image must include entire LV myocardium</li> </ul>   |
| ESA                              | 2DE: parasternal short-axis or subcostal sagittal (short-axis) view | Minimum area at end-systole           | LV size              | <ul style="list-style-type: none"> <li>• Used for LV volume calculation</li> <li>• Appropriate for abnormal LV shape</li> </ul>  | <ul style="list-style-type: none"> <li>• Depends on good blood-endocardium border</li> </ul>  |
| EDL                              | 2DE: apical four-chamber or subcostal coronal (long-axis) view      | Just after MV closure at end-diastole | LV size              | <ul style="list-style-type: none"> <li>• Used for LV volume and mass calculation</li> <li>• Appropriate for abnormal LV shape</li> </ul>   | <ul style="list-style-type: none"> <li>• Depends on good blood-endocardium border, especially at apex</li> <li>• Foreshortening can limit accuracy</li> </ul>   |

(Continued)

Table 16 (Continued)

| Measurement             | Modality/view  | Timing/calculation  | Utility | Strengths   | Weaknesses  |
|-------------------------|--|---|---------|---|---|
| EDL <sub>epi</sub>      | 2DE: apical four-chamber or subcostal coronal (long-axis) view | Just after MV closure at end-diastole   | LV size | <ul style="list-style-type: none"> <li>Used for LV volume and mass calculation</li> <li>Appropriate for abnormal LV shape</li> </ul>                            | <ul style="list-style-type: none"> <li>Depends on good display of apical epicardium</li> <li>Foreshortening can limit accuracy</li> </ul>   |
| ESL                     | 2DE: apical four-chamber or subcostal coronal (long-axis) view | Just before MV opening at end-systole   | LV size | <ul style="list-style-type: none"> <li>Used for LV volume calculation</li> <li>Appropriate for abnormal LV shape</li> </ul>                                     | <ul style="list-style-type: none"> <li>Depends on good blood-endocardium border, especially at apex</li> <li>Foreshortening can limit accuracy</li> </ul>                                   |
| EDA <sub>lax</sub>      | 2DE: apical four-chamber and two-chamber views                 | Just after MV closure at end-diastole   | LV size | <ul style="list-style-type: none"> <li>Same as above</li> </ul>   | <ul style="list-style-type: none"> <li>Same as above</li> </ul>   |
| ESA <sub>lax</sub>      | 2DE: apical four-chamber and two-chamber views                 | Just before MV opening at end-systole   | LV size | <ul style="list-style-type: none"> <li>Same as above</li> </ul>   | <ul style="list-style-type: none"> <li>Same as above</li> </ul>   |
| EDV                     | Area-length method   | $5/6 \times \text{EDA} \times \text{EDL}$   | LV size | <ul style="list-style-type: none"> <li>Used for EF and LV mass calculation</li> <li>Appropriate for abnormal LV shape</li> <li>Normal data available</li> </ul> | <ul style="list-style-type: none"> <li>Same as above</li> </ul>   |
| EDV <sub>epi</sub>      | Area-length method   | $5/6 \times \text{EDA}_{\text{epi}} \times \text{EDL}_{\text{epi}}$                             | LV size | <ul style="list-style-type: none"> <li>Used for LV mass calculation</li> <li>Appropriate for abnormal LV shape</li> <li>Normal data available</li> </ul>        | <ul style="list-style-type: none"> <li>Depends on good display of epicardium</li> <li>Foreshortening can limit accuracy</li> <li>Sector images must include entire LV myocardium</li> </ul> |
| ESV                     | Area-length method   | $5/6 \times \text{ESA} \times \text{ESL}$   | LV size | <ul style="list-style-type: none"> <li>Used for EF calculation</li> <li>Appropriate for abnormal LV shape</li> <li>Normal data available</li> </ul>             | <ul style="list-style-type: none"> <li>Depends on good blood-endocardium border, especially at apex</li> <li>Foreshortening can limit accuracy</li> </ul>                                   |
| LVM                     | Area-length method   | $(\text{EDV}_{\text{epi}} - \text{EDV}) \times 1.05$  | LV size | <ul style="list-style-type: none"> <li>Appropriate for abnormal LV shape</li> <li>Normal data available</li> </ul>  | <ul style="list-style-type: none"> <li>Same as above</li> </ul>   |
| LV mass-to-volume ratio | Area-length method   | LVM/EDV   | LV size | <ul style="list-style-type: none"> <li>Used to distinguish concentric vs eccentric hypertrophy</li> </ul>   | <ul style="list-style-type: none"> <li>Same as above</li> </ul>   |
| LVM                     | M-mode   | $\{0.8 \times [1.04 \times (\text{EDD} + \text{EDST} + \text{EDPWT})^3 - \text{EDD}^3]\} + 0.6$ | LV size | <ul style="list-style-type: none"> <li>Quick and simple</li> </ul>  | <ul style="list-style-type: none"> <li>No normal pediatric data available</li> </ul>  |
| LVMi                    | M-mode   | LVM/BSA or LVM/height <sup>2.7</sup>  | LV size | <ul style="list-style-type: none"> <li>Quick and simple</li> <li>Used to determine hypertrophy</li> </ul>   | <ul style="list-style-type: none"> <li>No consensus on which approach is preferred in children</li> </ul>   |
| EDV                     | Method of disks  | Summation of disks using EDA <sub>lax</sub> and EDL   | LV size | <ul style="list-style-type: none"> <li>Used for EF calculation</li> <li>Appropriate for abnormal LV shape</li> <li>Normal data available</li> </ul>             | <ul style="list-style-type: none"> <li>Depends on good blood-endocardium border, especially at apex</li> <li>Foreshortening can limit accuracy</li> </ul>                                   |
| ESV                     | Method of disks  | Summation of disks using ESA <sub>lax</sub> and ESL   | LV size | <ul style="list-style-type: none"> <li>Same as above</li> </ul>   | <ul style="list-style-type: none"> <li>Same as above</li> </ul>   |

(Continued)

**Table 16** (Continued)

| Measurement   | Modality/view                                      | Timing/calculation                    | Utility   | Strengths  | Weaknesses   |
|---|--|---------------------------------------|---|--|--|
| EDV   | 3DE: apical view                                   | Just after MV closure at end-diastole | LV size   | <ul style="list-style-type: none"> <li>• Single-beat global assessment</li> <li>• No geometric assumptions</li> <li>• Correlates well with MRI-derived LV volume</li> <li>• Normal data available</li> </ul> | <ul style="list-style-type: none"> <li>• 3DE volume calculation software needed</li> <li>• Lower temporal resolution for single-beat acquisition</li> <li>• Depends on good blood-endocardium border, especially at apex</li> <li>• Foreshortening can limit accuracy</li> </ul> |
| ESV   | 3DE: apical view                                   | Just before MV opening at end-systole | LV size   | <ul style="list-style-type: none"> <li>• Same as above</li> </ul>  | <ul style="list-style-type: none"> <li>• Same as above</li> </ul>  |
| LVEF  | Area-length method, method of disks, or 3DE method | $(EDV - ESV)/EDV \times 100\%$        | LV systolic function                            | <ul style="list-style-type: none"> <li>• Appropriate for abnormal LV shape</li> <li>• Normal data available</li> </ul>   | <ul style="list-style-type: none"> <li>• Depends on good blood-endocardium border, especially at apex</li> <li>• Foreshortening can limit accuracy</li> <li>• Depends on loading conditions</li> </ul>   |
| Peak MV inflow velocity in early diastole (E)       | PW: apical four-chamber view                       | Early diastole                        | LV diastolic function                           | <ul style="list-style-type: none"> <li>• Quick and simple</li> <li>• Normal data available</li> <li>• No geometric assumptions</li> </ul>  | <ul style="list-style-type: none"> <li>• Respiratory variation necessitates averaging over three cardiac cycles</li> <li>• Fast heart rates can limit accuracy</li> </ul>  |
| Peak MV inflow velocity at atrial contraction (A)   | PW: apical four-chamber view                       | Atrial contraction                    | LV diastolic function                           | <ul style="list-style-type: none"> <li>• Same as above</li> </ul>  | <ul style="list-style-type: none"> <li>• Same as above</li> </ul>  |
| Mitral inflow E/A ratio                             | PW: apical four-chamber view                       | Diastole                              | LV diastolic function                           | <ul style="list-style-type: none"> <li>• Same as above</li> </ul>  | <ul style="list-style-type: none"> <li>• Same as above</li> </ul>  |
| Peak MV annular velocity in systole (s')            | Tissue Doppler: apical four-chamber view           | Systole                               | LV systolic function                            | <ul style="list-style-type: none"> <li>• Good temporal resolution</li> <li>• Normal data available</li> </ul>  | <ul style="list-style-type: none"> <li>• Depends on alignment</li> <li>• Depends on loading conditions</li> <li>• Not useful when regional functional abnormalities are present</li> </ul>   |
| Peak MV annular velocity in early diastole (e')     | Tissue Doppler: apical four-chamber view           | Early diastole                        | LV diastolic function                           | <ul style="list-style-type: none"> <li>• Same as above</li> </ul>  | <ul style="list-style-type: none"> <li>• Same as above</li> </ul>  |
| Peak MV annular velocity at atrial contraction (a') | Tissue Doppler: apical four-chamber view           | Atrial contraction                    | LV diastolic function                           | <ul style="list-style-type: none"> <li>• Same as above</li> </ul>  | <ul style="list-style-type: none"> <li>• Same as above</li> </ul>  |
| MV early diastolic E/e' ratio                       | PW and tissue Doppler: apical four-chamber view    | Early diastole                        | LV diastolic function                           | <ul style="list-style-type: none"> <li>• Normal data available</li> </ul>  | <ul style="list-style-type: none"> <li>• Same as above</li> </ul>  |
| Recommendations (may be performed)                  |  |                                       |   |  |  |
| Pulmonary vein S velocity                           | PW: apical or parasternal short-axis views         | Systole                               | LV systolic function                            | <ul style="list-style-type: none"> <li>• Quick and simple</li> </ul>   | <ul style="list-style-type: none"> <li>• Depends on alignment</li> </ul>   |
| Pulmonary vein D velocity                           | PW: apical or parasternal short-axis views         | Diastole                              | LV diastolic function, LA function, MV function | <ul style="list-style-type: none"> <li>• Quick and simple</li> </ul>   | <ul style="list-style-type: none"> <li>• Depends on alignment</li> </ul>   |
| Pulmonary vein A-wave reversal velocity             | PW: apical or parasternal short-axis views         | Diastole                              | LV diastolic function, LA function, MV function | <ul style="list-style-type: none"> <li>• Quick and simple</li> </ul>   | <ul style="list-style-type: none"> <li>• Depends on alignment</li> </ul>   |

(Continued)

Table 16 (Continued)

| Measurement                             | Modality/view                              | Timing/calculation   | Utility   | Strengths   | Weaknesses  |
|---|--|--|---|---|---|
| Pulmonary vein A-wave reversal duration | PW: apical or parasternal short-axis views | Diastole   | LV diastolic function, LA function, MV function | <ul style="list-style-type: none"> <li>• Quick and simple</li> </ul>  | <ul style="list-style-type: none"> <li>• Depends on alignment</li> </ul>  |
| Peak LV4                                | STE: apical four-chamber view              | Systole  | LV systolic function                            | <ul style="list-style-type: none"> <li>• No geometric assumptions</li> <li>• Single measurement (no calculations needed)</li> </ul>   | <ul style="list-style-type: none"> <li>• STE software needed</li> <li>• Requires good 2DE images</li> <li>• Intervendor variability</li> <li>• Minor angular dependence</li> </ul>            |
| Peak LV3                                | STE: apical three-chamber view             | Systole  | LV systolic function                            | <ul style="list-style-type: none"> <li>• Same as above</li> </ul>   | <ul style="list-style-type: none"> <li>• Same as above</li> </ul>   |
| Peak LV2                                | STE: apical two-chamber view               | Systole  | LV systolic function                            | <ul style="list-style-type: none"> <li>• Same as above</li> </ul>   | <ul style="list-style-type: none"> <li>• Same as above</li> </ul>   |
| Average GLS                             | STE: apical views                          | Systole: average GLS from LV4, LV3, and LV2                          | LV systolic function                            | <ul style="list-style-type: none"> <li>• Same as above</li> </ul>   | <ul style="list-style-type: none"> <li>• Same as above</li> </ul>   |
| RWT                                     | 2DE or M-mode: parasternal short-axis      | (EDST + EDPWT)/EDD   | LV size   | <ul style="list-style-type: none"> <li>• Quick and simple</li> <li>• 2DE: adjustable alignment to measure along the axis of the largest diameter that bisects both septum and posterior wall</li> <li>• M-mode: better temporal resolution</li> </ul> | <ul style="list-style-type: none"> <li>• Depends on good blood-endocardium border</li> <li>• M-mode: cannot correct for lateral cardiac motion during respiratory cycle</li> </ul>            |
| MPI                                     | PW, CW, or tissue Doppler: apical          | (IVCT + IVRT)/ET   | Combined LV systolic and diastolic function     | <ul style="list-style-type: none"> <li>• Normal data available</li> </ul>   | <ul style="list-style-type: none"> <li>• Needs similar heart rate in both images</li> <li>• No information regarding individual contributions of systolic or diastolic dysfunction</li> </ul> |
| IVA                                     | Tissue Doppler: apical four-chamber view   | MV peak isovolumic annular velocity divided by time to peak velocity | LV systolic function                            |   | <ul style="list-style-type: none"> <li>• Depends on alignment</li> <li>• High measurement variability</li> </ul>  |
| IVCT                                    | Tissue Doppler: apical four-chamber view   | Time from end of a' wave to beginning of s' wave                     | LV systolic function                            |   | <ul style="list-style-type: none"> <li>• Same as above</li> </ul>   |
| IVRT                                    | Tissue Doppler: apical four-chamber view   | Time from end of s' wave to beginning of e' wave                     | LV diastolic function                           |   | <ul style="list-style-type: none"> <li>• Same as above</li> </ul>   |

BSA, body surface area; EDA, end-diastolic short-axis area;  $EDA_{epi}$ , end-diastolic short-axis epicardial area;  $EDA_{lax}$ , end-diastolic long-axis area; EDD, end-diastolic diameter; EDL, end-diastolic length;  $EDL_{epi}$ , end-diastolic epicardial length; EDPWT, end-diastolic posterior wall thickness; EDST, end-diastolic septal thickness; EDV, end-diastolic volume;  $EDV_{epi}$ , end-diastolic epicardial volume; ESA, end-systolic short-axis area;  $ESA_{lax}$ , end-systolic long-axis area; ESD, end-systolic diameter; ESL, end-systolic length; ESV, end-systolic volume; IVA, isovolumic acceleration; IVCT, isovolumic contraction time; IVRT, isovolumic relaxation time; LV2, LV GLS from the apical two-chamber view; LV3, LV GLS from the apical three-chamber view; LV4, LV GLS from the apical four-chamber view; LVM, LV mass;  $LVMi$ , LV mass index; RWT, relative wall thickness; STE, speckle-tracking echocardiography.

or ventricular septal defect or patent ductus arteriosus), PA hypertension from increased pulmonary vascular resistance, connective tissue disorders (Marfan syndrome), or autoimmune conditions (Behçet disease).<sup>108</sup>

The parasternal short-axis view is used to evaluate and measure the diameters of the main and branch PAs from inner edge to inner edge in mid-systole at their largest dimension (Figure 13). If the branch PAs do not originate symmetrically from the main PA, careful sweeps are important to exclude a left PA sling or branch PAs with superior-inferior relationship. The suprasternal short-axis view can show the right PA as it crosses behind the ascending aorta, and the high left

parasternal sagittal and suprasternal long-axis views are useful for evaluation of the left PA. Color mapping can evaluate for stenosis or for the presence of a patent ductus arteriosus with diastolic retrograde flow in the main PA (Figure 12). Doppler interrogation of the main PA should be performed in parasternal short-axis views or modified apical views with anterior tilting. Doppler interrogation of the branch PAs should be performed in parasternal, suprasternal, or high left parasternal short-axis views. The mean PA pressure can be estimated by adding the peak pulmonary regurgitation pressure gradient during early diastole to an assumed RA pressure of 5 to 10 mm Hg. The PA diastolic pressure can be estimated by adding

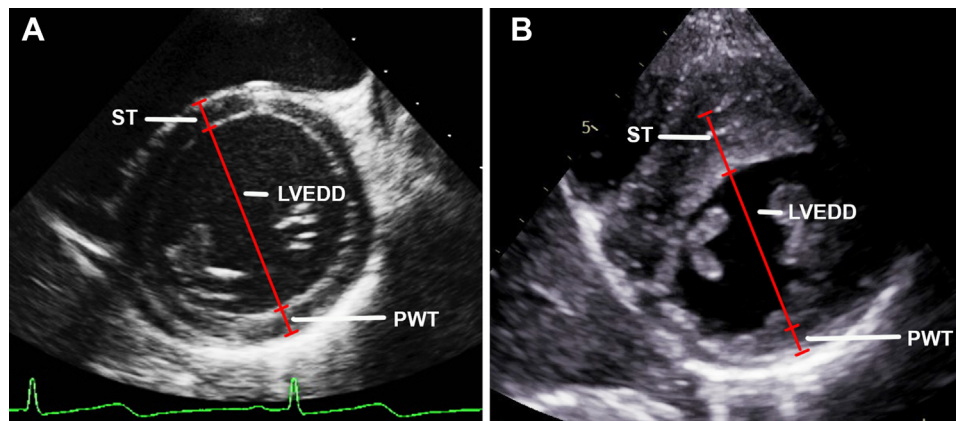


**Figure 28** Parasternal short-axis view showing left ventricular (LV) minor-axis internal diameter (LVEDD), posterior wall thickness (PWT), and septal wall thickness (ST; the internal diameter is a good surrogate of LV size only when the LV short-axis geometry is circular) in **(A)** a normal heart and **(B)** hypertrophic cardiomyopathy. Reproduced with permission from Lopez *et al.*<sup>2</sup>

the minimum pulmonary regurgitation pressure gradient at end-diastole to the same assumed RA pressure. It is important to remember that a high-velocity ductal jet can confound Doppler interrogation of the pulmonary regurgitant jet for estimating PA pressure.

**CAs.** The right and left CAs originate from the aortic sinuses of Valsalva and course along the coronary sulci of the myocardium. Imaging requires evaluation of the origin, size, and proximal course of individual CAs. Because they are small, superficial structures, CAs are best spatially resolved with high-frequency transducers. Frame rates should be optimized by reducing depth and sector size, and the zoom feature or increased magnification should be used when appropriate. Harmonics and increased compression should be used with caution because harmonics and too much gain may exaggerate echogenicity of the CA walls, making them appear abnormal, and excessive compression may filter out subtle abnormalities such as a thrombus within the lumen of the vessel.<sup>109</sup>

The parasternal short-axis view should be used to evaluate the left main, left anterior descending, circumflex, and proximal right CAs (Figure 10A). The parasternal long-axis view can show the anterior right CA origin from the aortic root (Figure 10B) and the circumflex

CA in the left AV groove. A modified parasternal long-axis view with rightward and posteroinferior tilting can show the posterior descending CA in the posterior interventricular groove (Figure 10C). A modified apical view with posterior tilting can show the distal right CA in the posterior right AV groove (Figure 10D), and one with anterior tilting can show the left main CA and its bifurcation into the left anterior descending and circumflex CAs. CA diameters should be measured at the point of maximum expansion. CA dilation occurs in the setting of Kawasaki disease, multisystem inflammatory syndrome in children after COVID-19 infection, juvenile rheumatoid arthritis, polyarteritis nodosa, ventricular hypertrophy, or a significant CA fistula.<sup>7,110</sup> Z scores help determine abnormal size, and serial measurements help evaluate disease progression and direct treatment strategies when needed. As previously discussed, the same Z score model should be used when determining growth trends over time in an individual patient and when assessing clinical outcomes and risk in a particular patient population because of the known differences among currently available Z score models.<sup>19</sup>

Color mapping of CA flow is crucial when abnormal origin must be excluded in the setting of cardiomyopathy, syncope, chest pain, or some CHDs,<sup>111</sup> using a low Nyquist limit to confirm appropriate antegrade

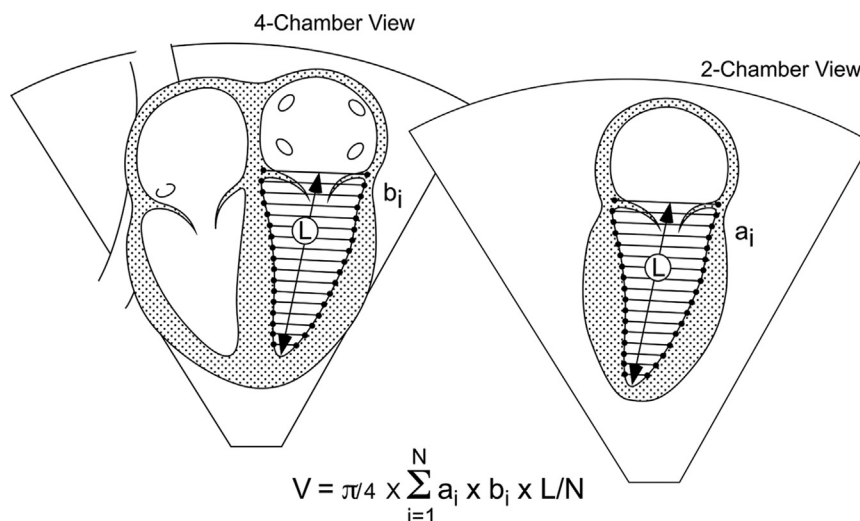


**Figure 29** Modified Simpson biplane method (method of disks) approach to estimate left ventricular volumes from apical four-chamber and two-chamber views. Reproduced with permission from Lopez *et al.*<sup>2</sup>

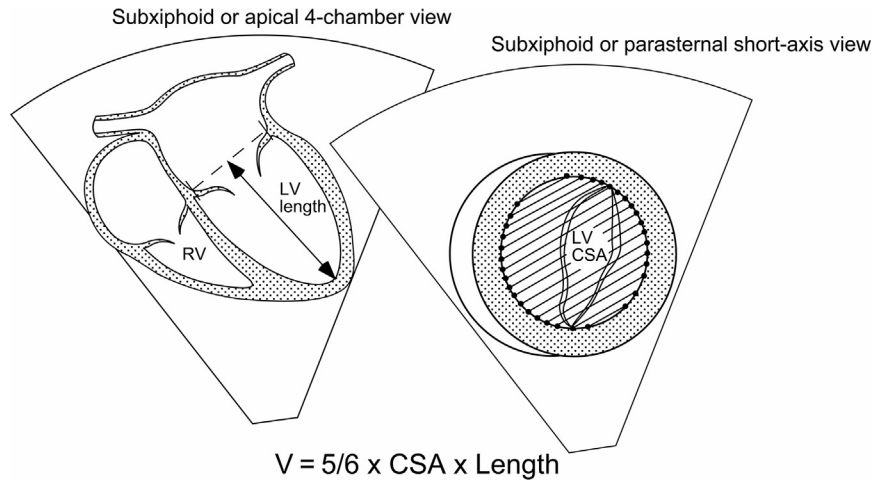


**Figure 30** Bullet (5/6 area-length) method to estimate left ventricular (LV) volumes from measurements of LV long-axis length and short-axis area. Reproduced with permission from Lopez *et al.*<sup>2</sup> CSA, Cross-sectional area; RV, right ventricle.

flow and differentiate CAs from coronary veins or artifact. Still images alone do not provide adequate diagnostic information. In fact, both 2DE and color mapping in parasternal short-axis views are needed to confirm normal origins of the right and left CAs. Doppler interrogation of flow should be performed with a real-time electrocardiogram to confirm timing of flow during the cardiac cycle. Flow reversal is suggestive of anomalous origin from the PA or coronary ostial atresia.<sup>112</sup>

**Aorta.** Serial aortic assessment is essential in the management of (1) aortic dilation as seen in connective tissue disease (Marfan or Loeys-Dietz syndrome), genetic disorders (Turner syndrome), and bicuspid AoVs<sup>113-116</sup>; (2) supralvalvar aortic stenosis as seen in Williams syndrome or other mutations of the *ELN* gene; or (3) aortic arch anomalies in isolation or with other cardiac abnormalities. The parasternal long-axis view should be used to visualize the proximal aorta, including the aortic root (at the sinuses of Valsalva), sinotubular junction, and ascending aorta (at the level of the right PA; **Figure 33**). High left or right parasternal views may provide better visualization of the proximal aorta. Aortic diameters in children should be measured from inner edge to inner edge at their maximum dimension during peak flow in mid-systole.<sup>2</sup> This guideline is distinct from those in adult echocardiography that recommend measurement of aortic diameters

from leading edge to leading edge in diastole,<sup>35</sup> particularly because pediatric aortic Z scores are all based on systolic measurements. In addition, the maximum effect of vascular size on vessel function occurs during peak flow, such that peak systolic wall stress becomes the primary determinant of dissection or rupture in patients with aortic dilation. Aortic diameters should be measured consistently so that they can be compared with prior studies and trends can be followed over time.

The aortic arch should be evaluated in suprasternal views with hyperextension of the neck. Both 2D imaging and color mapping during a superior sweep in the short-axis view can establish arch sidedness and display the innominate artery as it bifurcates into the carotid and subclavian arteries. Absence of this bifurcation raises the suspicion for an aberrant subclavian artery and its associated clinical implications. The suprasternal long-axis view should be used to visualize the transverse aortic arch, arch branches, and proximal descending aorta, with diameter measurements performed at the proximal and distal transverse arch and the aortic isthmus (**Figure 14B**). Increased distance between the left common carotid and left subclavian arteries, tapering or a posterior muscular shelf at the isthmus, and flow turbulence with color mapping should raise suspicion for aortic coarctation. Sweeps with color mapping in a high parasternal sagittal or suprasternal long-axis view

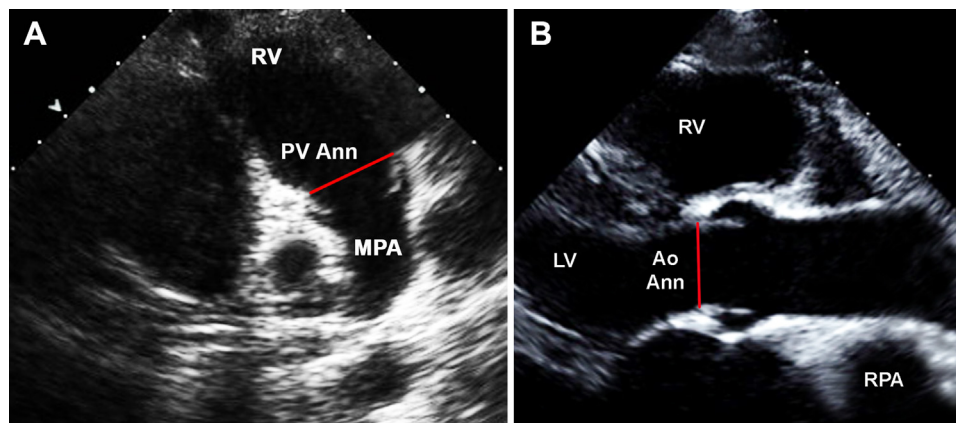


**Figure 31** Aortic valve and pulmonary valve (PV) annular diameter measurements during maximal valve opening in early to mid-systole: **(A)** PV annular diameter from the parasternal long-axis view with anterosuperior tilting and **(B)** Aortic valve annular diameter from the parasternal long-axis view. Reproduced with permission from Lopez *et al.*<sup>2</sup> Ann, Annulus; Ao, aortic; LV, left ventricle; MPA, main pulmonary artery; RPA, right PA; RV, right ventricle.

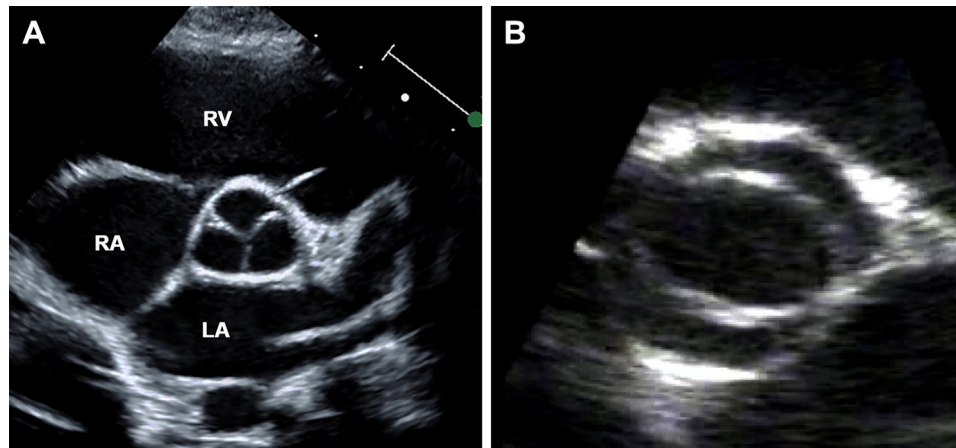


**Figure 32** Parasternal short-axis view: **(A)** trileaflet aortic valve and **(B)** bicuspid or bileaflet aortic valve with fusion of the intercoronary commissure. LA, Left atrium; RA, right atrium; RV, right ventricle.

should be used to exclude a patent ductus arteriosus. If present, spectral Doppler interrogation should evaluate the direction of ductal flow throughout the cardiac cycle and the degree of restriction. It is especially important to determine arch sidedness if a patent ductus arteriosus is likely to require surgical intervention to establish the side where the thoracotomy will be performed.

Doppler interrogation of flow in the ascending aorta should be performed in an apical three-chamber, suprasternal long-axis, right parasternal sagittal, or subcostal coronal view, especially if subvalvar, valvar, or supra-valvar aortic stenosis is suspected. Stepwise PW and CW Doppler interrogation should be performed along the aortic arch and proximal descending aorta to characterize potential areas of obstruction. PW Doppler interrogation of the abdominal aorta in the subcostal sagittal view should be performed when possible, and the spectral Doppler pattern should normally have a brisk upstroke and return to baseline (Figure 3A). The abdominal aortic Doppler pattern in the setting of significant aortic arch obstruction presents with a dampened upstroke and/or diastolic delay in return to baseline

(Figure 3B). In the setting of arch obstruction, CW Doppler interrogation of the aortic arch in suprasternal long-axis views may reveal a characteristic pattern with two peaks superimposed upon one another: the higher velocity outer envelope reflects flow across the obstructed area, and the lower velocity dense inner envelope represents flow proximal to the coarctation site. When there is a large aortopulmonary shunt (such as a patent ductus arteriosus, aortopulmonary window, or arteriovenous malformation) or at least moderate aortic regurgitation, the abdominal aortic Doppler pattern typically reveals holodiastolic flow reversal (Figure 3C).

### Key Points and Recommendations

- The main and branch PAs, aortic segments, and arch branches should be evaluated in parasternal and suprasternal views.
- The CAs should be evaluated in parasternal views.
- Sweeps with color mapping in a high left parasternal sagittal or suprasternal long-axis view should be used to evaluate for a patent ductus arteriosus.

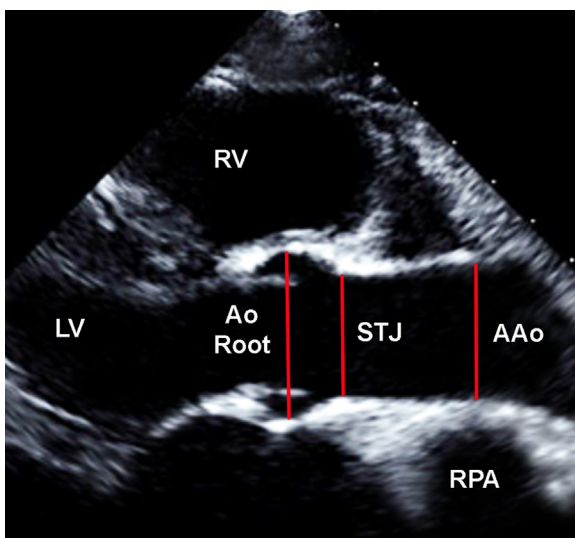


**Figure 33** Parasternal long-axis view during maximal valve opening in early to mid-systole: proximal aortic diameters at the aortic root (Ao Root), sinotubular junction (STJ), and ascending aorta (AAo). Reproduced with permission from Lopez et al.<sup>2</sup> LV, Left ventricle; RPA, right PA; RV, right ventricle.

### REPORTING

Two-dimensional echocardiographic data interpretation is a standard skill for all pediatric cardiologists and a major focus during training.<sup>1</sup> The core and advanced knowledge elements needed to perform pediatric TTE as listed in Table 5 are the same as those needed for interpretation. In addition, accurate interpretation also requires a review of the clinical history and an understanding of the indications for the

**Table 17** Common nomenclature systems for pediatric and congenital heart diseases

- International Society for Nomenclature of Paediatric and Congenital Heart Disease<sup>117</sup>
- Association for European Paediatric Cardiology: European Paediatric Cardiac Code
- Society of Thoracic Surgeons
- Robert Anderson, London
- Richard and Stella Van Praagh and Donald Fyler, Boston
- Paul Weinberg, Philadelphia

**Table 18** Standards and guidelines for the components of a pediatric transthoracic echocardiographic report<sup>119</sup>

| Standard report components   |
|--|
| Demographic data   |
| <ul style="list-style-type: none"> <li>Name</li> <li>Medical record number</li> <li>Date of birth</li> </ul>   |
| Clinical data  |
| <ul style="list-style-type: none"> <li>Indication(s) for study</li> <li>Prior diagnoses</li> <li>Prior interventions</li> <li>Height or length</li> <li>Weight</li> <li>Body surface area</li> <li>Body mass index</li> <li>Blood pressure</li> <li>Oxygen saturation if available</li> </ul>  |
| Study information  |
| <ul style="list-style-type: none"> <li>Date and time of study</li> <li>Location of study</li> <li>Echocardiographic modalities performed               <ul style="list-style-type: none"> <li>2D imaging</li> <li>M-mode echocardiography</li> <li>Color mapping</li> <li>Spectral Doppler interrogation</li> <li>3DE</li> <li>Strain analysis</li> </ul> </li> <li>Complete vs focused study</li> <li>Ordering clinician name and contact information</li> <li>Primary physician if different from ordering physician</li> <li>Sonographer or performing physician</li> <li>Interpreting physician</li> </ul> |
| Critical findings  |
| <ul style="list-style-type: none"> <li>Name of clinician notified of findings</li> <li>Timing of notification</li> </ul>   |
| Summary  |
| <ul style="list-style-type: none"> <li>Findings directly related to indication for study</li> <li>Organized list of pertinent positive and negative findings</li> <li>Limitations to study               <ul style="list-style-type: none"> <li>Poor windows</li> <li>Patient movement</li> <li>Clinical instability</li> <li>Physical barriers (tracheostomy, open chest, chest tubes)</li> </ul> </li> <li>Comparison with findings in prior study if appropriate</li> </ul>   |
| Measurements   |
| <ul style="list-style-type: none"> <li>Organized by segment</li> <li>Designation of each measurement as normal or abnormal               <ul style="list-style-type: none"> <li>Z scores if available</li> <li>Normal reference ranges if available</li> </ul> </li> </ul>   |
| Doppler evaluation   |
| <ul style="list-style-type: none"> <li>All measured mean and peak velocities and/or gradients               <ul style="list-style-type: none"> <li>Valves</li> <li>Vessels</li> <li>Shunts</li> </ul> </li> <li>Severity of stenotic structures if appropriate</li> <li>Severity of regurgitant valves if appropriate</li> <li>Estimation of RV systolic pressure on the basis of the velocity of the tricuspid regurgitation jet</li> </ul>   |
| Study findings   |
| <ul style="list-style-type: none"> <li>Visceral and cardiac situs</li> <li>Segmental anatomy</li> <li>Systemic and pulmonary veins</li> </ul>  |

(Continued)

**Table 18** (Continued)

| Standard report components  |
|---|
| <ul style="list-style-type: none"> <li>Atria and atrial septum.</li> <li>AV valves</li> <li>Ventricles and ventricular septum</li> <li>Outflow tracts</li> <li>Arteries (including CAs)</li> <li>Patent ductus arteriosus if present</li> <li>Pericardium</li> <li>Pleura and diaphragm if appropriate</li> <li>Documentation of any structure not well visualized</li> </ul> |
| Signature of interpreting physician   |
| Date and time of report completion  |

study as well as the specific questions that need to be answered. Challenges in image acquisition occur when the patient is uncooperative or when acoustic windows are poor because of obesity, a chest wall deformity, lung hyperexpansion or unilateral hypoplasia, a mediastinal mass, scarring from prior operations, surgical dressings, chest tubes, tracheostomy, mechanical circulatory support, or an open chest. In addition, the time to obtain images may be limited in a critically ill patient, such as a child being cannulated for extracorporeal membrane oxygenation support. All limitations should be documented on the report to suggest the potential need for repeat imaging or use of other diagnostic modalities. In addition, one should distinguish structures that are not well evaluated because of technical limitations vs structures that may be abnormally absent, occluded, or thrombosed, thereby requiring further evaluation. Lastly, tachycardia or bradycardia should be noted when present, and differences in heart rates should be documented when comparing ventricular function over serial studies.

Conveying a clear and universally understandable description of the findings is crucial in an echocardiographic report. Multiple nomenclature systems have been used to characterize and categorize abnormal morphology in CHD (Table 17), resulting in variable definitions and terminology for the same lesion or the same terminology for variable lesions. Coexistence of these systems within one center can lead to poor communication, confusion, and misunderstanding for sonographers, trainees, cardiologists, and cardiothoracic surgeons. International consensus documents to establish echocardiographic

**Table 19** Potential critical findings during the performance of pediatric TTE<sup>13</sup>

|   |
|---|
| <ul style="list-style-type: none"> <li>New critical CHD               <ul style="list-style-type: none"> <li>Duct-dependent lesion                   <ul style="list-style-type: none"> <li>Critical aortic stenosis</li> <li>Critical pulmonary stenosis</li> <li>Critical aortic coarctation</li> <li>Functional single ventricle with severe pulmonary stenosis or pulmonary atresia</li> <li>Hypoplastic left heart syndrome</li> </ul> </li> <li>Total anomalous pulmonary venous return                   <ul style="list-style-type: none"> <li>Infradiaphragmatic type</li> <li>Other type with obstruction</li> </ul> </li> </ul> </li> <li>New moderate or severe ventricular systolic dysfunction</li> <li>New severe valvar regurgitation or stenosis</li> <li>New moderate or large pericardial effusion</li> <li>New intracardiac vegetation or mass</li> <li>New pulmonary hypertension with pulmonary arterial pressure greater than two thirds systemic pressure</li> <li>Significant change compared with the previous study</li> </ul> |
|---|

**Table 20** Methods for QA using the dimensions of care framework<sup>120</sup>

| Quality elements      | QA methods  |
|-----------------------|---|
| Laboratory structure  | Accreditation through professional societies<br>Maintenance of standards for laboratory equipment<br>Training and credentialing of physicians and sonographers<br>Protocol for audit and feedback of quality issues<br>Participation in multicenter QI collaboratives |
| Patient selection     | Implementation of AUC<br>Utility of other guidelines for echocardiographic indications<br>Safety protocols for the use of sedation<br>Documentation of adverse events related to sedation   |
| Image acquisition     | Standardized imaging protocols<br>Protocol for audit and feedback of image quality<br>Protocol for audit and feedback of study comprehensiveness  |
| Image interpretation  | Evaluation of interreader and intrareader variability<br>Correlation with other imaging modalities, surgical findings, or pathology<br>Feedback of accuracy and reproducibility of image interpretation   |
| Results communication | Standardized reporting structure<br>Evaluation of timeliness of reporting critical results  |
| Improved outcomes     | Metrics for measuring patient outcomes<br>Patient satisfaction survey<br>Feedback from referring physicians   |

data standards and common nomenclature that cross-map terms from the various systems have been published to mitigate these challenges.<sup>117,118</sup> Until these systems are used routinely in everyday practice by all stakeholders, it is important for individual centers to agree upon common nomenclature that all members of the team know and understand.

The 2006 ASE pediatric guidelines list the minimum standard elements of a pediatric echocardiographic report.<sup>1</sup> In addition, the Intersocietal Accreditation Commission regularly publishes updated guidelines on the components of a report needed to achieve accreditation (Table 18).<sup>119</sup> Reports should be standardized and consistent within each center. A well-organized and succinct summary should convey the relevant anatomic and hemodynamic findings in an understandable and cohesive manner to facilitate optimal communication and patient care delivery. Comparison with findings from prior studies should be reported if appropriate. Measurements along with normal reference ranges and Z scores when available should be presented in an organized fashion, using tables when possible. All anatomic and hemodynamic findings should be organized and presented using the segmental approach. When structures that are important to the clinical question are not evaluated (such as CAs in the setting of chest pain), this should be documented in the report.

Standards for timely interpretation and reporting of pediatric TTE are available.<sup>119</sup> Stat or emergent studies should be interpreted shortly after completion. When possible, studies performed in a pediatric echo-

cardiography laboratory should be reviewed with a physician after image acquisition to ensure the absence of critical findings and to determine if additional imaging is needed. Finalized reports for routine inpatient TTE studies should be available within 24 hours of image acquisition. A list of critical findings should be created so that sonographers and fellows can immediately review a critical finding with an attending physician, who in turn should communicate the finding to the appropriate clinical caregiver or team (Table 19). The ACPC Quality Network has established a quality metric related to critical findings and determined that reporting of critical findings should occur within 1 to 2 hours of detection of the finding.<sup>13</sup> Critical findings should be communicated using nonroutine and urgent methods, including a direct phone call, in-person discussion, or text message, with the expectation of confirmation that the message has been received. If the referring caregiver or team is not available, another caregiver who can immediately address the critical finding should be contacted. Documentation of the time of communication and the clinical caregiver who was contacted should be included in the finalized report.

### Key Points and Recommendations

- Multiple nomenclature systems are available to describe CHDs.
- TTE reports should use nomenclature that everyone understands in a center.
- Standardized TTE reports should contain a succinct and focused summary, measurements with Z scores and/or normal reference ranges, and a description of all findings organized in a segmental fashion.
- Reports should be available in a reasonable period after study performance, and all critical findings should be communicated promptly to the appropriate caregiver.

### Quality Assurance

A robust QA and quality improvement (QI) program should be implemented. QA and QI activities require support from all stakeholders, including physicians, sonographers, hospital administrators, referring providers, patients, and their caregivers. Applying the “dimensions of care” framework for quality in cardiovascular imaging as defined by the American College of Cardiology, the ASE has used the structure-process-outcome model from Donabedian’s methodology to establish recommendations for quality echocardiography operations (Table 20).<sup>120</sup> Structural indicators of quality are the resources needed to provide effective TTE services, including appropriate facilities, equipment, staffing, training, and credentialing. The Intersocietal Accreditation Commission has established specific standards and guidelines related to these structural elements to achieve accreditation.<sup>119</sup> Process indicators are the activities and tasks needed to perform TTE, and the four domains of the imaging process that affect clinical outcomes are patient selection, image acquisition, interpretation, and results communication.

QA related to patient selection has been aided by the availability of AUC documents and disease-specific guidelines.<sup>4,9</sup> Because of the wide range in TTE order appropriateness among providers and echocardiography laboratories, educational interventions with audit and feedback for ordering clinicians and integration of AUC into the electronic health system as decision-support tools can improve quality in this domain.<sup>121,122</sup> QA related to image acquisition, interpretation, and reporting should occur in the setting of the significant practice variability within a center, particularly in terms of quantification.<sup>123</sup> Quality metrics have been published by the ACPC Quality

Network to help with best practices for image quality and performing a comprehensive pediatric TTE (Table 2),<sup>13</sup> and various QI methodologies related to image acquisition have been published.<sup>124,125</sup> Diagnostic accuracy and interobserver reproducibility are also important components of QA. Using the pediatric echocardiography error taxonomy model published in 2008,<sup>126</sup> another ACPC quality metric on diagnostic accuracy provides a framework for pediatric cardiac surgical programs to track diagnostic errors in echocardiography, categorize their severity in terms of clinical impact, and determine their preventability.<sup>13</sup> A similar initiative could be implemented in nonsurgical centers. The Intersocietal Accreditation Commission pediatric TTE standards and guidelines require two annual QI meetings for each facility to discuss diagnostic errors and establish corrective initiatives to address systemwide practices that contribute to the errors.<sup>119</sup> In addition, the accreditation process requires structured quarterly assessments of the following: (1) technical quality of TTE images; (2) correlation of reported findings with other modalities, surgical findings, or clinical outcomes; (3) physician interpretation variability; and (4) report completeness and timeliness.

QI activities related to the communication of results have been discussed above. Because patient satisfaction is a component of outcomes in this model, all facilities should establish a process in which feedback from patients, families, and referring providers is solicited regularly in an organized fashion. Finally, opportunities for using big data analysis from multicenter QI collaboratives and artificial intelligence to connect echocardiographic data with patient outcomes may also be explored.

## Key Points and Recommendations

- Centers and practices should develop and implement QA and QI programs to periodically review and measure the quality of echocardiographic services.

## SUMMARY

Pediatric TTE has provided valuable diagnostic information to the pediatric and congenital cardiology community for many decades. Since the publication of the ASE pediatric TTE guidelines in 2006 and 2010, there have been significant advances in the knowledge of pediatric and CHD as it relates to genetics, embryology, morphology, myocardial mechanics, vascular function, and blood flow dynamics. In addition, improvements in transducer technology and image processing as well as continued development of more robust and effective artificial intelligence algorithms have broadened the capabilities of TTE to provide accurate and reliable anatomic and physiologic information for children with heart disease. Two-dimensional echocardiography, M-mode, and Doppler evaluation continue to be the mainstay of pediatric TTE, but the armamentarium of adjunct diagnostic tools has expanded to include 3DE, STE, and the use of contrast agents. Although it is not discussed in this document because it is not an adjunct modality during standard pediatric TTE, transthoracic stress echocardiography is gaining increased use in children, particularly in the setting of valve disease, CA abnormalities, hypertrophic cardiomyopathy, and heart transplantation.<sup>127,128</sup> Minimal guidelines for its use and interpretation in pediatrics are included in the ASE stress echocardiography guidelines and standards for adults,<sup>129</sup> but detailed recommendations have not yet been published.

In developing this update to the 2006 and 2010 documents, there has been significant effort to distinguish between guidelines as practices that should be performed and additional or adjunct recommendations

as practices that may be performed during a complete pediatric TTE and to avoid describing practices that must be part of an examination. These recommendations result from a consensus of expert opinions based on published pediatric guidelines, reports of studies involving pediatric and congenital echocardiography, and clinical experience. It is important to recognize that the clinical scenario should always be considered during the performance of pediatric TTE, allowing flexibility when patients are unstable, uncomfortable, or uncooperative. Tables and figures in this document serve as guides for various aspects of pediatric and congenital TTE. They may need to be updated on a regular basis as knowledge and technology continue to evolve. In the current era, pediatric TTE is still limited in its ability to provide accurate data as it relates to cardiac output, relative flow between the pulmonary and systemic vascular beds, pulmonary vascular disease, and valve disease. In addition, many echocardiographic parameters used routinely in adult echocardiography laboratories have not yet been validated for standard pediatric use. Further research in children is needed for these and other areas, particularly in terms of the relationship between echocardiographic parameters and clinical outcomes in acquired and CHD, assessment of diastolic function in general, quantification of systolic and diastolic function for the right ventricle and the single ventricle, use of artificial intelligence and machine learning in pediatric echocardiography, and pediatric applications of strain imaging and contrast echocardiography. Advances in all these domains can only improve the care of children with suspected, acquired, or CHD.

## NOTICE AND DISCLAIMER

This report is made available by ASE as a courtesy reference source for members. This report contains recommendations only and should not be used as the sole basis to make medical practice decisions or for disciplinary action against any employee. The statements and recommendations contained in this report are primarily based on the opinions of experts, rather than on scientifically-verified data. ASE makes no express or implied warranties regarding the completeness or accuracy of the information in this report, including the warranty of merchantability or fitness for a particular purpose. In no event shall ASE be liable to you, your patients, or any other third parties for any decision made or action taken by you or such other parties in reliance on this information. Nor does your use of this information constitute the offering of medical advice by ASE or create any physician-patient relationship between ASE and your patients or anyone else.

## CONFLICTS OF INTEREST

The authors reported no actual or potential conflicts of interest in relation to this document.

## ACKNOWLEDGMENTS

This document was reviewed by members of the 2022-2023 ASE Guidelines and Standards Committee, ASE Board of Directors, ASE Executive Committee, and designated reviewers (Karima Addetia, MD, Brittany Byrd, RDCS, Noreen Kelly, MD, David Dudzinski, MD, David Orsinelli, MD, Anitha Parthiban, MD, Alan Pearlman, MD, Andrew Pellet, PhD, RDCS, Fadi Shamoun, MD, Kenan Stern, MD, Brian Soriano, MD, Elif Selamet Tierney, MD, Melissa Wasserman, RDCS, David H. Wiener, MD, Bo Xu, MD).

## REFERENCES

1. Lai WW, Geva T, Shirali GS, et al. Guidelines and standards for performance of a pediatric echocardiogram: a report from the task force of the Pediatric Council of the American Society of Echocardiography. *J Am Soc Echocardiogr* 2006;19:1413-30.
2. Lopez L, Colan SD, Frommelt PC, et al. Recommendations for quantification methods during the performance of a pediatric echocardiogram: a report from the pediatric measurements Writing group of the American Society of Echocardiography Pediatric and Congenital Heart Disease Council. *J Am Soc Echocardiogr* 2010;23:465-95.
3. Valente AM, Cook S, Festa P, et al. Multimodality imaging guidelines for patients with repaired tetralogy of Fallot: a report from the American Society of Echocardiography: developed in collaboration with the Society for Cardiovascular Magnetic Resonance and the Society for Pediatric Radiology. *J Am Soc Echocardiogr* 2014;27:111-41.
4. Campbell RM, Douglas PS, Eidem BW, et al. ACC/AAP/AHA/ASE/HRS/SCAI/SCCT/SCMR/SOPE 2014 appropriate use criteria for initial transthoracic echocardiography in outpatient pediatric cardiology: a report of the American College of Cardiology appropriate use criteria task force, American Academy of Pediatrics, American Heart Association, American Society of Echocardiography, Heart Rhythm Society, Society for Cardiovascular Angiography and Interventions, Society of Cardiovascular Computed Tomography, Society for Cardiovascular Magnetic Resonance, and Society of Pediatric Echocardiography. *J Am Coll Cardiol* 2014;64:2039-60.
5. Cohen MS, Eidem BW, Cetta F, et al. Multimodality imaging guidelines of patients with transposition of the great arteries: a report from the American Society of Echocardiography developed in collaboration with the Society for Cardiovascular Magnetic Resonance and the Society of Cardiovascular Computed Tomography. *J Am Soc Echocardiogr* 2016;29:571-621.
6. Simpson J, Lopez L, Acar P, et al. Three-dimensional echocardiography in congenital heart disease: an expert consensus document from the European Association of Cardiovascular Imaging and the American Society of Echocardiography. *J Am Soc Echocardiogr* 2017;30:1-27.
7. McCrindle BW, Rowley AH, Newburger JW, et al. Diagnosis, treatment, and long-term management of Kawasaki disease: a scientific statement for health professionals from the American Heart Association. *Circulation* 2017;135:e927-99.
8. Puchalski MD, Lui GK, Miller-Hance WC, et al. Guidelines for performing a comprehensive transesophageal echocardiographic examination in children and all patients with congenital heart disease: recommendations from the American Society of Echocardiography. *J Am Soc Echocardiogr* 2019;32:173-215.
9. Sachdeva R, Valente AM, Armstrong AK, et al. ACC/AHA/ASE/HRS/ISACHD/SCAI/SCCT/SCMR/SOPE 2020 appropriate use criteria for multimodality imaging during the follow-up care of patients with congenital heart disease: a report of the American College of cardiology solution set oversight committee and appropriate use criteria task force, American Heart Association, American Society of Echocardiography, Heart Rhythm Society, International Society for Adult Congenital Heart Disease, Society for Cardiovascular Angiography and Interventions, Society of Cardiovascular Computed Tomography, Society for Cardiovascular Magnetic Resonance, and Society of Pediatric Echocardiography. *J Am Coll Cardiol* 2020;75:657-703.
10. Frommelt P, Lopez L, Dimas VV, et al. Recommendations for multimodality assessment of congenital coronary anomalies: a guide from the American Society of Echocardiography developed in collaboration with the Society for Cardiovascular Angiography and Interventions, Japanese Society of Echocardiography, and Society for Cardiovascular Magnetic Resonance. *J Am Soc Echocardiogr* 2020;33:259-94.
11. Baggish AL, Battle RW, Beaver TA, et al. Recommendations on the use of multimodality cardiovascular imaging in young adult competitive athletes: a report from the American Society of Echocardiography in collaboration with the Society of Cardiovascular Computed Tomography and the Society for Cardiovascular Magnetic Resonance. *J Am Soc Echocardiogr* 2020;33:523-49.
12. Wasserman MA, Shea E, Cassidy C, et al. Recommendations for the adult cardiac sonographer performing echocardiography to screen for critical congenital heart disease in the newborn: from the American Society of Echocardiography. *J Am Soc Echocardiogr* 2021;34:207-22.
13. ACC. Adult Congenital and Pediatric Cardiology Quality Network Quality Metrics. <https://cvquality.acc.org/initiatives/acpc-quality-network/quality-metrics>; 2018.
14. Nagueh SF, Smiseth OA, Appleton CP, et al. Recommendations for the evaluation of left ventricular diastolic function by echocardiography: an update from the American Society of Echocardiography and the European Association of Cardiovascular Imaging. *J Am Soc Echocardiogr* 2016;29:277-314.
15. Coté CJ, Wilson S, American Academy of Pediatrics, et al. Guidelines for monitoring and management of pediatric patients before, during, and after sedation for diagnostic and therapeutic procedures. *Pediatrics* 2019;143:e20191000.
16. Van Praagh R. Diagnosis of complex congenital heart disease: morphologic-anatomic method and terminology. *Cardiovasc Intervent Radiol* 1984;7:115-20.
17. Anderson RH, Becker AE, Freedom RM, et al. Sequential segmental analysis of congenital heart disease. *Pediatr Cardiol* 1984;5:281-7.
18. Sluysmans T, Colan SD. Theoretical and empirical derivation of cardiovascular allometric relationships in children. *J Appl Physiol* 2005;99:445-57.
19. Lopez L, Frommelt PC, Colan SD, et al. Pediatric Heart Network echocardiographic Z scores: comparison with other published models. *J Am Soc Echocardiogr* 2021;34:185-92.
20. Lopez L, Colan S, Stylianou M, et al. Relationship of echocardiographic Z scores adjusted for body surface area to age, sex, race, and ethnicity: the pediatric heart Network normal echocardiogram database. *Circ Cardiovasc Imaging* 2017;10:e006979.
21. Boston Children's Hospital Z-Score Calculator. <http://zscore.chboston.org/>. Accessed December 13, 2023.
22. Cantinotti M, Giordano R, Scalse M, et al. Nomograms for two-dimensional echocardiography derived valvular and arterial dimensions in Caucasian children. *J Cardiol* 2017;69:208-15.
23. Pettersen MD, Du W, Skeens ME, et al. Regression equations for calculation of z scores of cardiac structures in a large cohort of healthy infants, children, and adolescents: an echocardiographic study. *J Am Soc Echocardiogr* 2008;21:922-34.
24. Cantinotti M, Scalse M, Molinaro S, et al. Limitations of current echocardiographic nomograms for left ventricular, valvular, and arterial dimensions in children: a critical review. *J Am Soc Echocardiogr* 2012;25:142-52.
25. PHN Z-Score Calculator. <https://www.pediatricheartnetwork.org/z-scores-calculator/>. Accessed December 13, 2023.
26. Parameter(Z). <http://www.parameterz.com/>. Accessed December 13, 2023.
27. Mahgerefteh J, Linder J, Silver EJ, et al. The prevalence of left ventricular hypertrophy in obese children varies depending on the method utilized to determine left ventricular mass. *Pediatr Cardiol* 2016;37:993-1002.
28. Silvestry FE, Cohen MS, Armsby LB, et al. Guidelines for the echocardiographic assessment of atrial septal defect and patent foramen ovale: from the American Society of Echocardiography and Society for Cardiac Angiography and Interventions. *J Am Soc Echocardiogr* 2015;28:910-58.
29. Mitchell C, Rahko PS, Blauwet LA, et al. Guidelines for performing a comprehensive transthoracic echocardiographic examination in adults: recommendations from the American Society of Echocardiography. *J Am Soc Echocardiogr* 2019;32:1-64.
30. Porter TR, Mulvagh SL, Abdelmoneim SS, et al. Clinical applications of ultrasonic enhancing agents in echocardiography: 2018 American Society of Echocardiography guidelines update. *J Am Soc Echocardiogr* 2018;31:241-74.

31. Muskula PR, Main ML. Safety with echocardiographic contrast agents. *Circ Cardiovasc Imaging* 2017;10:e006979.
32. Lang RM, Badano LP, Tsang W, et al. EAE/ASE recommendations for image acquisition and display using three-dimensional echocardiography. *J Am Soc Echocardiogr* 2012;25:3-46.
33. Jolley MA, Ghelani SJ, Adar A, et al. Three-dimensional mitral valve morphology and age-related trends in children and young adults with structurally normal hearts using transthoracic echocardiography. *J Am Soc Echocardiogr* 2017;30:561-71.
34. Perrin DP, Vasilyev NV, Marx GR, et al. Temporal enhancement of 3D echocardiography by frame reordering. *JACC Cardiovasc Imaging* 2012;5:300-4.
35. Lang RM, Badano LP, Mor-Avi V, et al. Recommendations for cardiac chamber quantification by echocardiography in adults: an update from the American Society of Echocardiography and the European Association of Cardiovascular Imaging. *J Am Soc Echocardiogr* 2015;28:1-39.e14.
36. Pignatelli RH, Ghazi P, Reddy SC, et al. Abnormal myocardial strain indices in children receiving anthracycline chemotherapy. *Pediatr Cardiol* 2015;36:1610-6.
37. Yim D, Hui W, Larios G, et al. Quantification of right ventricular electromechanical dyssynchrony in relation to right ventricular function and clinical outcomes in children with repaired tetralogy of Fallot. *J Am Soc Echocardiogr* 2018;31:822-30.
38. Alghamdi MH, Mertens L, Lee W, et al. Longitudinal right ventricular function is a better predictor of right ventricular contribution to exercise performance than global or outflow tract ejection fraction in tetralogy of Fallot: a combined echocardiography and magnetic resonance study. *Eur Heart J Cardiovasc Imaging* 2013;14:235-9.
39. Rösner A, Khalapyan T, Dalen H, et al. Classic-pattern dyssynchrony in adolescents and adults with a Fontan circulation. *J Am Soc Echocardiogr* 2018;31:211-9.
40. Lin LQ, Conway J, Alvarez S, et al. Reduced right ventricular fractional area change, strain, and strain rate before bidirectional cavopulmonary anastomosis is associated with medium-term mortality for children with hypoplastic left heart syndrome. *J Am Soc Echocardiogr* 2018;31:831-42.
41. Sanchez AA, Levy PT, Sekarski TJ, et al. Effects of frame rate on two-dimensional speckle tracking-derived measurements of myocardial deformation in premature infants. *Echocardiography* 2015;32:839-47.
42. Voigt JU, Pedrizzetti G, Lysyansky P, et al. Definitions for a common standard for 2D speckle tracking echocardiography: consensus document of the EACVI/ASE/industry task force to standardize deformation imaging. *J Am Soc Echocardiogr* 2015;28:183-93.
43. Ramlogan S, Aly D, France R, et al. Reproducibility and intervendor agreement of left ventricular global systolic strain in children using a layer-specific analysis. *J Am Soc Echocardiogr* 2020;33:110-9.
44. Mirea O, Pagourelis ED, Duchenne J, et al. Variability and reproducibility of segmental longitudinal strain measurement: a report from the EACVI-ASE Strain Standardization task force. *JACC Cardiovasc Imaging* 2018;11:15-24.
45. Forsha D, Slorach C, Chen CK, et al. Classic-pattern dyssynchrony and electrical activation delays in pediatric dilated cardiomyopathy. *J Am Soc Echocardiogr* 2014;27:956-64.
46. Forsha D, Slorach C, Chen CKS, et al. Patterns of mechanical inefficiency in pediatric dilated cardiomyopathy and their relation to left ventricular function and clinical outcomes. *J Am Soc Echocardiogr* 2016;29:226-36.
47. Dallaire F, Slorach C, Bradley T, et al. Pediatric reference values and Z score equations for left ventricular systolic strain measured by two-dimensional speckle-tracking echocardiography. *J Am Soc Echocardiogr* 2016;29:786-93.e788.
48. Levy PT, Machevsky A, Sanchez AA, et al. Reference ranges of left ventricular strain measures by two-dimensional speckle-tracking echocardiography in children: a systematic review and meta-analysis. *J Am Soc Echocardiogr* 2016;29:209-25.e206.
49. Koopman LP, Rebel B, Gnanam D, et al. Reference values for two-dimensional myocardial strain echocardiography of the left ventricle in healthy children. *Cardiol Young* 2019;29:325-37.
50. Ferraro AM, Adar A, Ghelani SJ, et al. Speckle tracking echocardiographically-based analysis of ventricular strain in children: an intervendor comparison. *Cardiovasc Ultrasound* 2020;18:15.
51. Sabatino J, Di Salvo G, Prota C, et al. Left atrial strain to identify diastolic dysfunction in children with cardiomyopathies. *J Clin Med* 2019;8:1243.
52. Steele JM, Urbina EM, Mazur WM, et al. Left atrial strain and diastolic function abnormalities in obese and type 2 diabetic adolescents and young adults. *Cardiovasc Diabetol* 2020;19:163.
53. Russell K, Eriksen M, Aaberge L, et al. A novel clinical method for quantification of regional left ventricular pressure-strain loop area: a non-invasive index of myocardial work. *Eur Heart J* 2012;33:724-33.
54. Sabatino J, Borrelli N, Fraise A, et al. Abnormal myocardial work in children with Kawasaki disease. *Sci Rep* 2021;11:7974.
55. Navarini S, Bellsham-Revell H, Chubb H, et al. Myocardial deformation measured by 3-dimensional speckle tracking in children and adolescents with systemic arterial hypertension. *Hypertension* 2017;70:1142-7.
56. Jone PN, Duchateau N, Pan Z, et al. Right ventricular area strain from 3-dimensional echocardiography: mechanistic insight of right ventricular dysfunction in pediatric pulmonary hypertension. *J Heart Lung Transplant* 2021;40:138-48.
57. Salte IM, Østvik A, Smistad E, et al. Artificial intelligence for automatic measurement of left ventricular strain in echocardiography. *JACC Cardiovasc Imaging* 2021;14:1918-28.
58. Rajagopal H, Uppu SC, Weigand J, et al. Validation of right atrial area as a measure of right atrial size and normal values of in healthy pediatric population by two-dimensional echocardiography. *Pediatr Cardiol* 2018;39:892-901.
59. Mertens L, Seri I, Marek J, et al. Targeted neonatal echocardiography in the neonatal intensive care unit: practice guidelines and recommendations for training. *Eur J Echocardiogr* 2011;12:715-36.
60. Bhatla P, Nielsen JC, Ko HH, et al. Normal values of left atrial volume in pediatric age group using a validated allometric model. *Circ Cardiovasc Imaging* 2012;5:791-6.
61. Ghelani SJ, Brown DW, Kuebler JD, et al. Left atrial volumes and strain in healthy children measured by three-dimensional echocardiography: normal values and maturational changes. *J Am Soc Echocardiogr* 2018;31:187-93.e181.
62. Huttin O, Voilliot D, Mandry D, et al. All you need to know about the tricuspid valve: tricuspid valve imaging and tricuspid regurgitation analysis. *Arch Cardiovasc Dis* 2016;109:67-80.
63. Cantinotti M, Giordano R, Koestenberger M, et al. Echocardiographic examination of mitral valve abnormalities in the paediatric population: current practices. *Cardiol Young* 2020;30:1-11.
64. Cohen MS, Jacobs ML, Weinberg PM, et al. Morphometric analysis of unbalanced common atrioventricular canal using two-dimensional echocardiography. *J Am Coll Cardiol* 1996;28:1017-23.
65. Prakash A, Lacro RV, Sleeper LA, et al. Challenges in echocardiographic assessment of mitral regurgitation in children after repair of atrioventricular septal defect. *Pediatr Cardiol* 2012;33:205-14.
66. Kutty S, Colen TM, Smallhorn JF. Three-dimensional echocardiography in the assessment of congenital mitral valve disease. *J Am Soc Echocardiogr* 2014;27:142-54.
67. Mah K, Khoo NS, Tham E, et al. Tricuspid regurgitation in hypoplastic left heart syndrome: three-dimensional echocardiography provides additional information in describing jet location. *J Am Soc Echocardiogr* 2021;34:529-36.
68. Jain A, Mohamed A, El-Khuffash A, et al. A comprehensive echocardiographic protocol for assessing neonatal right ventricular dimensions and function in the transitional period: normative data and z scores. *J Am Soc Echocardiogr* 2014;27:1293-304.
69. Rösner A, Bharucha T, James A, et al. Impact of right ventricular geometry and left ventricular hypertrophy on right ventricular mechanics and clinical outcomes in hypoplastic left heart syndrome. *J Am Soc Echocardiogr* 2019;32:1350-8.
70. Heng EL, Gatzoulis MA, Uebing A, et al. Immediate and midterm cardiac remodeling after surgical pulmonary valve replacement in adults with

- repaired tetralogy of Fallot: a prospective cardiovascular magnetic resonance and clinical study. *Circulation* 2017;136:1703-13.
71. van der Zwaan HB, Geleijnse ML, McGhie JS, et al. Right ventricular quantification in clinical practice: two-dimensional vs. three-dimensional echocardiography compared with cardiac magnetic resonance imaging. *Eur J Echocardiogr* 2011;12:656-64.
  72. Driessen MMP, Meijboom FJ, Hui W, et al. Regional right ventricular remodeling and function in children with idiopathic pulmonary arterial hypertension vs those with pulmonary valve stenosis: insights into mechanics of right ventricular dysfunction. *Echocardiography* 2017;34:888-97.
  73. Koestenberger M, Avian A, Gamillscheg A, et al. Right ventricular base/apex ratio in the assessment of pediatric pulmonary arterial hypertension: results from the European Pediatric Pulmonary Vascular Disease Network. *Clin Cardiol* 2018;41:1144-9.
  74. Alghamdi MH, Grosse-Wortmann L, Ahmad N, et al. Can simple echocardiographic measures reduce the number of cardiac magnetic resonance imaging studies to diagnose right ventricular enlargement in congenital heart disease? *J Am Soc Echocardiogr* 2012;25:518-23.
  75. Kamińska H, Małek Ł, Barczuk-Fałęcka M, et al. Usefulness of three-dimensional echocardiography for assessment of left and right ventricular volumes in children, verified by cardiac magnetic resonance. Can we overcome the discrepancy? *Arch Med Sci* 2021;17:71-83.
  76. Kutty S, Zhou J, Gauvreau K, et al. Regional dysfunction of the right ventricular outflow tract reduces the accuracy of Doppler tissue imaging assessment of global right ventricular systolic function in patients with repaired tetralogy of Fallot. *J Am Soc Echocardiogr* 2011;24:637-43.
  77. Koestenberger M, Ravekes W, Everett AD, et al. Right ventricular function in infants, children and adolescents: reference values of the tricuspid annular plane systolic excursion (TAPSE) in 640 healthy patients and calculation of z score values. *J Am Soc Echocardiogr* 2009;22:715-9.
  78. Mercer-Rosa L, Parnell A, Forfia PR, et al. Tricuspid annular plane systolic excursion in the assessment of right ventricular function in children and adolescents after repair of tetralogy of Fallot. *J Am Soc Echocardiogr* 2013;26:1322-9.
  79. Di Maria MV, Campbell KR, Burkett DA, et al. Parameters of right ventricular function reveal ventricular-vascular mismatch as determined by right ventricular stroke work versus pulmonary vascular resistance in children with pulmonary hypertension. *J Am Soc Echocardiogr* 2020;33:218-25.
  80. Bitterman Y, Hauck A, Manlhiot C, et al. Serial assessment of tricuspid annular plane systolic excursion is associated with death or lung transplant in children with pulmonary arterial hypertension. *J Am Soc Echocardiogr* 2021;34:1320-2.
  81. Khoo NS, Young A, Occlshaw C, et al. Assessments of right ventricular volume and function using three-dimensional echocardiography in older children and adults with congenital heart disease: comparison with cardiac magnetic resonance imaging. *J Am Soc Echocardiogr* 2009;22:1279-88.
  82. Alkon J, Humpl T, Manlhiot C, et al. Usefulness of the right ventricular systolic to diastolic duration ratio to predict functional capacity and survival in children with pulmonary arterial hypertension. *Am J Cardiol* 2010;106:430-6.
  83. Tan JL, Prati D, Gatzoulis MA, et al. The right ventricular response to high afterload: comparison between atrial switch procedure, congenitally corrected transposition of the great arteries, and idiopathic pulmonary arterial hypertension. *Am Heart J* 2007;153:681-8.
  84. Okumura K, Humpl T, Dragulescu A, et al. Longitudinal assessment of right ventricular myocardial strain in relation to transplant-free survival in children with idiopathic pulmonary hypertension. *J Am Soc Echocardiogr* 2014;27:1344-51.
  85. Bhatt SM, Wang Y, Elci OU, et al. Right ventricular contractile reserve is impaired in children and adolescents with repaired tetralogy of Fallot: an exercise strain imaging study. *J Am Soc Echocardiogr* 2019;32:135-44.
  86. Aly D, Ramlogan S, France R, et al. Intervendor agreement for right ventricular global longitudinal strain in children. *J Am Soc Echocardiogr* 2021;34:786-93.
  87. Colquitt JL, Wilkinson JC, Liu AM, et al. Single systemic right ventricle longitudinal strain: intravendor reproducibility and intervendor agreement in children. *Echocardiography* 2021;38:402-9.
  88. DiLorenzo M, Hwang WT, Goldmuntz E, et al. Diastolic dysfunction in tetralogy of Fallot: comparison of echocardiography with catheterization. *Echocardiography* 2018;35:1641-8.
  89. Mercer-Rosa L, Fogel MA, Paridon SM, et al. Revisiting the end-diastolic forward flow (restrictive physiology) in tetralogy of Fallot: an exercise, echocardiographic, and magnetic resonance study. *JACC Cardiovasc Imaging* 2018;11:1547-8.
  90. Friedberg MK. Imaging right-left ventricular interactions. *JACC Cardiovasc Imaging* 2018;11:755-71.
  91. Jone PN, Hinzman J, Wagner BD, et al. Right ventricular to left ventricular diameter ratio at end-systole in evaluating outcomes in children with pulmonary hypertension. *J Am Soc Echocardiogr* 2014;27:172-8.
  92. Ebata R, Fujioka T, Diab SG, et al. Asymmetric regional work contributes to right ventricular fibrosis, inefficiency, and dysfunction in pulmonary hypertension versus regurgitation. *J Am Soc Echocardiogr* 2021;34:537-50.e533.
  93. Okumura K, Slorach C, Mroczek D, et al. Right ventricular diastolic performance in children with pulmonary arterial hypertension associated with congenital heart disease: correlation of echocardiographic parameters with invasive reference standards by high-fidelity micromanometer catheter. *Circ Cardiovasc Imaging* 2014;7:491-501.
  94. Villemain O, Baranger J, Friedberg MK, et al. Ultrafast ultrasound imaging in pediatric and adult cardiology: techniques, applications, and perspectives. *JACC Cardiovasc Imaging* 2020;13:1771-91. <https://doi.org/10.1016/j.jcmg.2019.09.019>.
  95. Feigenbaum H. Role of M-mode technique in today's echocardiography. *J Am Soc Echocardiogr* 2010;23:240-57. 335-247.
  96. Frommelt PC, Minich LL, Trachtenberg FL, et al. Challenges with left ventricular functional parameters: the pediatric heart Network normal echocardiogram database. *J Am Soc Echocardiogr* 2019;32:1331-8.e1331.
  97. Nascimento R, Pereira D, Freitas A, et al. Comparison of left ventricular ejection fraction in congenital heart disease by visual versus algorithmic determination. *Am J Cardiol* 1997;80:1331-5.
  98. Friedberg MK, Su X, Tworetzky W, et al. Validation of 3D echocardiographic assessment of left ventricular volumes, mass, and ejection fraction in neonates and infants with congenital heart disease: a comparison study with cardiac MRI. *Circ Cardiovasc Imaging* 2010;3:735-42.
  99. Balluz R, Liu L, Zhou X, et al. Real time three-dimensional echocardiography for quantification of ventricular volumes, mass, and function in children with congenital and acquired heart diseases. *Echocardiography* 2013;30:472-82.
  100. Jashari H, Rydberg A, Ibrahim P, et al. Left ventricular response to pressure afterload in children: aortic stenosis and coarctation: a systematic review of the current evidence. *Int J Cardiol* 2015;178:203-9.
  101. Dragulescu A, Mertens L, Friedberg MK. Interpretation of left ventricular diastolic dysfunction in children with cardiomyopathy by echocardiography: problems and limitations. *Circ Cardiovasc Imaging* 2013;6:254-61.
  102. Lopez L, Houyel L, Colan SD, et al. Classification of ventricular septal defects for the eleventh iteration of the International Classification of diseases - striving for consensus: a report from the International society for nomenclature of paediatric and congenital heart disease. *Ann Thorac Surg* 2018;106:1578-89.
  103. Anderson RH, Mori S, Spicer DE, et al. Development and morphology of the ventricular outflow tracts. *World J Pediatr Congenit Heart Surg* 2016;7:561-77.
  104. Vlahos AP, Marx GR, McElhinney D, et al. Clinical utility of Doppler echocardiography in assessing aortic stenosis severity and predicting need for intervention in children. *Pediatr Cardiol* 2008;29:507-14.
  105. Barker PC, Ensing G, Ludomirsky A, et al. Comparison of simultaneous invasive and noninvasive measurements of pressure gradients in congenital aortic valve stenosis. *J Am Soc Echocardiogr* 2002;15:1496-502.
  106. Schlingmann TR, Gauvreau K, Colan SD, et al. Correction of Doppler gradients for pressure recovery improves agreement with subsequent catheterization gradients in congenital aortic stenosis. *J Am Soc Echocardiogr* 2015;28:1410-7.

107. Fenster BE, Schroeder JD, Hertzberg JR, et al. 4-Dimensional cardiac magnetic resonance in a patient with bicuspid pulmonic valve: characterization of post-stenotic flow. *J Am Coll Cardiol* 2012;59:e49.
108. Gupta M, Agrawal A, Iakovou A, et al. Pulmonary artery aneurysm: a review. *Pulm Circ* 2020;10:2045894020908780.
109. Brown LM, Duffy CE, Mitchell C, et al. A practical guide to pediatric coronary artery imaging with echocardiography. *J Am Soc Echocardiogr* 2015;28:379-91.
110. Wu EY, Campbell MJ. Cardiac manifestations of multisystem inflammatory syndrome in children (MIS-C) following COVID-19. *Curr Cardiol Rep* 2021;23:168.
111. Camarda J, Berger S. Coronary artery abnormalities and sudden cardiac death. *Pediatr Cardiol* 2012;33:434-8.
112. Cohen MS, Herlong RJ, Silverman NH. Echocardiographic imaging of anomalous origin of the coronary arteries. *Cardiol Young* 2010;20(Suppl 3):26-34.
113. Ekhomu O, Naheed ZJ. Aortic involvement in pediatric Marfan syndrome: a review. *Pediatr Cardiol* 2015;36:887-95.
114. Velchev JD, Van Laer L, Luyckx I, et al. Loeys-Dietz syndrome. *Adv Exp Med Biol* 2021;1348:251-64.
115. Silberbach M, Roos-Hesselink JW, Andersen NH, et al. Cardiovascular health in Turner syndrome: a scientific statement from the American Heart Association. *Circ Genom Precis Med* 2018;11:e000048.
116. Borger MA, Fedak PWM, Stephens EH, et al. The American Association for Thoracic Surgery consensus guidelines on bicuspid aortic valve-related aortopathy: full online-only version. *J Thorac Cardiovasc Surg* 2018;156:e41-74.
117. Jacobs JP, Franklin RCC, Béland MJ, et al. Nomenclature for pediatric and congenital cardiac care: unification of clinical and administrative nomenclature—the 2021 International paediatric and congenital cardiac Code (IPCCC) and the eleventh revision of the International Classification of Diseases (ICD-11). *Cardiol Young* 2021;31:1057-188.
118. Douglas PS, Carabello BA, Lang RM, et al. 2019 ACC/AHA/ASE key data elements and definitions for transthoracic echocardiography: a report of the American College of Cardiology/American Heart Association task force on clinical data standards (Writing committee to develop clinical data standards for transthoracic echocardiography) and the American Society of Echocardiography. *J Am Soc Echocardiogr* 2019;32:1161-248.
119. IAC. The intersocietal accreditation commission standards and guidelines for pediatric echocardiography accreditation. <https://intersocietal.org/document/pediatric-echocardiography-accreditation-standards/>; 2021. Accessed December 13, 2023.
120. Picard MH, Adams D, Bierig SM, et al. American Society of Echocardiography recommendations for quality echocardiography laboratory operations. *J Am Soc Echocardiogr* 2011;24:1-10.
121. Sachdeva R, Douglas PS, Kelleman MS, et al. Educational intervention for improving the appropriateness of transthoracic echocardiograms ordered by pediatric cardiologists. *Congenit Heart Dis* 2017;12:373-81.
122. Dasgupta S, Kelleman M, Sachdeva R. Improvement in appropriateness of pediatric outpatient echocardiography orders following integration of the appropriate use criteria within the electronic medical record ordering system. *J Am Soc Echocardiogr* 2020;33:1152-3.
123. Camarda JA, Patel A, Carr MR, et al. Practice variations in pediatric echocardiography laboratories. *Pediatr Cardiol* 2019;40:537-45.
124. Parthiban A, Levine JC, Nathan M, et al. Implementation of a quality improvement bundle improves echocardiographic imaging after congenital heart surgery in children. *J Am Soc Echocardiogr* 2016;29:1163-70.e1163.
125. Statile C, Statile A, Brown J, et al. Using improvement methodology to optimize echocardiographic imaging of coronary arteries in children. *J Am Soc Echocardiogr* 2016;29:247-52.
126. Benavidez OJ, Gauvreau K, Jenkins KJ, et al. Diagnostic errors in pediatric echocardiography: development of taxonomy and identification of risk factors. *Circulation* 2008;117:2995-3001.
127. Cifra B, Dragulescu A, Border WL, et al. Stress echocardiography in paediatric cardiology. *Eur Heart J Cardiovasc Imaging* 2015;16:1051-9.
128. El Asaad I, Gauvreau K, Rizwan R, et al. Value of exercise stress echocardiography in children with hypertrophic cardiomyopathy. *J Am Soc Echocardiogr* 2020;33:888-94.e882.
129. Pellikka PA, Arruda-Olson A, Chaudhry FA, et al. Guidelines for performance, interpretation, and application of stress echocardiography in ischemic heart disease: from the American Society of Echocardiography. *J Am Soc Echocardiogr* 2020;33:1-41.e48.